

AD_____

Award Number: DAMD17-03-1-0299

TITLE: Regulation of MDM2 Activity by Nucleolin

PRINCIPAL INVESTIGATOR: James A. Borowiec, Ph.D.

CONTRACTING ORGANIZATION: New York University School of Medicine
New York, NY 10016

REPORT DATE: June 2005

TYPE OF REPORT: Annual

PREPARED FOR: U.S. Army Medical Research and Materiel Command
Fort Detrick, Maryland 21702-5012

DISTRIBUTION STATEMENT: Approved for Public Release;
Distribution Unlimited

The views, opinions and/or findings contained in this report are those of the author(s) and should not be construed as an official Department of the Army position, policy or decision unless so designated by other documentation.

20050927 096

REPORT DOCUMENTATION PAGEForm Approved
OMB No. 074-0188

Public reporting burden for this collection of information is estimated to average 1 hour per response, including the time for reviewing instructions, searching existing data sources, gathering and maintaining the data needed, and completing and reviewing this collection of information. Send comments regarding this burden estimate or any other aspect of this collection of information, including suggestions for reducing this burden to Washington Headquarters Services, Directorate for Information Operations and Reports, 1215 Jefferson Davis Highway, Suite 1204, Arlington, VA 22202-4302, and to the Office of Management and Budget, Paperwork Reduction Project (0704-0188), Washington, DC 20503

1. AGENCY USE ONLY (Leave blank)		2. REPORT DATE June 2005	3. REPORT TYPE AND DATES COVERED Annual (1 May 2004 - 30 Apr 2005)	
4. TITLE AND SUBTITLE Regulation of MDM2 Activity by Nucleolin			5. FUNDING NUMBERS DAMD17-03-1-0299	
6. AUTHOR(S) James A. Borowiec, Ph.D.				
7. PERFORMING ORGANIZATION NAME(S) AND ADDRESS(ES) New York University School of Medicine New York, NY 10016 E-Mail: James.borowiec@med.nyu.edu			8. PERFORMING ORGANIZATION REPORT NUMBER	
9. SPONSORING / MONITORING AGENCY NAME(S) AND ADDRESS(ES) U.S. Army Medical Research and Materiel Command Fort Detrick, Maryland 21702-5012			10. SPONSORING / MONITORING AGENCY REPORT NUMBER	
11. SUPPLEMENTARY NOTES Original contains color plates: All DTIC reproductions will be in black and white.				
12a. DISTRIBUTION / AVAILABILITY STATEMENT Approved for Public Release; Distribution Unlimited				12b. DISTRIBUTION CODE
13. ABSTRACT (Maximum 200 Words) <p>A key antagonist of the p53 tumor suppressor is human MDM2 (Hdm2). We examined the significance of a recently identified complex between Hdm2 and nucleolin, a c-Myc-induced gene product with defined roles in ribosomal RNA processing and the inhibition of chromosomal DNA replication following stress. Changes in the level of nucleolin protein in unstressed cells cause parallel changes in the amount of p53 protein. Alterations in p53 levels arise from nucleolin binding to the p53-antagonist Hdm2, resulting in the inhibition of both p53 ubiquitination and Hdm2 auto-ubiquitination. Unexpectedly, we find that nucleolin also reduces Hdm2 protein levels, demonstrating that nucleolin inhibits Hdm2 using multiple mechanisms. Increases in nucleolin levels in unstressed cells led to higher expression of p21^{cip1/waf1}, a reduced rate of cellular proliferation, and an increase in apoptosis. Thus, nucleolin has a number of properties in common with the tumor suppressor ARF. We propose that nucleolin, like ARF, responds to hyper-proliferative signals by up-regulation of p53 through Hdm2 inhibition. These findings have important implications on the progression of breast cells to cancer, and have the potential to provide new therapeutic routes to treat breast cancers.</p>				
14. SUBJECT TERMS MDM2, HDM2, nucleolin, p53, estrogen receptor alpha, ubiquitination				15. NUMBER OF PAGES 83
				16. PRICE CODE
17. SECURITY CLASSIFICATION OF REPORT Unclassified	18. SECURITY CLASSIFICATION OF THIS PAGE Unclassified	19. SECURITY CLASSIFICATION OF ABSTRACT Unclassified	20. LIMITATION OF ABSTRACT Unlimited	

Table of Contents

Cover.....	1
SF 298.....	2
Introduction.....	4
Body.....	4
Key Research Accomplishments.....	9
Reportable Outcomes.....	10
Conclusions.....	11
References.....	11
Appendices.....	12

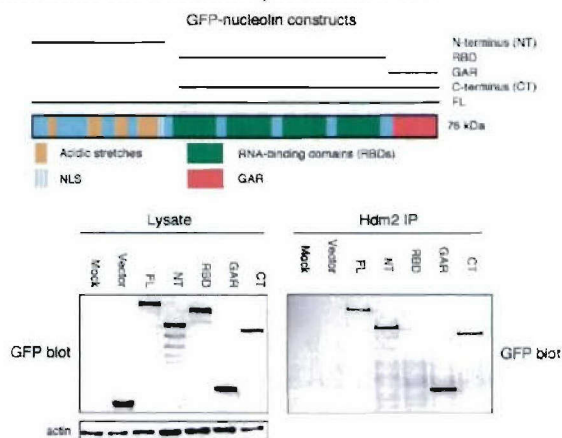
INTRODUCTION

The human MDM2 (Hdm2) protein is overexpressed in one-third of benign breast lesions and two-thirds of malignant lesions. As Hdm2 normally causes rapid p53 turnover and reduces p53 transactivation, heightened Hdm2 levels will therefore inhibit p53-mediated cell-cycle arrest and apoptosis. We have found a novel interaction between Hdm2 and nucleolin, an abundant nucleolar protein, and this interaction apparently inhibits Hdm2 activity. The hypothesis to be tested in our studies is that nucleolin normally serves to inhibit Hdm2 activity *in vivo*. Increases in nucleolin protein levels will therefore inhibit Hdm2 ubiquitination activity, p53 nuclear exclusion, and ER α activity. The objective of the proposed work is to characterize the nucleolin-Hdm2 interaction and to understand the modulation of Hdm2 activities by nucleolin. The specific Aims of the project are: (1) To identify the domains on both nucleolin and Hdm2 necessary for interaction, (2) to examine the effect of nucleolin on the ubiquitin ligase activity of Hdm2 for itself and for p53, (3) to examine the effect of nucleolin on the Hdm2-mediated nuclear exclusion of p53, and on Hdm2 localization, and (4) to characterize the effect of nucleolin on ER α activity and Hdm2-ER α complex formation *in vivo*.

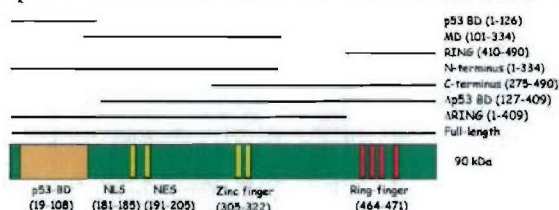
BODY

Over the past year, we have made significant progress analyzing the effect of nucleolin on modulating the activity of Hdm2 on p53. Our work primarily relates to Task 1 (Identification of nucleolin- and Hdm2-interaction domains) and Task 3 (Effect of nucleolin on the ubiquitin ligase activity of Hdm2) of the application. The key experimental findings are described below:

Identification of Hdm2 and nucleolin domains required for nucleolin-Hdm2 complex formation (Task 1). We have completed generating vectors that express nucleolin and Hdm2 truncation mutants for analysis in mammalian cells, or that allow purification for cell-free study. Specifically, we have constructed a number of vectors for nucleolin expression in mammalian cells (see figure to the right). All mutants are tagged at their N-terminus with GFP. In preliminary studies, p53-null H1299 cells were transiently transfected with each of these vectors. Subsequently, lysates were prepared and subjected to immunoprecipitation with an anti-Hdm2 antibody, and the immunoprecipitate subjected to Western blotting using GFP antibody. As shown in the figure to the right, Hdm2 was found to associate with the nucleolin NT and GAR domains, but not with the central RBD domain. These results are being verified in other cell lines. For study of purified proteins, we initially proposed generating nucleolin mutants in yeast. However, the yield of the isolated protein was low and was often obtained in a degraded form. We have therefore altered our



strategy to express nucleolin mutants in insect cells. The viruses have been constructed and purification of the different nucleolin mutants is currently taking place.



We have also constructed eight different myc-tagged Hdm2 vectors for mammalian expression (see figure to the left), or for purification from bacterial cells. These are currently undergoing testing to identify the nucleolin

interaction domain. The interacting regions will be identified in the very near future.

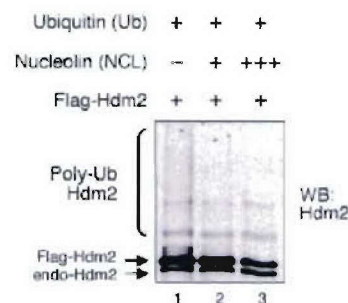
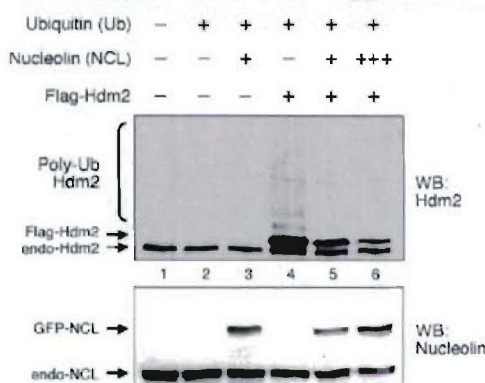
Effect of nucleolin on Hdm2 ubiquitination activity (Aim 2). We examined the effect of nucleolin on Hdm2 ubiquitination activity. We previously found that nucleolin over-expression inhibits p53 ubiquitination. Because we found that nucleolin interacts with the C-terminal ubiquitination domain on p53 (Daniely et al. 2002. MCB 22:6014-6022) as well as Hdm2, it was unclear whether nucleolin sterically prevented Hdm2 from modifying p53, or instead directly inhibited the Hdm2 E3 ubiquitin ligase activity. To address this question, we examined the influence of nucleolin on the Hdm2 auto-ubiquitination activity. Very preliminary investigation of this issue that we previously reported (Year 1 Progress Report) did not reveal any clear effects. However, we have now more rigorously examined this issue and can now report some definitive findings.

p53-null H1299 cells were transfected with Flag-tagged Hdm2, ubiquitin, and two different levels of GFP-tagged nucleolin (see figure to the left). Cells were subsequently lysed and the lysate examined for the presence of Hdm2 and nucleolin by Western blotting (WB). Auto-ubiquitinated Hdm2 is clearly visible ('Poly-Ub Hdm2') when cells are transfected with both Flag-Hdm2 and ubiquitin (upper panel; lane 4). In the presence of increasing nucleolin levels (lanes 5 and 6), loss of ubiquitinated Hdm2 is seen. However, note that nucleolin causes a reduction of both Flag-tagged and endogenous Hdm2 (total; compare the levels of the quickly-migrating Hdm2 doublet between lanes 4 and 6 [upper panel]).

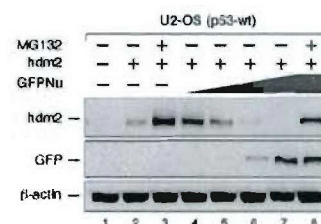
These data suggest that increased nucleolin expression reduces the level of Hdm2 protein, a point also addressed below.

Because the loss of ubiquitinated-Hdm2 may merely be a consequence of less total Hdm2, we repeated the experiment but loaded equivalent amounts of total Hdm2 on the blot. As shown in the figure to the right, increased nucleolin expression again reduced the level of ubiquitinated-Hdm2, demonstrating that nucleolin inhibits Hdm2 auto-ubiquitination activity. This is an important result that we can now confirm.

As indicated above, nucleolin caused an apparent loss of Hdm2 protein, even though inhibiting Hdm2 auto-ubiquitination. We therefore further characterized the effect of nucleolin on Hdm2 levels. Because endogenous Hdm2 levels are normally very low, U2-



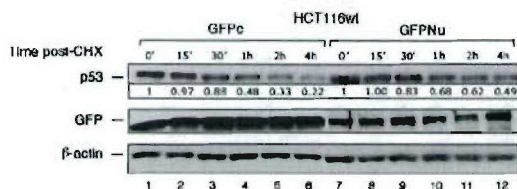
OS cells were transfected with Hdm2 and various amounts of the nucleolin expression constructs. Increases in the level of nucleolin caused a drastic reduction in Hdm2 protein levels (see figure to the right), with Hdm2 found to be virtually undetectable at the highest level of nucleolin (lane 7). Note that nucleolin had only slight effects on Hdm2 levels when cells were treated with MG132 (compare lanes 3 and 8), perhaps suggesting that nucleolin primarily stimulates Hdm2 degradation through a proteasome-dependent mechanism. A similar decrease in Hdm2 protein levels was observed in H1299 cells, indicating that the presence of p53 was not required for nucleolin to mediate this effect (data not shown). Overall, these data indicate that nucleolin reduces Hdm2 protein, with this reduction not strongly influenced by p53. Thus, a therapeutic increase in nucleolin levels and/or activity have the potential of providing a tumor suppressor role in cells, thus pointing towards a novel route to prevent breast cancer development or to treat existing breast tumors.



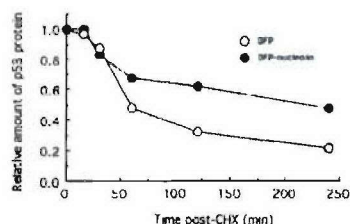
These data lead to one other very interesting conclusion. It has been found that increased Hdm2 auto-ubiquitination causes Hdm2 degradation and therefore less Hdm2 protein (Stommel and Wahl. 2004. EMBO J. 23:1547-56). Intriguingly, we find that nucleolin *decreases* Hdm2 auto-ubiquitination, but still causes a *reduction* in Hdm2 protein levels. These data indicate that nucleolin alters Hdm2 protein levels using a mechanism distinct from its control on Hdm2 ubiquitin activity. We do not yet have any data providing clues as to the identity of this mechanism. That said, nucleolin is known to affect the stability of various mRNAs (e.g., Bcl-2) and our current hypothesis is that nucleolin reduces Hdm2 mRNA stability, thereby reducing Hdm2 protein levels. A more general conclusion is that nucleolin regulates Hdm2 by at two least two different mechanisms – regulation of Hdm2 ubiquitination activity and modulation of Hdm2 protein levels. This is another important result. Because breast cancer cells often express higher levels of Hdm2, it is foreseeable that nucleolin peptides or compounds that mimic nucleolin action can be developed that serve to stimulate p53 levels and thereby inhibit breast cancer growth.

The results above predict that nucleolin would stabilize p53 protein. We therefore

A



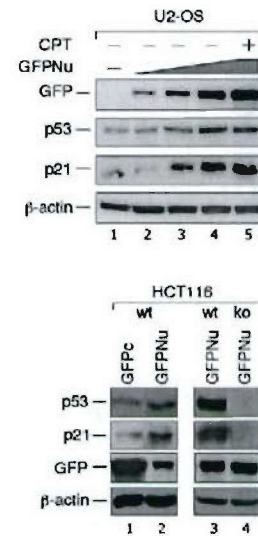
B



examined the influence of nucleolin on the p53 protein half-life. Following transfection of HCT116-wt cells with either GFPNu or GFPc expression vectors, cells were treated with cycloheximide and then harvested at various times post-treatment. Probing the lysates for p53 protein levels indicated a longer p53 half-life in cells expressing GFP-nucleolin (see figure to the left). Densitometric analysis of the p53 levels, corrected for the level of β-actin in the same sample, confirmed this result (lower panel). These data indicate that

heightened nucleolin expression results in significant stabilization of the p53 protein.

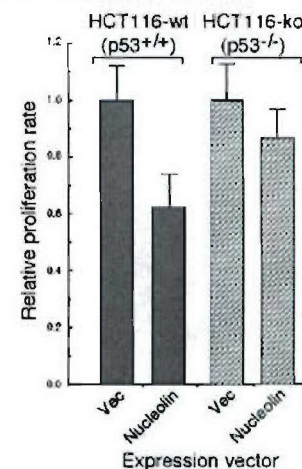
To complete experiments for this part of the study, we measured the effect of nucleolin expression on the level of endogenous p21^{cip1/waf1} protein. p21^{cip1/waf1} protein is a key p53-responsive cell-cycle regulator whose activity is critical for blocking cells at the G1/S transition. We found that nucleolin increased the level of this key cell-cycle regulator (see figure to the right; top panel). At the highest level of nucleolin, the expression of p53 or p21^{cip1/waf1} protein was not further stimulated by genotoxic stress (top panel; compare lanes 4 and 5). Further, when the isogenic cell lines HCT116-wt and -ko were examined, higher levels of p21^{cip1/waf1} were again seen following expression of GFP-nucleolin (lower panel). Only very low levels of p21^{cip1/waf1} were observed in HCT116-ko cells expressing GFP-nucleolin, demonstrating that the stimulation is p53-specific. Similar results were noted for the pro-apoptotic Bax gene product (data not shown). These data indicate that up-regulation of p53 levels by nucleolin can also lead to heightened expression of various p53-responsive genes.



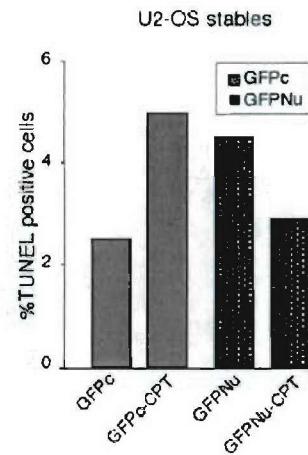
Because nucleolin increases p21^{cip1/waf1} expression, we examined the effect of nucleolin expression on cell proliferation. As a simple indicator of proliferation, we expressed either GFP or GFP-nucleolin in U2-OS or SJSA cells (both of which express wild-type p53), plated the cells at equal low densities, and then grew the cells under G418 selection for ~three weeks (see figure to the left). Visual inspection found that cells expressing GFP-nucleolin had a clear growth disadvantage over cells expressing GFP. To quantitate this effect, we expressed nucleolin in HCT116-wt cells and observed that nucleolin inhibited cell growth to levels ~60% of these same cells transfected with the empty vector (see figure to the right). In contrast, nucleolin expression in HCT116-ko cells had lesser effect as compared to cells transfected with an empty vector control, with this residual effect potentially due to

the ability of nucleolin to inhibit the replication factor RPA (Daniely and Borowiec. 2000. *JCB* 149, 799-810; Wang et al. 2001. *JBC* 276, 20579-20588; Kim et al. 2005. *MCB* 25, 2463-2474). These data indicate that heightened expression of nucleolin inhibits cell proliferation in a p53-dependent manner.

Because p53 regulates numerous genes involved in the cellular apoptotic program, we determined if p53-mediated apoptosis was modulated by nucleolin. Stable clones of U2-OS cells were generated that expressed either GFP-nucleolin or GFP alone. Interestingly, although cells were maintained under G418 selection, it was found that GFP-nucleolin expression was lost in



~50% of cells following two weeks of growth, compared to ~25% of cells losing GFP expression (data not shown). Cells were either mock-treated, or incubated with CPT, and the fraction of GFP-positive cells undergoing apoptosis was then quantitated using a TUNEL assay (see figure to the right). Approximately 1500 cells were examined for each condition. Control (i.e., non-CPT treated) cells expressing GFP-nucleolin were found to have a ~two-fold higher level of apoptosis (4.5%) compared to cells expressing GFP (2.5%). When cells were treated with CPT, the GFP-expressing cells showed increased apoptosis (from 2.5 to 5.0%), as expected, while cells expressing GFP-nucleolin actually showed a reduced level of apoptosis, compared to the mock-treated cells (from 4.5 to 2.9%). In other words, over-expression of nucleolin stimulates apoptosis under normal growth conditions, but under genotoxic stress conditions apparently has anti-apoptotic effects. Combined, our data indicate that nucleolin acts during normal growth conditions to inhibit cellular proliferation and stimulate apoptosis, while inhibiting apoptosis under conditions of genotoxic stress.



The ability of nucleolin to modulate the p53-Hdm2 circuitry suggests a potential therapeutic route to prevent breast cancer development. Recent work has shown that, at the earliest stages of tumorigenesis, early pre-cancer lesions demonstrate a DNA damage response such as p53 activation, ATM activation, and phosphorylation of histone H2AX (Bartkova et al. 2005. *Nature* **434**:864-870; Gorgoulis et al. 2005. *434*:907-13). Thus, manipulating the levels and/or activity of nucleolin may allow clinicians to slightly increase the p53 surveillance machinery, and thereby reduce breast tumorigenesis.

The manuscript describing these results has been submitted to the EMBO Journal (a high-impact journal) and is currently under review. A copy is provided in the Appendix.

Note that the results described above are the most important *scientific* results. In terms of our progress on specific *technical* aspects of the proposal, we have completed:

Task 1 (~85%; a to c complete; d in final stages).

Task 2 (~75%; a to c complete; d is in progress).

Task 3 (~20% complete with sub-task 'a' finished. Sub-task 'b' is in progress. Note that we initially concentrated on examining ubiquitination in vivo, as described above. We also modified our nucleolin expression system from yeast to insect cells infected with recombinant baculoviruses. The insect expression system provides higher expression and more active proteins. We are now re-focusing on the in vitro studies).

Task 4 (~30% complete; a and b complete; preliminary work on c and d is ongoing).

Task 5 (Not yet started)

KEY RESEARCH ACCOMPLISHMENTS

The accomplishments arising over the last twelve months are starred (*).

- Nucleolin inhibits Hdm2-mediated ubiquitination of p53 in vivo.
- Nucleolin inhibits Hdm2 auto-ubiquitination in vivo.*
- Nucleolin reduces Hdm2 protein levels in vivo.*
- Heightened nucleolin expression results in significant stabilization (increased half-life) of the p53 protein. *
- Knockdown of endogenous nucleolin by RNAi methodology has the opposite effect of nucleolin overexpression, namely, p53 levels are reduced.
- The previous two points indicate that alterations in the amount of nucleolin in vivo cause parallel changes in the level of p53.
- Up-regulation of p53 levels by nucleolin causes heightened expression of various p53-responsive genes. *
- Over-expression of nucleolin inhibits cell proliferation in a p53-dependent manner. *
- Higher nucleolin expression increases cellular apoptosis in a p53-dependent manner, in non-stressed cells.*

REPORTABLE OUTCOMES

A. Manuscripts, abstracts, presentations

Much of the work described above was submitted to EMBO Journal and is currently under review. The reference therefore is:

Saxena, A., Rorie, C.J., Dimitrova, D.D., Daniely, Y., and Borowiec, J.A. (2005). Nucleolin inhibits Hdm2 by multiple pathways leading to p53 stabilization. EMBO J. Submitted.

Nucleolin constructs made with DOD funding were subsequently used in work examining the ability of nucleolin to cause a checkpoint response. Thus, DOD funding was used in the following study involving nucleolin:

Kim, K., Dimitrova, D.D., Carta, K., Daras, M., and Borowiec, J.A. (2004). A novel checkpoint response to genotoxic stress mediated by nucleolin-RPA complex formation. *Mol. Cell. Biol.*, 25, 2463-2474.

As mentioned in the previous Annual Report, DOD funding was used to purchase two expression constructs that were also used for a study on another novel cellular S phase checkpoint mechanism:

Vassin, V.M., Wold, M.S., and Borowiec, J.A. (2004). Replication protein A (RPA) phosphorylation prevents RPA association with replication centers. *Mol. Cell. Biol.* 24, 1930-1943.

We also have recently written a review:

Borowiec, J.A. (2004). The Toposome – A new twist on topoisomerase II α . *Cell Cycle* 3, 627-8.

In all four cases, DOD funding was acknowledged.

Over the last year, we gave presentations at the 1) Indiana University School of Medicine, 2) Genomic Integrity Meeting in Galway, Ireland, 3) University of Milan, Italy, and 4) Vanderbilt University. In addition, an abstract was submitted to the '12th International p53 Workshop' in Dunedin, New Zealand. Support from the Department of Defense was publicized in each case.

In the near future, the work will be discussed at the 'Cold Spring Harbor Meeting on Eukaryotic DNA replication', and potentially at 'The Wilhelm Bernhard Workshop - 19th International Workshop on the Cell Nucleus' in Münsterschwarzach, Germany.

Note that nearly all of the funding for these trips was supplied by non-DOD sources, allowing the DOD support to be used directly for laboratory research.

B. Development of cell lines

We have developed stable cells lines that express GFP-nucleolin and control GFP alone using the parental HCT116^{+/+} cell line.

C. Employment or research opportunities applied for and/or received based on experience/training supported by this award.

As mentioned previously, I recruited Checo Rorie, a talented minority (African-American) scientist with a Ph.D. from UNC-Chapel Hill, to work on the project. After ~18 productive months in the lab, he was accepted into the highly competitive SPIRE (Seeding Postdoctoral Innovators in Research and Education), back in North Carolina. He is leaving my laboratory with a 2nd author manuscript – mentioned above – and another publication to be submitted in the upcoming year.

CONCLUSIONS

Our data implicate nucleolin as a key regulatory factor in the p53-Hdm2 circuitry and suggest that nucleolin is a novel tumor suppressor protein. Specifically, we have found that nucleolin binds and inhibits the p53-antagonist Hdm2. The consequences of elevated p53 levels are enhanced expression of p21^{cip1/waf1}, a corresponding reduction of cellular proliferation rate, and an increased rate of apoptosis. Importantly, nucleolin expression is significantly stimulated by c-Myc, suggesting that it is directly responsive to proliferative signals. Our data indicate that nucleolin increases p53 protein levels in response to hyper-proliferative signals, and thereby provide a check against uncontrolled cellular growth.

Because Hdm2 is found upregulated in a significant fraction of breast tumors, our findings suggest new routes to treat breast tumors. Further study of the effect of nucleolin on Hdm2 activity could lead to the identification of molecular compounds that can be used therapeutically. In addition, manipulating the levels and/or activity of nucleolin may allow clinicians to modulate the p53 surveillance machinery, and thereby reduce breast tumorigenesis.

REFERENCES

Provided in text body.

APPENDICES

Four publications are attached that acknowledge DOD funding:

- 1) Saxena, A., Rorie, C.J., Dimitrova, D.D., Daniely, Y., and Borowiec, J.A. (2005). Nucleolin inhibits Hdm2 by multiple pathways leading to p53 stabilization. EMBO J. Submitted.
- 2) Kim, K., Dimitrova, D.D., Carta, K., Daras, M., and Borowiec, J.A. (2004). A novel checkpoint response to genotoxic stress mediated by nucleolin-RPA complex formation. Mol. Cell. Biol., **25**:2463-2474.
- 3) Vassin, V.M., Wold, M.S., and Borowiec, J.A. (2004). Replication protein A (RPA) phosphorylation prevents RPA association with replication centers. Mol. Cell. Biol. **24**:1930-1943.
- 4) Borowiec, J.A. (2004). The toposome – a new twist on topoisomerase II α . Cell Cycle **3**:627-8.

Nucleolin inhibits Hdm2 by multiple pathways leading to p53 stabilization

Running title: ARF-like properties of nucleolin

**Anjana Saxena¹, Checo J. Rorie¹, Diana Dimitrova¹, Yaron Daniely^{1,2}, and James A.
Borowiec^{1,*}**

¹Dept. of Biochemistry and New York University Cancer Institute, New York University School
of Medicine, New York, New York 10016.

*Correspondence should be addressed to J.A.B. Tel.: 212-263-8453. Fax: 212-263-8166.

E-mail: james.borowiec@med.nyu.edu

²Current address: Gamida-Cell, Ltd., 5 Nahum Hafzadi Street, Jerusalem 95484

Character count (including spaces) = 64,311

Abstract

Nucleolin is a c-Myc-induced gene product with defined roles in ribosomal RNA processing and the inhibition of chromosomal DNA replication following stress. Here we find that changes in the level of nucleolin protein in unstressed cells cause parallel changes in the amount of p53 protein. Alterations in p53 levels arise from nucleolin binding to the p53-antagonist Hdm2, resulting in the inhibition of both p53 ubiquitination and Hdm2 auto-ubiquitination. Although the inhibition of ligase activity would be expected to stabilize Hdm2, we instead find that nucleolin also reduces Hdm2 protein levels, demonstrating that nucleolin inhibits Hdm2 using multiple mechanisms. Increases in nucleolin levels in unstressed cells led to higher expression of p21^{cip1/waf1}, a reduced rate of cellular proliferation, and an increase in apoptosis. Thus, nucleolin has a number of properties in common with the tumor suppressor ARF. We propose that nucleolin, like ARF, responds to hyper-proliferative signals by up-regulation of p53 through Hdm2 inhibition.

Keywords: ARF/Mdm2/nucleolin/p53/ubiquitination

Introduction

The transcription factor p53 exerts a pivotal role in controlling cell cycle progression and apoptosis in response to various forms of genotoxic and cellular stress [Anderson and Appella, 2004]. Although normally existing in a latent state, stress conditions cause p53 to become activated, allowing transcriptional modulation of a large body of genes. Mice engineered to lack p53 expression have a high propensity for development of a broad spectrum of tumors [Donehower *et al*, 1992]. In humans, altered p53 regulation is a common step along the pathway of tumorigenesis with ~50% of human cancers showing mutation of the TP53 gene, often a loss of one gene copy and a point mutation within the second. p53 overexpression is also deleterious with heightened p53 levels during development causing organ atrophy [Nakamura *et al*, 1995; Godley *et al*, 1996; Allemand *et al*, 1999]. One hypermorphic p53 mutant, although decreasing the susceptibility to tumor development, results in reduced longevity [Tyner *et al*, 2002]. Control of the intracellular level of p53 therefore represents a critical feature for maintenance of normal cell proliferation and life span.

p53 activity is regulated by various means including protein turnover. Stability of p53 is primarily mediated by the mouse double minute 2 (Mdm2) gene product. Mdm2 (also known as Hdm2 in humans), an E3 ubiquitin ligase, directly interacts with and ubiquitinates p53, promoting its cytoplasmic degradation through the 26S proteasome [Haupt *et al*, 1997; Honda *et al*, 1997; Kubbutat *et al*, 1997; Roth *et al*, 1998; Freedman and Levine, 1998]. Mdm2 also regulates p53 by binding and occluding its N-terminal transactivation domain [Momand *et al*, 1992; Oliner *et al*, 1993]. Upon exposure to various stress stimuli, levels of p53 rise as a consequence of alterations in the p53 modification state that facilitate loss of association with Mdm2. In response to genotoxic stress, for example, p53 N-terminal sites are targeted by

members of the phosphatidylinositol 3-kinase-like kinase (PIKK) family including ATM, ATR, and DNA-PK, as well as downstream effector kinases Chk1 and Chk2 [Anderson and Appella, 2004]. Such modifications both reduce p53 proteolytic degradation and increase the accessibility of the transactivation domain, among other effects. Activation of these kinases also leads to heightened Mdm2 auto-ubiquitination and Mdm2 destabilization [Stommel and Wahl, 2004]. The importance of Mdm2 in appropriately regulating p53 is demonstrated both by the lethality of Mdm2-null mice, and the fact that viability can be rescued by simultaneous deletion of the p53 gene [Jones *et al*, 1995; Montes de Oca Luna *et al*, 1995]. In addition, a hypomorphic allele of Mdm2 exhibits increased p53 transcriptional activity and apoptosis in homeostatic tissue [Mendrysa *et al*, 2003]. In humans, overexpression of Hdm2 is common in a variety of different tumor types, particularly in soft tissue tumors and osteosarcomas, that express wild-type p53 [Momand *et al*, 1998]. These data attest to the conclusion that Mdm2 levels, like those of p53, must be exquisitely controlled.

A number of factors have been identified that alter the p53-Mdm2 circuitry. One prominent member of this group is the ARF tumor suppressor (p14ARF in humans, p19ARF in mice) [Lowe and Sherr, 2003]. Oncogene overexpression increases ARF levels [de Stanchina *et al*, 1998; Palmero *et al*, 1998; Radfar *et al*, 1998; Zindy *et al*, 1998] and stimulates ARF-Mdm2 complex formation [Kamijo *et al*, 1998; Pomerantz *et al*, 1998; Stott *et al*, 1998; Zhang *et al*, 1998; Xirodimas *et al*, 2001]. This in turn causes a decrease both in Mdm2 auto-ubiquitination (indicative of reduced ubiquitin ligase activity) and in the ubiquitination of p53, thus stabilizing p53. Nevertheless, the increase in p53 levels in response to oncogene expression is only partially abrogated in ARF-null cells [Zindy *et al*, 1998] and, in certain tumorigenesis models, p53 up-regulation following oncogenic stress does not involve ARF [Tolbert *et al*, 2002; Verschuren *et*

al, 2002]. Thus, ARF-independent pathways that stimulate p53 in response to hyper-proliferative signals surely exist. Other Mdm2-interacting proteins that can regulate the degradation of p53 include the tumor susceptibility gene 101 (TSG101; [Li *et al*, 2001]), the retinoblastoma protein (Rb; [Hsieh *et al*, 1999]), and the transcription factor Yin Yang 1 (YY1; [Gronroos *et al*, 2004; Sui *et al*, 2004]). A role for the nucleolus in the regulation of p53 has also recently become apparent with nucleolar disruption leading to p53 stabilization [Rubbi and Milner, 2003; Olson, 2004]. ARF has been found to sequester Mdm2 in the nucleolus [Weber *et al*, 1999], although this activity does not appear to be requisite for ARF-dependent p53 stabilization [Llanos *et al*, 2001; Korgaonkar *et al*, 2002]. Recently, nucleophosmin (also called B23), a nucleolar phosphoprotein implicated in ribosome biogenesis and other diverse activities (e.g., see [Okuda, 2002]) was found to interact with Mdm2 and cause p53 stabilization [Kurki *et al*, 2004], and to bind and inhibit ARF [Bertwistle *et al*, 2004; Korgaonkar *et al*, 2005].

Another prominent nucleolar phosphoprotein is nucleolin (also called C23; [Ginisty *et al*, 1999]), an abundant c-Myc-induced gene product [Greasley *et al*, 2000]. In response to c-Myc or a heightened cellular proliferation rate, nucleolin levels can increase ~4-fold [Sirri *et al*, 1997; Greasley *et al*, 2000]. Nucleolin functions at an early step in precursor ribosomal RNA (rRNA) processing [Ginisty *et al*, 1998; Borovjagin and Gerbi, 2004], and disruption of nucleolin homologues in yeast causes unbalanced production of the large and small ribosome subunits [Kondo and Inouye, 1992; Lee *et al*, 1992; Gulli *et al*, 1995]. Although the yeast strains lacking expression of the homologues are viable, they show severe defects in growth strongly suggesting that knockouts of the mammalian protein will be lethal. Nucleolin has stress-regulated interactions with numerous mRNA molecules [Yang *et al*, 2002], and regulates the turnover of particular mRNAs including those encoding the apoptosis inhibitor Bcl-2 and the cell-cycle

regulatory factor gadd45 γ [Sengupta *et al*, 2004; Zheng *et al*, 2005]. Nucleolin is also directly involved in the transcriptional regulation of various genes including rRNA [Bouche *et al*, 1984; Egyhazi *et al*, 1988; Roger *et al*, 2002]. In response to heat shock or genotoxic stress, nucleolin serves to inhibit chromosomal DNA replication by binding and repressing replication protein A (RPA) [Daniely and Borowiec, 2000; Wang *et al*, 2001; Kim *et al*, 2005], the cellular single-stranded DNA-binding protein. These stresses also cause a fraction of the nucleolin pool to relocate from the nucleolus to the nucleoplasm in a reaction stimulated by physical interaction with p53, but independent of the ability of p53 to activate transcription [Daniely *et al*, 2002]. Together, these data indicate that nucleolin globally modulates DNA and RNA metabolism following stress.

Here we examine the effect of nucleolin on the p53-Hdm2 regulatory loop. We find that nucleolin stabilizes p53 by binding and inhibiting Hdm2. Although the effects of nucleolin mimic those seen previously for ARF, nucleolin can exert these effects in cells lacking ARF expression. Because nucleolin levels are increased by proliferative signals, we propose that nucleolin acts in a pathway parallel to ARF to increase p53 levels in response to oncogenic stress.

Results

Nucleolin modulates p53 levels in vivo

To understand the significance of the previously identified nucleolin-p53 interaction [Daniely *et al*, 2002], we characterized the effect of nucleolin on p53 protein levels in cells that normally express wild-type p53 (U2-OS, HCT116-wt) or in p53-null cell lines (H1299 or HCT116-ko) transfected with wild-type p53. In contrast to H1299 cells, both U2-OS and HCT116 cells lack detectable expression of ARF [Burri *et al*, 2001; Park *et al*, 2002; Stott *et al* 1998], and these expression patterns are not altered by nucleolin (data not shown). Transfection of U2-OS cells with increasing levels of a plasmid expressing GFP-tagged nucleolin (GFPNu) was found to raise p53 levels nearly 4-fold relative to mock-transfected cells and nearly to the level of p53 found in cells treated with proteasome inhibitor MG132 (Fig. 1A). There was a ~2-fold increase in total nucleolin protein at the highest levels of nucleolin-vector transfected (data not shown; see Fig. 6A below), indicating that the effects on p53 levels are not a result of extreme nucleolin overexpression. Transient or stable expression of nucleolin increased the level of p53 in other cell lines including HCT116-wt cells (Fig. 1B). Our data demonstrate that nominal increases in nucleolin expression significantly elevate p53 levels in unstressed cells.

It is possible that even a slight increase in nucleolin expression results in genotoxic stress, leading to p53 activation and stabilization. A hallmark of human p53 activation is phosphorylation of Ser15 by members of the PIKK family. Testing the status of Ser15, we found that nucleolin only slightly raised the level of phospho-Ser15, and this followed the increase in total p53 levels (Fig. 1C, compare lanes 1 and 3). In contrast, when cells transfected with GFPc or GFPNu were treated with the DNA-damaging agent camptothecin (CPT), a robust level of p53 activation was observed (lanes 2 and 4). CPT-treated cells expressing nucleolin had similar

or slightly reduced levels of total p53 (lane 4 and data not shown). These data indicate that nucleolin increases p53 levels in a pathway distinct from that utilized by cells undergoing genotoxic stress.

Silencing of nucleolin down-regulates p53 levels

To more clearly show that nucleolin causes coordinate changes in the level of p53, we performed silencing experiments using two different nucleolin-specific short-interfering RNA (siRNA) molecules, siNu1 and siNu2. Twenty-four hours post-transfection, both siNu1 and siNu2 molecules down-regulated the amount of nucleolin protein to 20% and 50%, respectively, of that observed in cells treated with a control siRNA molecule directed against luciferase (siLuc) (Fig. 2A; compare lanes 2 and 5 with lane 1). Comparable reductions in the amount of p53 were observed. At later times post-transfection, as the level of nucleolin returned to more normal levels, comparable increases in the amount of p53 were also detected. Similar effects were seen by immunofluorescence microscopy (Fig. 2B). Using either siRNA molecule, cells with reduced nucleolin staining were also found to be deficient in p53. No overt changes in the localization of the residual p53 were noted. In addition, upon nucleolin silencing, cell morphology remained apparently normal during the course of the experiment, although a significant amount of death was noted at late times post-transfection (>72 h; data not shown). Thus, we find that alterations in the level of nucleolin cause parallel changes in the amount of p53 protein.

Nucleolin regulates the half-life of p53

Because p53 levels are primarily governed through the regulation of p53 stability, we examined the influence of nucleolin on the p53 protein half-life. Following transfection of HCT116-wt cells with either GFPNu or GFPc expression vectors, cells were treated with cycloheximide and then harvested at various times post-treatment. Probing the lysates for p53 protein levels indicated a longer p53 half-life in cells expressing GFP-nucleolin (Fig. 3A). Densitometric analysis of the p53 levels, corrected for the level of γ -actin in the same sample, confirmed this result (Fig. 3B). These data indicate that heightened nucleolin expression results in significant stabilization of the p53 protein.

Nucleolin inhibits Hdm2-mediated ubiquitination of p53 in vivo and in vitro

The primary pathway of p53 turnover involves ubiquitination by Hdm2 and subsequent proteasomal degradation. Because our data suggest that nucleolin might interfere with this pathway, we examined the effect of Hdm2 on the ability of nucleolin to modulate p53 levels. We observed that nucleolin had a more pronounced effect on p53 levels in U2-OS cells expressing ectopic Hdm2 (Fig. 4A). In the absence of exogenous Hdm2, titration of a nucleolin expression vector had only minor effects on p53 levels (Fig. 4A, lanes 9 to 12, compare to lane 1). Expression of Hdm2 by itself reduced the amount of p53 (lane 2), and ectopic nucleolin expression in these cells increased the amount of p53 by ~8-fold over these lower levels (lanes 4 to 7; 0.1 vs. 0.8 relative levels). Similar effects were noted in p53-null H1299 cells that were transiently transfected with p53 (Fig. 4B), although the stimulation observed in the presence of ectopic Hdm2 (3.6-fold, lanes 7 and 9) compared to the absence of Hdm2 (2.4-fold, lanes 1 and 2) was not as pronounced.

The effect of nucleolin on the Hdm2-mediated ubiquitination of p53 was next characterized (Fig. 4C). In U2-OS cells, as expected, expression of ectopic Hdm2 resulted in the accumulation of poly-ubiquitinated p53 (lower panel, lane 2), which was further heightened by treatment with MG132 (lane 3). Strikingly, co-expression of nucleolin diminished p53 poly-ubiquitination, particularly at the higher nucleolin levels, and led to the formation of putative mono- and di-ubiquitinated p53 (lanes 4 to 7). Loss of the residual poly-ubiquitinated p53 at the higher levels of nucleolin correlated with an increase in the amount of p53. Interestingly, the inhibition of ubiquitination was persistent even in the presence of proteasomal inhibitor (lane 8). A similar loss of p53 poly-ubiquitination was observed in H1299 cells following high nucleolin expression, even after MG132 treatment (Fig. 4D, lower panel), and, to a lesser extent, in HCT116-wt cells that expressed both endogenous p53 and exogenous flag-tagged p53 (Fig. 4E, lower panel, compare lane 3 to lane 1). Control experiments found that nucleolin did not appreciably alter the overall pattern of protein ubiquitination (data not shown). Our evidence indicates that nucleolin selectively disrupts p53 ubiquitination by Hdm2, resulting in p53 stabilization and an increase in cellular p53.

To provide direct evidence that nucleolin affects p53 ubiquitination, we utilized an *in vitro* reconstitution system for p53 ubiquitination by Hdm2, using purified proteins [Wang *et al*, 2004]. This system catalyzed robust p53 ubiquitination in an Hdm2-dependent reaction (Fig. 4F; lane 2). While purified nucleolin had no effect on p53 modification in the absence of Hdm2 (lane 3), the addition of increasing amounts of nucleolin to Hdm2 dramatically reduced p53-ubiquitination (lanes 4 and 5). These results demonstrate that nucleolin inhibits Hdm2-mediated ubiquitination of p53 *in vivo* and *in vitro*.

Nucleolin associates with Hdm2 and inhibits the Hdm2 ubiquitin ligase activity

The inhibition of p53 ubiquitination could be a consequence of nucleolin binding to the C-terminal regulatory region of p53 [Daniely *et al*, 2002], which contains multiple lysines that are ubiquitination targets [Rodriguez *et al*, 2000], and hence sterically block Hdm2 action. Alternatively, nucleolin might directly bind Hdm2 and thereby alter its ability to modify p53. As a first test of this hypothesis, we tested the interaction of endogenous nucleolin and Hdm2 in co-immunoprecipitation studies. In p53-positive U2-OS or p53-negative H1299 cells, use of either of two different antibodies to immunoprecipitate Hdm2 also co-precipitated nucleolin (Fig. 5A, lanes 3 and 4). The control IgG did not pull down either Hdm2 or nucleolin (lane 1). The reverse immunoprecipitation reaction involving anti-nucleolin antibodies also precipitated Hdm2 from extracts of these two cells lines as well as the SJSA line (which overexpresses endogenous Hdm2) (Fig. 5B). Further, test of lysates from either U2-OS or H1299 cells found that endogenous Hdm2 formed a complex with ectopic GFP-nucleolin (Fig. 5C, lanes 3 and 6), but not with GFP alone (Fig. 5C, lanes 2 and 5). Similarly, U2-OS and H1299 cells were transfected with both Flag-Hdm2 and GFP-nucleolin, or the corresponding empty vectors. Use of anti-Flag antibodies co-precipitated Flag-Hdm2 and GFP-nucleolin (Fig. 5D, lanes 3 and 6). We consistently observe a slightly higher level of nucleolin-Hdm2 complex in H1299 cells as compared to U2-OS cells. As mentioned, inhibition of p53-ubiquitination was also found to be more striking in H1299 cells than in U2-OS cells (Fig. 4C and D, above). While these differences may merely be a consequence of the use of two different cell types, we note that H1299 cells are p53-negative/ARF-positive while U2-OS cells are p53-positive/ARF-negative. We are currently examining the possibilities that p53 inhibits nucleolin-Hdm2 association, or alternatively that

ARF facilitates nucleolin-Hdm2 complex formation. In sum, these data indicate that nucleolin and Hdm2 can complex *in vivo* in a p53-independent manner.

The ability of nucleolin and Hdm2 to physically interact suggests that nucleolin might inhibit the Hdm2 ubiquitination activity directly, thereby explaining the effect of nucleolin on p53 modification. To test this possibility, we examined Hdm2 auto-ubiquitination as an indicator of the overall ubiquitin ligase activity. In H1299 cells transfected with Hdm2 and His-tagged ubiquitin (Ub-His), a significant level of ubiquitinated Hdm2 was observed (Fig. 6A, lane 4). When these cells were co-transfected with increasing levels of nucleolin, the level of ubiquitinated-Hdm2 *and* total Hdm2 (n.b., the ubiquitinated proteins were not isolated in this experiment) progressively declined (lanes 5 and 6). At the highest level of nucleolin, ubiquitinated-Hdm2 was barely detected (lane 6). Note that this level corresponds to only a ~two-fold increase in total nucleolin (compare endogenous and GFP-tagged nucleolin in lane 6, lower panel). Because nucleolin has an effect on Hdm2 protein levels (described in greater detail below), we more rigorously tested the influence of nucleolin on Hdm2 auto-ubiquitination. H1299 cells were transfected with Hdm2, Ub-His, and two different levels of nucleolin (Fig. 6B). Aliquots that contained equivalent total Hdm2 protein were removed from each lysate, and then analyzed by Western blotting to determine the level of modified Hdm2. Using this approach, we observed that heightened expression of nucleolin resulted in a loss of the ubiquitinated form of Hdm2 (compares lanes 2 and 3 to control lane 1). We conclude that nucleolin inhibits the auto-ubiquitination activity of Hdm2, and this reduced ubiquitin ligase activity contributes to decreased p53 ubiquitination.

Nucleolin diminishes Hdm2 protein levels

As indicated above, nucleolin caused an apparent loss of Hdm2 protein, even though inhibiting Hdm2 auto-ubiquitination (a surprising observation because heightened auto-ubiquitination has been reported to destabilize Hdm2 [Stommel and Wahl, 2004]). We therefore further characterized the effect of nucleolin on Hdm2 levels in various cell lines. Because endogenous Hdm2 levels are normally very low, cells were transfected with Hdm2 and various amounts of the nucleolin expression constructs. In U2-OS cells, increases in the level of nucleolin caused a drastic reduction in Hdm2 protein levels (Fig. 6C, lanes 3 to 7), with Hdm2 found to be virtually undetectable at the highest level of nucleolin (lane 7). Note that nucleolin had only slight effects on Hdm2 levels when cells were treated with MG132 (compare lanes 3 and 8), perhaps suggesting that nucleolin primarily stimulates Hdm2 degradation through a proteasome-dependent mechanism. A similar decrease in Hdm2 protein levels was observed in H1299 cells, indicating that the presence of p53 was not required for nucleolin to mediate this effect (Fig. 6D; compare lanes 4 and 9). To elucidate if the nucleolin-Hdm2 interaction is influenced by the presence of p53, we directly tested the effect of p53 (Fig. 6E). Nucleolin again diminished the level of Hdm2 to an almost undetectable amount (Fig. 6E, compare lane 7 to lane 2). The down-regulation of Hdm2 expression by nucleolin was similar in the presence or absence of p53. Overall, these data indicate that nucleolin reduces Hdm2 protein, with this reduction not strongly influenced by p53.

Nucleolin stimulates p53 transcriptional activity and inhibits cellular proliferation

Because changes in the level of nucleolin can alter the amount of p53 protein, we determined the effect of nucleolin on various p53-mediated activities, first testing p53

transcriptional activity in H1299 cells. Using p53-responsive elements from the promoters of the cyclin-dependent kinase (cdk) inhibitor p21^{cip1/waf1} or Mdm2 genes, we found that nucleolin stimulated expression from 1.9 to 3.4-fold in the presence of p53 (Fig. 7A). Nucleolin in the absence of p53 had no significant effect. We also measured the expression of endogenous p21^{cip1/waf1} protein, and found that nucleolin increased the level of this key cell-cycle regulator (Fig. 7B). At the highest level of nucleolin, genotoxic stress did not markedly stimulate the expression of p53 or p21^{cip1/waf1} protein (Fig. 7B, compare lanes 4 and 5). Further, when the isogenic cell lines HCT116-wt and -ko were examined, higher levels of p21^{cip1/waf1} were again seen following expression of GFP-nucleolin (Fig. 7C, lane 2). Only very low levels of p21^{cip1/waf1} were observed in HCT116-ko cells expressing GFP-nucleolin (Fig. 7C, lane 4), demonstrating that the stimulation is p53-specific. Similar results were noted for the pro-apoptotic Bax gene product (data not shown). These data indicate that up-regulation of p53 levels by nucleolin can also lead to heightened expression of various p53-responsive genes.

Because nucleolin increases p21^{cip1/waf1} expression, we examined the effect of nucleolin expression on cell proliferation. As a simple indicator of proliferation, we expressed either GFP or GFP-nucleolin in U2-OS or SJSA cells, plated the cells at equal low densities, and then grew the cells under G418 selection for ~three weeks (Fig. 8A). Visual inspection found that cells expressing GFP-nucleolin had a clear growth disadvantage over cells expressing GFP. To quantitate this effect, we expressed nucleolin in HCT116-wt cells and observed that nucleolin inhibited cell growth to levels ~60% of these same cells transfected with the empty vector (Fig. 8B). In contrast, nucleolin expression in HCT116-ko cells had lesser effect as compared to cells transfected with an empty vector control, with this residual effect potentially due to the ability of nucleolin to inhibit the replication factor RPA [Daniely and Borowiec, 2000; Wang *et al*, 2001;

Kim *et al*, 2005]. These data indicate that heightened expression of nucleolin inhibits cell proliferation in a p53-dependent manner.

Because p53 regulates numerous genes involved in the cellular apoptotic program, we determined if p53-mediated apoptosis was modulated by nucleolin. Stable clones of U2-OS cells were generated that expressed either GFP-nucleolin or GFP alone. Interestingly, although cells were maintained under G418 selection, it was found that GFP-nucleolin expression was lost in ~50% of cells following two weeks of growth, compared to ~25% of cells losing GFP expression (data not shown). Cells were either mock-treated, or incubated with CPT, and the fraction of GFP-positive cells undergoing apoptosis was then quantitated using a TUNEL assay (Fig. 8C). Approximately 1500 cells were examined for each condition. Control (i.e., non-CPT treated) cells expressing GFP-nucleolin were found to have a ~two-fold higher level of apoptosis (4.5%) compared to cells expressing GFP (2.5%). When cells were treated with CPT, the GFP-expressing cells showed increased apoptosis (from 2.5 to 5.0%), as expected, while cells expressing GFP-nucleolin actually showed a reduced level of apoptosis, compared to the mock-treated cells (from 4.5 to 2.9%). In other words, over-expression of nucleolin stimulates apoptosis under normal growth conditions, but under genotoxic stress conditions apparently has anti-apoptotic effects. Combined, our data indicate that nucleolin acts during normal growth conditions to inhibit cellular proliferation and stimulate apoptosis, while inhibiting apoptosis under conditions of genotoxic stress.

Discussion

The ability to increase p53 protein levels through binding and inhibition of the p53-antagonist Hdm2 implicates nucleolin as a key regulatory factor in the p53-Hdm2 circuitry. The consequences of elevated p53 levels are enhanced expression of p21^{cip1/waf1}, a corresponding reduction of cellular proliferation rate, and an increased rate of apoptosis. Importantly, the nucleolin gene contains a c-Myc binding site (E-box) in the first intron and nucleolin transcription is stimulated ~4-fold by c-Myc, suggesting that it is directly responsive to proliferative signals [Greasley *et al*, 2000]. Indeed, nucleolin protein expression is coupled to the cellular growth rate with proliferating cells having a >3-fold higher nucleolin protein levels compared to quiescent cells (e.g., see [Sirri *et al*, 1997]). We observe significant effects on p53 levels when the amount of nucleolin is changed only ~0.5 to 2-fold. Combined, these data indicate that nucleolin increases p53 protein levels in response to hyper-proliferative signals, and thereby provide a check against uncontrolled cellular growth.

The number of parallels between nucleolin and the ARF tumor suppressor are striking. First, similar to the nucleolin properties that we have described, ARF expression is up-regulated in response to proliferative signals [de Stanchina *et al*, 1998; Palmero *et al*, 1998; Radfar *et al*, 1998; Zindy *et al*, 1998]. At these elevated levels, ARF stabilizes p53 by associating with Mdm2 [Kamijo *et al*, 1998; Pomerantz *et al*, 1998; Stott *et al*, 1998; Zhang *et al*, 1998]. Second, ARF inhibits the E3 ubiquitin ligase activity of Mdm2 [Honda and Yasuda, 1999; Midgley *et al*, 2000], and has been reported to reduce Hdm2 levels [Zhang *et al*, 1998]. Third, both factors function in rRNA processing, although nucleolin is instrumental in facilitating an early cleavage event [Ginisty *et al*, 1998], while p19^{ARF} inhibits downstream processing steps, likely by interference with the nucleophosmin/B23 endoribonuclease [Savkur and Olson, 1998; Itahana *et*

al, 2003; Sugimoto *et al*, 2003; Bertwistle *et al*, 2004]. Fourth, as would be expected of proteins with ribosome biogenic functions, both nucleolin and ARF are primarily nucleolar [Ginisty *et al*, 1999; Zhang and Xiong, 1999; Weber *et al*, 2000]. Importantly, while ARF and nucleolin can associate [Korgaonkar *et al*, 2005], our observed effects of nucleolin on Hdm2 activity and p53 protein levels are not dependent upon ARF because they can occur in cells that lack detectable p14^{ARF} mRNA and protein expression. It is worth emphasizing that ARF-null cells can still raise p53 levels partially or completely when confronted with oncogenic stress, demonstrating the existence of ARF-independent mechanism(s) [Zindy *et al*, 1998; Tolbert *et al*, 2002; Verschuren *et al*, 2002]. We hypothesize that nucleolin functions in such an ARF-independent pathway to regulate p53 and Hdm2 in response to hyper-proliferative signals.

Because nucleolin has numerous activities in common with ARF, a reasonable question to ask is if nucleolin is a tumor suppressor itself. While our data suggest that the answer to this question is likely to be yes, we are not aware of any cancer cells expressing nucleolin mutants. This may simply be a consequence of the critical role that nucleolin plays in rRNA maturation. Budding and fission yeasts deleted for the gene encoding a nucleolin homologue (NSR1 and *gar2*⁺, respectively) are viable but show severe growth defects and have aberrant pre-rRNA processing [Kondo and Inouye, 1992; Lee *et al*, 1992; Gulli *et al*, 1995]. Similarly, our RNAi-mediated silencing of nucleolin causes toxic effects on cell viability (data not shown), likely resulting from an inability to properly process rRNA. These data indicate that mammalian cells lacking nucleolin will be non-viable, or at least have an extreme growth restriction. That said, it is conceivable that nucleolin mutants can be constructed that have selective defects in the interactions with Mdm2 and p53 and thus directly tested for their tumor suppressor properties.

We find that nucleolin binds Hdm2, inhibits its E3 ubiquitin ligase activity, and reduces Hdm2 protein levels, and these collectively lead to an increase in p53 levels in non-stressed cells. Although we have previously observed that nucleolin can associate with the C-terminal domain of p53 (which is the target for ubiquitination [Rodriguez *et al*, 2000]), nucleolin-p53 complex formation is minimal unless cells are subjected to genotoxic stress [Daniely *et al*, 2002]. Taken together, these data suggests that nucleolin regulates p53 by different pathways in unstressed cells compared to cells undergoing genotoxic stress. The ability of nucleolin to both inhibit Hdm2 auto-ubiquitination and cause a reduction in Hdm2 protein levels is surprising. Heightened Mdm2 auto-ubiquitination has been found to stimulate its degradation [Stommel and Wahl, 2004], yet we find that nucleolin both inhibits auto-ubiquitination *and* decreases Hdm2 protein levels. Because the effect of nucleolin can be partly reversed by use of a proteasomal inhibitor (MG132; Fig. 6C), nucleolin likely facilitates Hdm2 degradation. Other mechanisms may facilitate the nucleolin-mediated loss of Hdm2 protein, such as export to the cytoplasm. Although nucleolin is predominantly a nucleolar protein, it constantly shuttles between the nucleus and cytoplasm [Borer *et al*, 1989]. Thus, it is possible that nucleolin aids Hdm2 export to the cytoplasm and stimulates its degradation. Because nucleolin regulates the stability of specific mRNAs (e.g., Bcl-2 and gadd45 γ ; [Sengupta *et al*, 2004; Zheng *et al*, 2005]), we do not rule out the possibility that nucleolin might also regulate Hdm2 (and p53) mRNA stability. The mechanism by which nucleolin inhibits the ubiquitin ligase activity of Hdm2 is similarly unclear. Complex formation with nucleolin may cause conformational changes in Hdm2 that inhibit the ubiquitin ligase reaction. Alternatively, the presence of nucleolin has the potential to sterically block the association of Hdm2 with the E2 ubiquitin-conjugating enzyme or p53. These and other possibilities are under investigation.

Previous data from our laboratory and others indicate that nucleolin can inhibit chromosomal DNA replication following heat shock and genotoxic stress via complex formation with the essential DNA replication factor RPA [Daniely and Borowiec, 2000; Wang *et al*, 2001; Kim *et al*, 2005]. Thus, nucleolin can regulate cell cycle progression both through a p53-independent pathway, as well as the p53-dependent pathway described here. Combined with the defined involvement of nucleolin in rRNA-processing [Ginisty *et al*, 1998], these findings show nucleolin to be a central factor that integrates critical cellular processes including ribosome biogenesis, proliferation and the response to stress.

Materials and Methods

Nucleolin, p53, and Hdm2 expression vectors. The expression constructs for human nucleolin full length (aa 1-707) containing an N-terminal GFP- (GFPNu) or Flag-tag were described previously [Kim *et al*, 2005]. To generate suitable vectors for stable expression in the human cell lines, the puromycin-resistance gene was cloned into GFPNu and GFPc (GFP-only; pEGFP-C1 from BD Biosciences Clontech) expression vectors. The Flag-p53 wt (human), Hdm2 wt and His₆-tagged ubiquitin (Ub-His) constructs were kindly provided by M. Oren (Weizmann Institute), B. Vogelstein (John Hopkins University) and M. Pagano (New York University School of Medicine), respectively.

Antibodies. The primary antibodies used for immunoprecipitation or Western blotting were as follows: nucleolin, either the mouse monoclonal MS-3 or rabbit polyclonal H250 (Santa Cruz Biotechnology); GFP, the rabbit polyclonal anti-GFP antibody (Molecular Probes); p53, mouse monoclonal DO-1 (Santa Cruz Biotechnology); p53 phosphorylated on Ser15, rabbit polyclonal pS15p53 (Cell Signaling Technology); p21, mouse monoclonal CIP1 (BD Biosciences Pharmingen); and Hdm2, mouse monoclonal SMP14 (Santa Cruz Biotechnology) or Ab1 (Oncogene Res. Products). The secondary antibodies used were anti-mouse and anti-rabbit HRP-conjugated antibodies (Amersham), and fluorescent-conjugates antibodies (Jackson ImmunoResearch).

Cell Culture and transfection. HCT116 p53 wild (wt) and knockout (ko) cell lines [Bunz *et al*, 1998] were kindly provided by Dr. Bert Vogelstein (Johns Hopkins University). All other cell lines were obtained from ATCC. Plasmid transfections were performed using Effectene

transfection reagent (Qiagen). When required, CPT (Sigma-Aldrich; a stock concentration of 10 mM in DMSO) was directly added to the growth media to a final concentration of 2 μ M for 90 min. To determine the p53 half-life, HCT116-wt cells were transfected with either GFPc or GFPNu vectors. Thirty-six hours post-transfection, cells were treated with cycloheximide (200 μ g/ml), and harvested at various times. Lysates were prepared and analyzed by Western blotting with anti-p53 antibodies (DO-1).

To generate stable cell lines, U2-OS cells were seeded at 5×10^5 cells per 60-mm plate and transfected with 1 μ g of GFPNu or 0.5 μ g of GFPc vectors. Post-transfection (18 h), the cells were replated at the density of 10^4 cells/10 cm dish in duplicates. GFP-expressing cells were selected in McCoy's 5A media containing 400 or 800 μ g/ml G418 (Cellgro) medium for 21 days, with the drug-containing media replaced every week. Individual clones were subsequently isolated and expanded over a 2 to 4 week period.

For nucleolin silencing experiments, siRNA duplexes (Dharmacon) corresponding to nucleolin positions 2215-2235 (siNu1) or 2292-2310 (siNu2; in the 3' untranslated sequence) were employed, using nucleolin sequence information from Accession NM_005381. U2-OS cells in 24-well plates were transfected with 200 nM of either siNu1 or siNu2, and then harvested at 24, 48 and 72 h post-transfection. Luciferase siRNA (siLuc) was used as a control. Immunofluorescence microscopy was performed as described by Vassin *et al* [2004].

Assay of p53 and Hdm2 ubiquitination. Purification of His₆-ubiquitinated p53 conjugates was performed essentially as described in Rodriguez *et al* [1999]. Cells were processed 36 h post-transfection with 3xFlag-p53 and Hdm2 (at a ratio of 1:20), Ub-His, GFPNu, and pBluescript pIIKS+ (the latter reagent used to equalize the total amount of DNA transfected). An aliquot of

the cell suspension (20%) was directly used for Western blot analysis (see below). The remaining cells were lysed with denaturing buffer (6 M guanidinium-HCl, 0.1 M $\text{Na}_2\text{HPO}_4/\text{NaH}_2\text{PO}_4$, 0.01 M Tris-HCl, pH 8.0, 5 mM imidazole and 10 mM γ -mercaptoethanol), the His-tagged ubiquitinated proteins purified on Ni^{2+} -NTA-agarose beads (Qiagen), and then analyzed by Western blotting using specific antibodies against p53.

For identifying the ubiquitinated-Hdm2 species, H1299 cells were transfected for 24 to 36 h with Flag-Hdm2 and GFPNu (at ratios of 1:1 to 1:3), Ub-His, and pBluescript pIIKS+ vectors. When required, cells were treated with the proteasome inhibitor MG132 (30 μM ; Calbiochem) for 4 h prior to harvest. Following washing with 1x PBS, cells were lysed directly on 100 mm dishes in 50 mM Tris-HCl, pH 7.6, 0.5 mM EDTA, 1% (w/v) SDS and 1 mM DTT, scraped into eppendorf tubes and boiled for 10 min. The concentration of the cell lysate was determined and Western blot analysis was performed with an anti-Hdm2 (SMP14) antibody.

In vitro ubiquitination was performed as described by Wang *et al* [2004]. Reactions (15 μl) containing bacterially expressed human E1, E2 (GST-UbcH5), p53 (1 μl produced in a wheat germ transcription-coupled in vitro translation system [Promega]), GST-Mdm2 (400 ng) and 10 μg ubiquitin (Sigma), GST-nucleolin [Kim *et al*, 2005], 1 $\mu\text{g/ml}$ ATP γ S (Boehringer), 40 mM Tris-HCl, pH 7.5, 2 mM DTT, and 5 mM MgCl_2 were incubated for 60 min at 30°C. Reactions were quenched by addition of 15 μl of SDS-PAGE buffer, boiled for 5 min, and analyzed by 8% SDS-PAGE and Western blotting with an anti-p53 antibody (DO-1).

Immunoprecipitation. Transfected cells were lysed in 20 mM HEPES, pH 7.4, 100 mM NaCl, 0.5% (v/v) NP-40, 10% glycerol, 2 mM EDTA, 1 mM phenylmethylsulfonyl fluoride (PMSF), 0.1 mM Na_3VO_4 , 1 mM NaF, and 1 μg per ml each of aprotinin, leupeptin, and pepstatin. Cell

extracts were incubated with the desired primary antibody for 2 h at 4°C, and the immuno-complex captured using either protein A or Protein G-plus beads at 4°C overnight. The beads were then washed five times with BC100 buffer (20 mM Tris-HCl, pH 7.9, 0.1 mM EDTA, 10% glycerol, 100 mM KCl, 4 mM MgCl₂, 0.2 mM PMSF, 1 mM dithiothreitol, and 0.25 µg per ml of pepstatin), eluted with 2x SDS-PAGE lysis buffer and boiled for 10 min. The proteins were resolved by SDS-PAGE gels and analyzed by Western blotting.

Western blot analysis. To visualize the His-tagged ubiquitinated conjugates, the cell suspension was pelleted and lysed in NP-40 lysis buffer (150 mM NaCl, 50 mM Tris-HCl, pH 8.0, 5 mM EDTA, pH 8.0, 1% NP-40, 2 mM DTT, 2 mM PMSF), and incubated on ice for 30 min. Lysates were similarly obtained from the Hdm2 ubiquitination experiments. Proteins were subjected to Western blot analysis using standard conditions and visualized using ECL-Plus (Perkin-Elmer). Digital images were analyzed using Image SXM and ImageJ software. γ -actin was used for normalization when quantitating band intensities.

Transcription assays. Plasmids encoding firefly luciferase under the control of the p21 or Hdm2 promoter were kindly provided by M. Oren. Briefly, p21 and Hdm2 promoter sequences (both of which contain a p53 response element) were amplified by PCR and ligated into pGL3-Basic reporter plasmid (Promega), upstream of the luciferase gene. H1299 cells were transfected with Flag-p53 and/or GFPNu plasmids, along with either the p21-Luc or Hdm2-Luc reporter constructs. Renilla luciferase under the control of CMV promoter was co-transfected as a control. Cells were harvested 24 h post-transfection and luciferase assayed with a commercial

double luciferase kit (Promega), employing a TD-20e luminometer (Turner BioSystems).

Luciferase activities were normalized against the level of Renilla luciferase in the same extracts.

Proliferation assay. For visual examination of proliferation rates, U2-OS and SJSA cells stably-transfected with GFPNu or GFPc cells were plated at constant density and grown for 3 to 4 weeks under G418 selection. Cells were fixed with 10% TCA for 10 min at RT, and then stained with crystal violet (0.5% in 80% methanol) for 15 min. For assessing the effect of nucleolin expression on growth rate, HCT116-wt and -ko cell lines were transiently transfected with Flag-nucleolin or empty Flag vectors. Twenty-four hours post-transfection, cells were counted and replated at equivalent densities into 96-well plates in triplicate. Cells were harvested at different time points (40, 48, 72, 96 and 120 h post-transfection), stained with 0.1% crystal violet in 80% methanol. After the cells were washed thoroughly with 1x PBS, the crystal violet was eluted in absolute ethanol and measured at 600nm in a 96-plate reader (Dynatech MR7000) as a measure of cell density. The experiment was performed on three independent occasions in triplicate. The relative growth rates were determined at each time point and averaged.

TUNEL. Apoptosis was assayed by TdT-mediated dUTP nick-end labeling (*TUNEL*) using the In Situ Cell Death Detection Kit (TMR Red; Roche) following the manufacturer's protocol.

Following end-labeling, the cells were viewed by fluorescence microscopy to visualize the TUNEL stain, GFP, and Hoechst. GFPc- or GFPNu-positive cells with either complete or granular nuclear TUNEL staining were considered as positive apoptotic cells. More than 1500 of total cells were counted for each construct and treatment.

Acknowledgments

We thank Moshe Oren for various constructs and reagents for the cell-free ubiquitination assay, Michele Pagano for the His-Ub vector, Bert Vogelstein for the HCT116-wt and HCT116-ko cell lines. We also thank A. Wilson, P. Bhatt, and V. Vassin for critical comments on the manuscript, and Elena Sokolova for technical assistance. JAB was supported by the DOD Breast Cancer Research Program (DAMD17-03-1-0299), NIH grant AI29963, Philip Morris USA Inc (15-B0001-42171), and the NYU Cancer Institute and the Rita J. and Stanley Kaplan Comprehensive Cancer Center (NCI P30CA16087).

References

- Allemand I, Anglo A, Jeantet AY, Cerutti I, May E (1999) Testicular wild-type p53 expression in transgenic mice induces spermiogenesis alterations ranging from differentiation defects to apoptosis. *Oncogene* **18**: 6521-6530
- Anderson CW, Appella E (2004) Signaling to the p53 tumor suppressor through pathways activated by genotoxic and non-genotoxic stresses. In *Handbook of Cell Signaling*, Bradshaw RA & Dennis EA (eds) Vol 3, pp 237-247. Academic Press
- Bertwistle D, Sugimoto M, Sherr CJ (2004) Physical and functional interactions of the Arf tumor suppressor protein with nucleophosmin/B23. *Mol Cell Biol* **24**: 985-996
- Borer RA, Lehner CF, Eppenberger HM, Nigg EA (1989) Major nucleolar proteins shuttle between nucleus and cytoplasm. *Cell* **56**: 379-390
- Borovjagin AV, Gerbi SA (2004) Xenopus U3 snoRNA docks on pre-rRNA through a novel base-pairing interaction. *RNA* **10**: 942-953
- Bouche G, Caizergues-Ferrer M, Bugler B, Amalric F (1984) Interrelations between the maturation of a 100 kDa nucleolar protein and pre rRNA synthesis in CHO cells. *Nucl Acids Res* **12**: 3025-3035
- Bunz F, Dutriaux A, Lengauer C, Waldman T, Zhou S, Brown JP, Sedivy JM, Kinzler KW, Vogelstein B (1998) Requirement for p53 and p21 to sustain G2 arrest after DNA damage. *Science* **282**: 1497-1501
- Burri N, Shaw P, Bouzourene H, Sordat I, Sordat B, Gillet M, Schorderet D, Bosman FT, Chaubert P (2001) Methylation silencing and mutations of the p14ARF and p16INK4a genes in colon cancer. *Lab Invest* **81**: 217-229
- Daniely Y, Borowiec JA (2000) Formation of a complex between nucleolin and replication protein A after cell stress prevents initiation of DNA replication. *J Cell Biol* **149**: 799-810
- Daniely Y, Dimitrova DD, Borowiec JA (2002) Stress-dependent nucleolin mobilization mediated by p53-nucleolin complex formation. *Mol Cell Biol* **22**: 6014-6022
- de Stanchina E, McCurrach ME, Zindy F, Shieh SY, Ferbeyre G, Samuelson AV, Prives C, Roussel MF, Sherr CJ, Lowe SW (1998) E1A signaling to p53 involves the p19(ARF) tumor suppressor. *Genes Dev* **12**: 2434-2442
- Donehower LA, Harvey M, Slagle BL, McArthur MJ, Montgomery CA, Butel JS, Bradley A (1992) Mice deficient for p53 are developmentally normal but susceptible to spontaneous tumours. *Nature* **356**: 215-221
- Egyhazi E, Pigon A, Chang JH, Ghaffari SH, Dreesen TD, Wellman SE, Case ST, Olson MO (1988) Effects of anti-C23 (nucleolin) antibody on transcription of ribosomal DNA in Chironomus salivary gland cells. *Exp Cell Res* **178**: 264-272
- Freedman DA, Levine AJ (1998) Nuclear export is required for degradation of endogenous p53 by MDM2 and human papillomavirus E6. *Mol Cell Biol* **18**: 7288-7293
- Ginisty H, Amalric F, Bouvet P (1998) Nucleolin functions in the first step of ribosomal RNA processing. *EMBO J* **17**: 1476-1486
- Ginisty H, Sicard H, Roger B, Bouvet P (1999) Structure and functions of nucleolin. *J Cell Sci* **112**: 761-772
- Godley LA, Kopp JB, Eckhaus M, Paglino JJ, Owens J, Varmus HE (1996) Wild-type p53 transgenic mice exhibit altered differentiation of the ureteric bud and possess small kidneys. *Genes Dev* **10**: 836-850

- Greasley PJ, Bonnard C, Amati B (2000) Myc induces the nucleolin and BN51 genes: possible implications in ribosome biogenesis. *Nucl Acids Res* **28**: 446-453
- Gronroos E, Terentiev AA, Punga T, Ericsson J (2004) YY1 inhibits the activation of the p53 tumor suppressor in response to genotoxic stress. *Proc Natl Acad Sci USA* **101**: 12165-12170
- Gulli MP, Girard JP, Zabetakis D, Lapeyre B, Melese T, Caizergues-Ferrer M (1995) gar2 is a nucleolar protein from *Schizosaccharomyces pombe* required for 18S rRNA and 40S ribosomal subunit accumulation. *Nucl Acids Res* **23**: 1912-1918
- Haupt Y, Maya R, Kazaz A, Oren M (1997) Mdm2 promotes the rapid degradation of p53. *Nature* **387**: 296-299
- Honda R, Tanaka H, Yasuda H (1997) Oncoprotein MDM2 is a ubiquitin ligase E3 for tumor suppressor p53. *FEBS Lett* **420**: 25-27
- Honda R, Yasuda H (1999) Association of p19(ARF) with Mdm2 inhibits ubiquitin ligase activity of Mdm2 for tumor suppressor p53. *EMBO J* **18**: 22-27
- Hsieh JK, Chan FS, O'Connor DJ, Mitnacht S, Zhong S, Lu X (1999) RB regulates the stability and the apoptotic function of p53 via MDM2. *Mol Cell* **3**: 181-193
- Itahana K, Bhat KP, Jin A, Itahana Y, Hawke D, Kobayashi R, Zhang Y (2003) Tumor suppressor ARF degrades B23, a nucleolar protein involved in ribosome biogenesis and cell proliferation. *Mol Cell* **12**: 1151-1164
- Jones SN, Roe AE, Donehower LA, Bradley A (1995) Rescue of embryonic lethality in Mdm2-deficient mice by absence of p53. *Nature* **378**: 206-208
- Kamijo T, Weber JD, Zambetti G, Zindy F, Roussel MF, Sherr CJ (1998) Functional and physical interactions of the ARF tumor suppressor with p53 and Mdm2. *Proc Natl Acad Sci USA* **95**: 8292-8297
- Kim K, Dimitrova DD, Carta KM, Saxena A, Daras M, Borowiec JA (2005) Novel checkpoint response to genotoxic stress mediated by nucleolin-replication protein A complex formation. *Mol Cell Biol* **25**: 2463-2474
- Kondo K, Inouye M (1992) Yeast NSR1 protein that has structural similarity to mammalian nucleolin is involved in pre-rRNA processing. *J Biol Chem* **267**: 16252-16258
- Korgaonkar C, Hagen J, Tompkins V, Frazier AA, Allamargot C, Quelle FW, Quelle DE (2005) Nucleophosmin (B23) targets ARF to nucleoli and inhibits its function. *Mol Cell Biol* **25**: 1258-1271
- Korgaonkar C, Zhao L, Modestou M, Quelle DE (2002) ARF function does not require p53 stabilization or Mdm2 relocalization. *Mol Cell Biol* **22**: 196-206
- Kubbutat MH, Jones SN, Vousden KH (1997) Regulation of p53 stability by Mdm2. *Nature* **387**: 299-303
- Kurki S, Peltonen K, Latonen L, Kiviharju TM, Ojala PM, Meek D, Laiho M (2004) Nucleolar protein NPM interacts with HDM2 and protects tumor suppressor protein p53 from HDM2-mediated degradation. *Cancer Cell* **5**: 465-475
- Lee WC, Zabetakis D, Melese T (1992) NSR1 is required for pre-rRNA processing and for the proper maintenance of steady-state levels of ribosomal subunits. *Mol Cell Biol* **12**: 3865-3871
- Li L, Liao J, Ruland J, Mak TW, Cohen SN (2001) A TSG101/MDM2 regulatory loop modulates MDM2 degradation and MDM2/p53 feedback control. *Proc Natl Acad Sci USA* **98**: 1619-1624

- Llanos S, Clark PA, Rowe J, Peters G (2001) Stabilization of p53 by p14ARF without relocation of MDM2 to the nucleolus. *Nat Cell Biol* 3: 445-452
- Lowe SW, Sherr CJ (2003) Tumor suppression by Ink4a-Arf: progress and puzzles. *Curr Opin Genet Dev* 13: 77-83
- Mendrysa SM, McElwee MK, Michalowski J, O'Leary KA, Young KM, Perry ME (2003) mdm2 is critical for inhibition of p53 during lymphopoiesis and the response to ionizing irradiation. *Mol Cell Biol* 23: 462-472
- Midgley CA, Desterro JM, Saville MK, Howard S, Sparks A, Hay RT, Lane DP (2000) An N-terminal p14ARF peptide blocks Mdm2-dependent ubiquitination in vitro and can activate p53 in vivo. *Oncogene* 19: 2312-2323
- Momand J, Jung D, Wilczynski S, Niland J (1998) The MDM2 gene amplification database. *Nucl Acids Res* 26: 3453-3459
- Momand J, Zambetti GP, Olson DC, George D, Levine AJ (1992) The mdm-2 oncogene product forms a complex with the p53 protein and inhibits p53-mediated transactivation. *Cell* 69: 1237-1245
- Montes de Oca Luna R, Wagner DS, Lozano G (1995) Rescue of early embryonic lethality in mdm2-deficient mice by deletion of p53. *Nature* 378: 203-206
- Nakamura T, Pichel JG, Williams-Simons L, Westphal H (1995) An apoptotic defect in lens differentiation caused by human p53 is rescued by a mutant allele. *Proc Natl Acad Sci USA* 92: 6142-6146
- Okuda M (2002) The role of nucleophosmin in centrosome duplication. *Oncogene* 21: 6170-6174
- Oliner JD, Pietenpol JA, Thiagalingam S, Gyuris J, Kinzler KW, Vogelstein B (1993) Oncoprotein MDM2 conceals the activation domain of tumour suppressor p53. *Nature* 362: 857-860
- Olson, MO (2004) Sensing cellular stress: another new function for the nucleolus? *Sci STKE* 2004: pe10
- Palmero I, Pantoja C, Serrano M (1998) p19ARF links the tumour suppressor p53 to Ras. *Nature* 395: 125-126
- Park YB, Park MJ, Kimura K, Shimizu K, Lee SH, Yokota J (2002) Alterations in the INK4a/ARF locus and their effects on the growth of human osteosarcoma cell lines. *Cancer Genet Cytogenet* 133: 105-111
- Pomerantz J, Schreiber-Agus N, Liegeois NJ, Silverman A, Alland L, Chin L, Potes J, Chen K, Orlov I, Lee HW, Cordon-Cardo C, DePinho RA (1998) The Ink4a tumor suppressor gene product, p19Arf, interacts with MDM2 and neutralizes MDM2's inhibition of p53. *Cell* 92: 713-723
- Radfar A, Unnikrishnan I, Lee HW, DePinho RA, Rosenberg N (1998) p19(Arf) induces p53-dependent apoptosis during abelson virus-mediated pre-B cell transformation. *Proc Natl Acad Sci USA* 95: 13194-13199
- Rodriguez MS, Desterro JM, Lain S, Lane DP, Hay RT (2000) Multiple C-terminal lysine residues target p53 for ubiquitin-proteasome-mediated degradation. *Mol Cell Biol* 20: 8458-8467
- Rodriguez MS, Desterro JM, Lain S, Midgley CA, Lane DP, Hay RT (1999) SUMO-1 modification activates the transcriptional response of p53. *EMBO J* 18: 6455-6461

- Roger B, Moisand A, Amalric F, Bouvet P (2002) Repression of RNA polymerase I transcription by nucleolin is independent of the RNA sequence that is transcribed. *J Biol Chem* **277**:10209-19
- Roth J, Dobbstein M, Freedman DA, Shenk T, Levine AJ (1998) Nucleo-cytoplasmic shuttling of the hdm2 oncoprotein regulates the levels of the p53 protein via a pathway used by the human immunodeficiency virus rev protein. *EMBO J* **17**: 554-564
- Rubbi CP, Milner J (2003) Disruption of the nucleolus mediates stabilization of p53 in response to DNA damage and other stresses. *EMBO J* **22**: 6068-6077
- Savkur RS, Olson MO (1998) Preferential cleavage in pre-ribosomal RNA by protein B23 endoribonuclease. *Nucl Acids Res* **26**: 4508-4515
- Sengupta TK, Bandyopadhyay S, Fernandes DJ, Spicer EK (2004) Identification of nucleolin as an AU-rich element binding protein involved in bcl-2 mRNA stabilization. *J Biol Chem* **279**: 10855-10863
- Sirri V, Roussel P, Gendron MC, Hernandez-Verdun D (1997) Amount of the two major Ag-NOR proteins, nucleolin, and protein B23 is cell-cycle dependent. *Cytometry* **28**: 147-156
- Stommel JM, Wahl GM (2004) Accelerated MDM2 auto-degradation induced by DNA-damage kinases is required for p53 activation. *EMBO J* **23**: 1547-1556
- Stott FJ, Bates S, James MC, McConnell BB, Starborg M, Brookes S, Palmero I, Ryan K, Hara E, Vousden KH, Peters G (1998) The alternative product from the human CDKN2A locus, p14(ARF), participates in a regulatory feedback loop with p53 and MDM2. *EMBO J* **17**: 5001-5014
- Sugimoto M, Kuo ML, Roussel MF, Sherr CJ (2003) Nucleolar Arf tumor suppressor inhibits ribosomal RNA processing. *Mol Cell* **11**: 415-424
- Sui G, Affar EB, Shi Y, Brignone C, Wall NR, Yin P, Donohoe M, Luke MP, Calvo D, Grossman SR (2004) Yin Yang 1 is a negative regulator of p53. *Cell* **117**: 859-872
- Tolbert D, Lu X, Yin C, Tantama M, Van Dyke T (2002) p19(ARF) is dispensable for oncogenic stress-induced p53-mediated apoptosis and tumor suppression in vivo. *Mol Cell Biol* **22**: 370-377
- Tyner SD, Venkatachalam S, Choi J, Jones S, Ghebranious N, Igelmann H, Lu X, Soron G, Cooper B, Brayton C, Hee Park S, Thompson T, Karsenty G, Bradley A, Donehower LA (2002) p53 mutant mice that display early ageing-associated phenotypes. *Nature* **415**: 45-53
- Verschuren EW, Klefstrom J, Evan GI, Jones N (2002) The oncogenic potential of Kaposi's sarcoma-associated herpesvirus cyclin is exposed by p53 loss in vitro and in vivo. *Cancer Cell* **2**: 229-241
- Wang Y, Guan J, Wang H, Leeper D, Iliakis G (2001) Regulation of DNA replication after heat shock by replication protein A- nucleolin interactions. *J Biol Chem* **276**: 20579-20588
- Wang X, Taplick J, Geva N, Oren M (2004) Inhibition of p53 degradation by Mdm2 acetylation. *FEBS Lett* **561**: 195-201
- Weber JD, Kuo ML, Bothner B, DiGiammarino EL, Kriwacki RW, Roussel MF, Sherr CJ (2000) Cooperative signals governing ARF-mdm2 interaction and nucleolar localization of the complex. *Mol Cell Biol* **20**: 2517-2528
- Weber JD, Taylor LJ, Roussel MF, Sherr CJ, Bar-Sagi D (1999) Nucleolar Arf sequesters Mdm2 and activates p53. *Nat Cell Biol* **1**: 20-26
- Vassin VM, Wold MS, Borowiec JA (2004) Replication protein A (RPA) phosphorylation prevents RPA association with replication centers. *Mol Cell Biol* **24**: 1930-1943

- Xirodimas D, Saville MK, Edling C, Lane DP, Lain S (2001) Different effects of p14ARF on the levels of ubiquitinated p53 and Mdm2 in vivo. *Oncogene* **20**: 4972-4983
- Yang C, Maiguel DA, Carrier F (2002) Identification of nucleolin and nucleophosmin as genotoxic stress-responsive RNA-binding proteins. *Nucl Acids Res* **30**: 2251-2260
- Zhang Y, Xiong Y (1999) Mutations in human ARF exon 2 disrupt its nucleolar localization and impair its ability to block nuclear export of MDM2 and p53. *Mol Cell* **3**: 579-591
- Zhang Y, Xiong Y, Yarbrough WG (1998) ARF promotes MDM2 degradation and stabilizes p53: ARF-INK4a locus deletion impairs both the Rb and p53 tumor suppression pathways. *Cell* **92**: 725-734
- Zheng X, Zhang Y, Chen YQ, Castranova V, Shi X, Chen F (2005) Inhibition of NF-kappaB stabilizes gadd45alpha mRNA. *Biochem Biophys Res Commun* **329**: 95-99
- Zindy F, Eischen CM, Randle DH, Kamijo T, Cleveland JL, Sherr CJ, Roussel MF (1998) Myc signaling via the ARF tumor suppressor regulates p53-dependent apoptosis and immortalization. *Genes Dev* **12**: 2424-2433

Figure Legends

Figure 1. Nucleolin overexpression increases p53 protein levels. Lysates were prepared from (A) U2-OS cells that were transiently transfected with increasing levels of a nucleolin-expression plasmid (GFPNu; 0.3 and 0.6 μ g in a 6-well plate), or from (B) HCT116-wt cells that were either transiently or stably transfected with the GFPNu or GFPc plasmids, as indicated. When required, cells were treated with 30 μ M MG132 for 4 h to inhibit the proteasome. Lysates were then subjected to SDS-PAGE and Western blotting with antibodies against GFP (to reveal GFP-nucleolin), p53, and γ -actin, the latter as a loading control. For panels A and B, the relative amount of p53 was calculated after correction for the amount of γ -actin. These experiments show that nucleolin expression increases p53 protein levels. (C) U2-OS cells were transiently transfected with either GFPc or GFPNu expression vectors. As indicated, cells were treated with 2 μ M CPT for 90 min to cause DNA damage. The lysates were blotted for p53 phosphorylated on Ser15 (pS15-p53), total p53 (p53), GFP and γ -actin. Nucleolin overexpression did not result in any significant changes to either the cellular or nucleolar appearance.

Figure 2. Silencing of nucleolin causes a corresponding decrease in p53. U2-OS cells were transfected with nucleolin (siNu1 or siNu2) or luciferase (siLuc) siRNA duplexes. (A) Lysates were prepared at various times post-transfection (indicated), and nucleolin, p53, and γ -actin was then detected by Western blotting. (B) At 24 h post-transfection, cells were stained with anti-nucleolin and p53 antibodies, and visualized by epifluorescence microscopy. Identical exposure times were used. Both the initial depletion of nucleolin protein and its subsequent recovery caused parallel changes in p53 levels. Note that silencing of nucleolin did not result in any obvious nucleolar disruption.

Figure 3. Nucleolin increases the p53 half-life. **(A)** HCT116-wt cells were transfected with either GFPNu or GFPc. At 48 h post-transfection, cells were treated with 200 μ g/ml cycloheximide (CHX) for indicated times. Lysates were prepared and analyzed by Western blotting for p53, GFP (for GFP and GFP-nucleolin), and the γ -actin loading control. **(B)** Plot of the p53-expression levels following cycloheximide treatment in cells expressing either GFP-nucleolin (solid circles) or GFP alone (open circles), corrected for the levels of γ -actin.

Figure 4. Nucleolin inhibits Hdm2-mediated p53 ubiquitination in vivo and in vitro. Lysates were prepared from **(A)** U2-OS or **(B)** H1299 cells transfected with Hdm2 and various levels of GFPNu (panel A, 0.1 to 0.9 μ g; panel B, 1x and 2x corresponds to 0.3 and 0.6 μ g). H1299 cells were also transfected with p53. Western blotting was used to assay p53 and γ -actin. The level of p53, determined by densitometric analysis and corrected by comparison to the amount of γ -actin, is shown below the p53 panels. The data indicate that the increase in p53 upon nucleolin overexpression is more pronounced in the presence of exogenous Hdm2. **(C)** U2-OS, **(D)** H1299, and **(E)** HCT116-wt cells were transfected with 3x-Flag p53 (15 ng), Hdm2 (300 ng), Ub-His (150 ng) and increasing concentration of GFPNu (100, 300, 600 and 900 ng) plasmids. The His-tagged (ubiquitinated) species were then immunoprobed for the presence of p53. Total lysates were probed for GFP (i.e., nucleolin), p53 (total), and γ -actin. In panels A to D, cells were treated with 30 μ M of MG132 for 4 h, where indicated. With increasing nucleolin expression, higher molecular weight species of p53 reduced significantly, even with the presence of proteasomal inhibitor (panel C, lane 8). A similar loss of p53 poly-ubiquitination was observed with H1299 cells (panel D) and, to a lesser extent, in HCT116-wt cells (panel E). **(F)** In vitro p53

ubiquitination was carried out as described in Materials and Methods, in the presence of increasing amounts of GST-nucleolin (1 to 5 ng) purified from yeast. Ubiquitinated p53 was visualized by immunoblotting with a p53-specific monoclonal antibody (DO-1).

Figure 5. Nucleolin and Hdm2 interact in vivo. Lysates from non-transfected p53-wt (U2-OS, SJSA), and p53-null (H1299) cells, as indicated, were subjected to immunoprecipitation using (A) two different antibodies against Hdm2 (Ab-1 and SMP14), control IgG, or (B) anti-nucleolin antibodies. The immunoprecipitates were subjected to Western analysis using anti-nucleolin, Hdm2, or γ -actin antibodies. These data indicate that endogenous nucleolin and Hdm2 associate in a p53-independent manner. (C) U2-OS or H1299 cells were mock-transfected (Cont), or transfected with the empty GFPc (vec) or GFP-nucleolin (nucleolin) vectors, as indicated. (D) Similarly, U2-OS or H1299 cells were mock-transfected (no DNA control; '-'), or transfected with the empty Flag and GFP vectors (vec), or GFPNu (nuc) and Flag-Hdm2 (hdm2) vectors. Aliquots of the resulting lysates were subjected to immunoprecipitation with anti-Hdm2 (panel C), or anti-Flag (panel D) antibodies. The immunoprecipitates, or aliquots of the original lysates, were immunoblotted with antibodies directed against nucleolin, Hdm2, the GFP or Flag tags, or γ -actin. 'ns' indicates a non-specific band. These data indicate that endogenous and exogenous nucleolin and Hdm2 associate in a p53-independent manner.

Figure 6. Nucleolin inhibits Hdm2 auto-ubiquitination and reduces Hdm2 levels in a p53-independent manner. (A, B) Lysates prepared from H1299 cells transfected with Hdm2, Ub-His and GFPNu plasmids (1x and 3x correspond to 0.25 and 0.75 μ g of the GFPNu vector, respectively) were analyzed for Hdm2 and nucleolin (lower panel) using specific antibodies.

With higher nucleolin expression (i.e., a ~2-fold increase in total nucleolin), Hdm2 poly-ubiquitinated products as well as total Hdm2 levels were decreased. In panel B, lysate samples used in lanes 4 to 6 of panel A were first normalized for total Hdm2 levels, and then again immunoblotted for Hdm2. Although the same blot image was used for upper and lower panels, the signal in the upper panel was digitally-enhanced to more clearly show the Hdm2-ubiquitination products. (C) U2-OS and (D and E) H1299 cells were transfected with Hdm2 (300 ng) and GFPNu (panel C and E, 100, 300, 600 and 900 ng; panel D, 25, 100, 300, 600 and 900 ng). H1299 cells were either used as a p53-null cell line (panel D) or transfected with 3x-Flag p53 (25 ng; panel E). Cells were treated with 30 μ M MG132 for 4 h prior to harvest, where indicated. Aliquots of the lysates were probed by Western blot for GFP (i.e., nucleolin), Hdm2 and γ -actin.

Figure 7. Nucleolin stimulates p53-dependent p21^{cip1/waf1} expression. (A) H1299 cells were transfected with GFPNu (nucleolin) and/or 3xFlag p53 plasmids, as indicated, and the Hdm2- or p21-promoter reporter constructs driving expression of firefly luciferase. The fold-change in firefly luciferase activity is plotted relative to the level of Renilla luciferase in the same extracts. All transfections were performed in triplicates in two independent experiments. (B) Lysates of U2-OS cells transfected with increasing levels of GFPNu (100, 300, and 900 ng) were analyzed for GFP (i.e., nucleolin), p53, p21^{cip1/waf1}, and γ -actin by Western blotting. To generate a genotoxic stress response, cells were treated with 2 μ M CPT for 90 min (lane 5). The data indicate that overexpression of nucleolin in U2-OS cells increases the protein level of the p53 transcriptional target gene product, p21^{cip1/waf1}. (C) Isogenic cell lines HCT116-wt and -ko were

transfected with either GFP or GFPNu. Lysates were then subjected to Western blotting to reveal p53, p21^{cip1/waf1}, GFP, and γ -actin.

Figure 8. Nucleolin inhibits cell proliferation and increases apoptosis in non-stressed cells. **(A)** (Upper two panels) U2-OS and SJSA cells expressing either GFPc or GFPNu were grown under G418 drug selection for ~3 weeks. (Lower panel) Individual stable U2-OS clones expressing either GFP or GFPNu were plated at equal density and grown under selection for 21 days. Colony formation was viewed after staining with crystal violet. **(B)** Transiently transfected HCT116-wt and -ko cells were harvested at 40, 48, 72, 96, and 120 h, and the cell density determined. The relative growth rates were determined at each time point, and averaged for each cell line-transfection combination. **(C)** The TUNEL assay was performed in U2-OS stable clones expressing either GFPc or GFPNu. 1500 cells were carefully examined to determine cells that were positive for both GFP and TUNEL staining. Cells were treated with 5 μ M CPT for 4 h, as indicated.

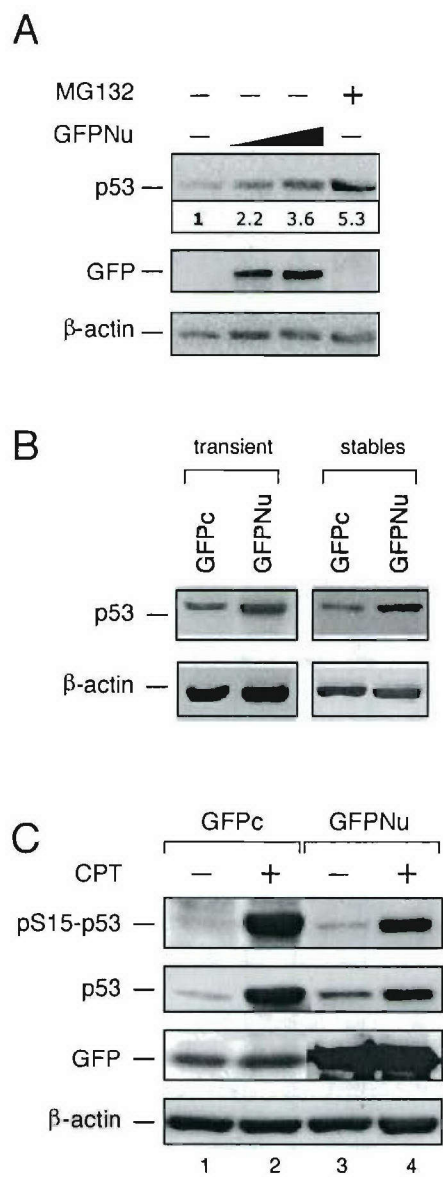
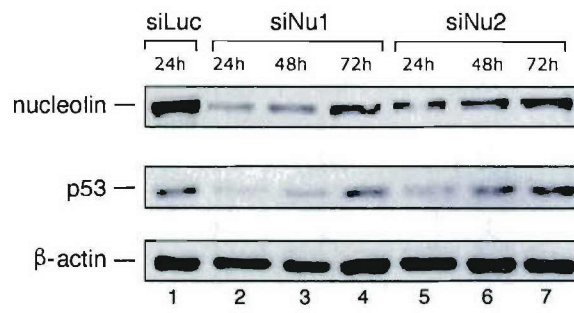


Figure 1

A



B

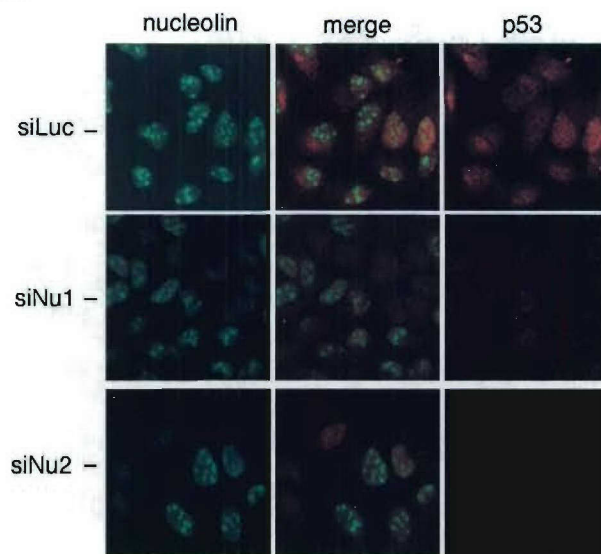
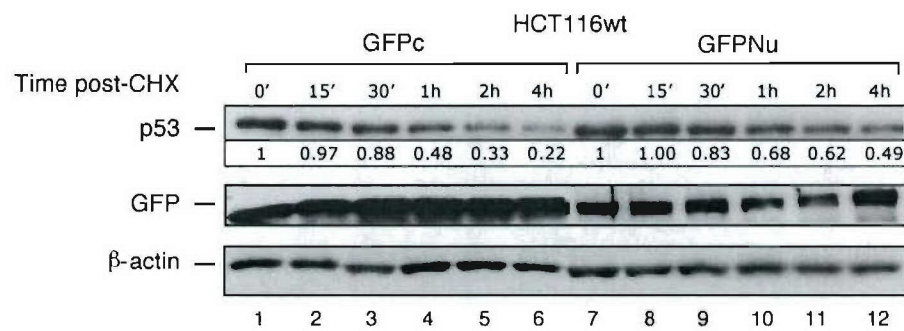


Figure 2

A



B

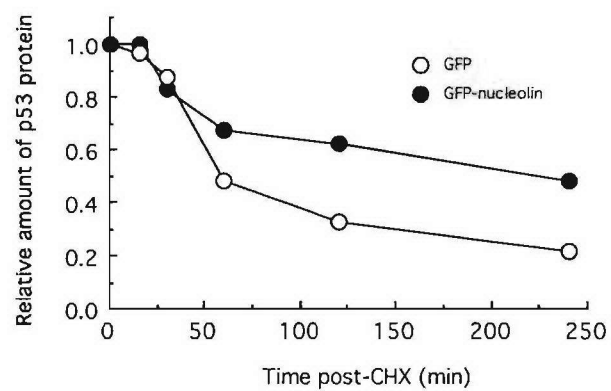


Figure 3

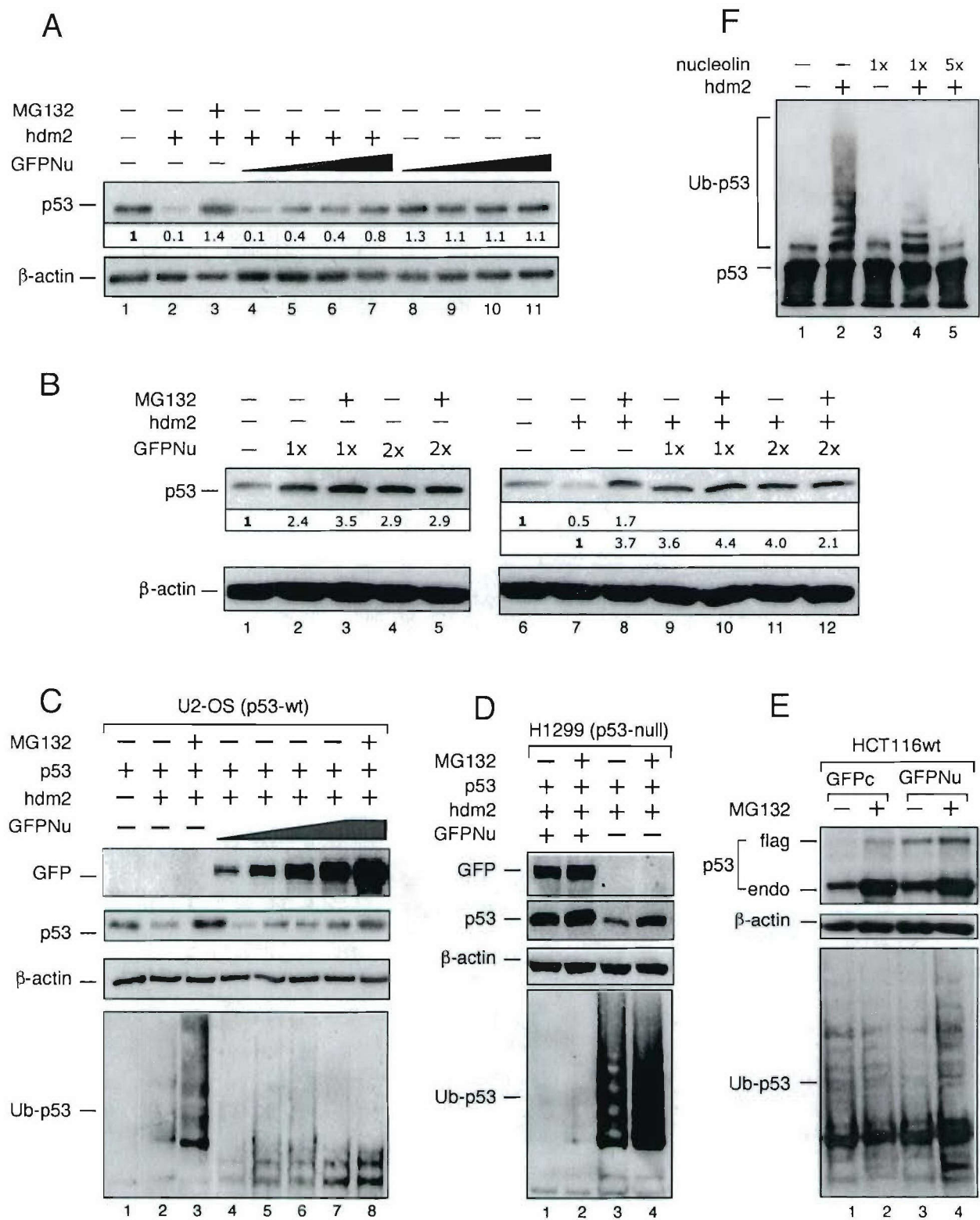


Figure 4

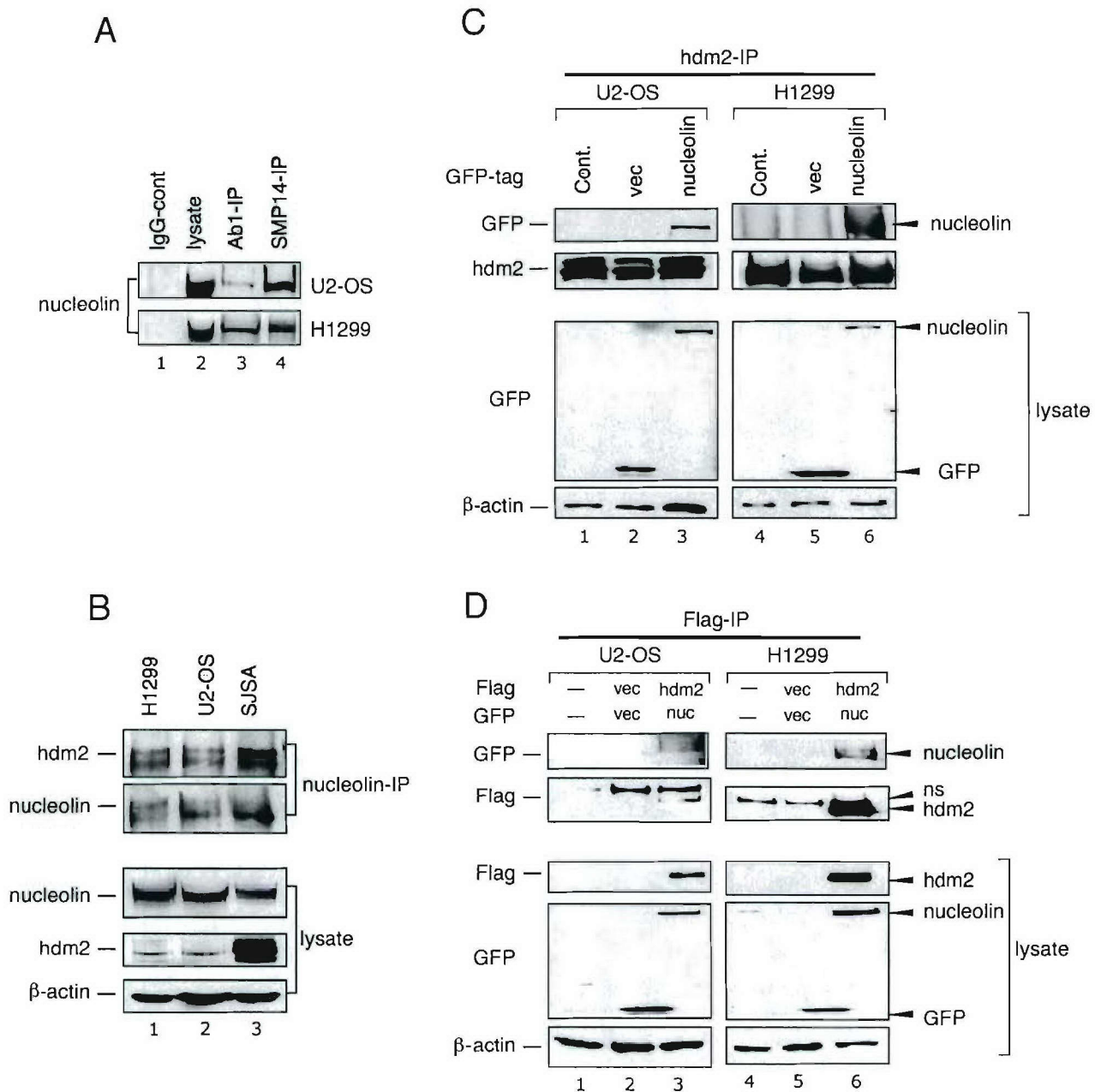


Figure 5

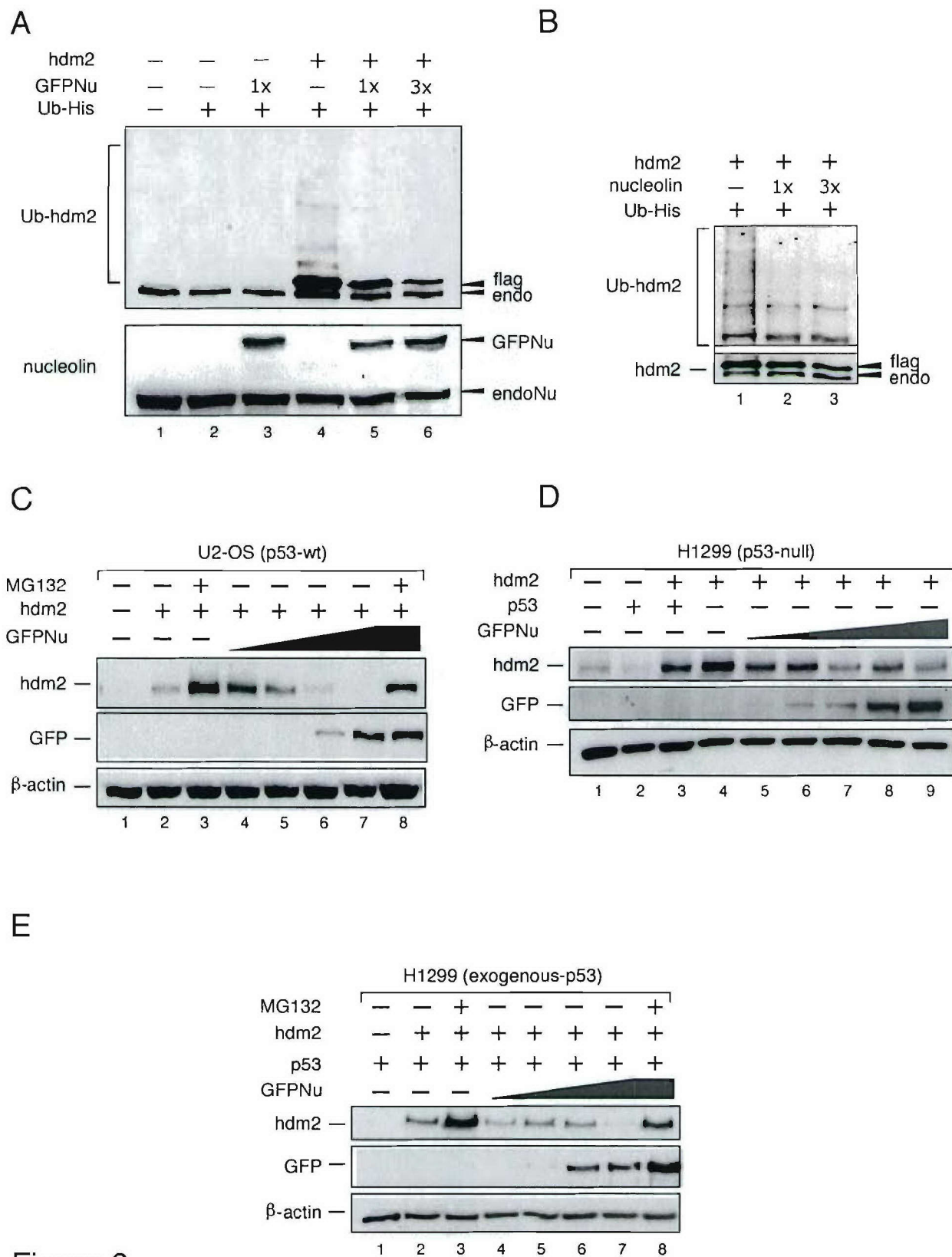
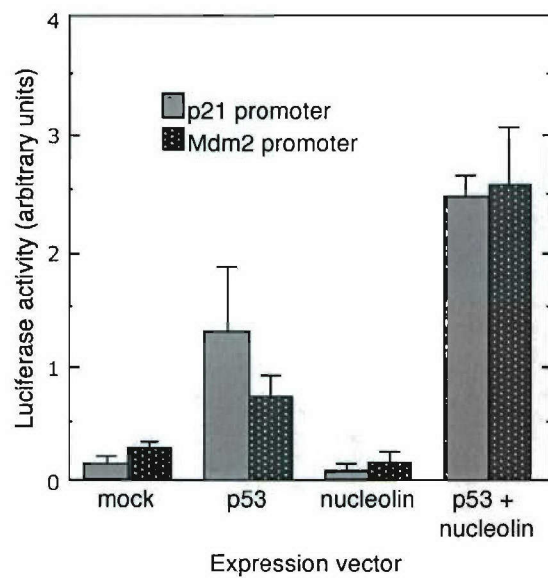
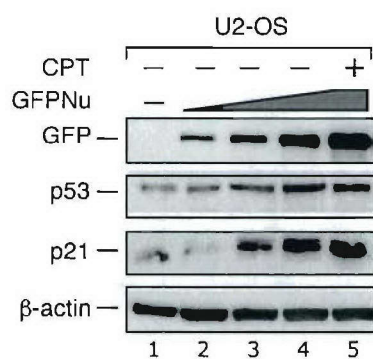


Figure 6

A



B



C

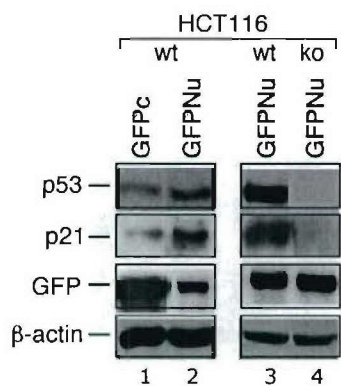


Figure 7

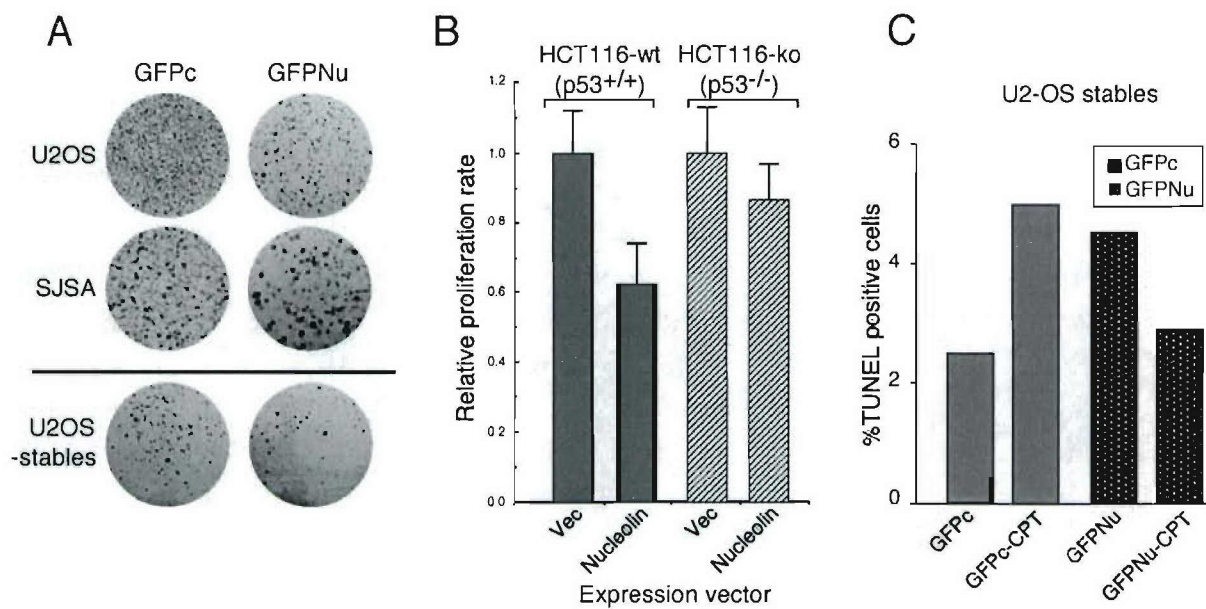


Figure 8

Novel Checkpoint Response to Genotoxic Stress Mediated by Nucleolin-Replication Protein A Complex Formation

Kyung Kim, Diana D. Dimitrova, Kristine M. Carta, Anjana Saxena, Mariza Daras, and James A. Borowiec*

Department of Biochemistry and New York University Cancer Institute, New York University School of Medicine, New York, New York

Received 19 May 2004/Returned for modification 14 June 2004/Accepted 13 December 2004

Human replication protein A (RPA), the primary single-stranded DNA-binding protein, was previously found to be inhibited after heat shock by complex formation with nucleolin. Here we show that nucleolin-RPA complex formation is stimulated after genotoxic stresses such as treatment with camptothecin or exposure to ionizing radiation. Complex formation in vitro and in vivo requires a 63-residue glycine-arginine-rich (GAR) domain located at the extreme C terminus of nucleolin, with this domain sufficient to inhibit DNA replication in vitro. Fluorescence resonance energy transfer studies demonstrate that the nucleolin-RPA interaction after stress occurs both in the nucleoplasm and in the nucleolus. Expression of the GAR domain or a nucleolin mutant (TM) with a constitutive interaction with RPA is sufficient to inhibit entry into S phase. Increasing cellular RPA levels by overexpression of the RPA2 subunit minimizes the inhibitory effects of nucleolin GAR or TM expression on chromosomal DNA replication. The arrest is independent of p53 activation by ATM or ATR and does not involve heightened expression of p21. Our data reveal a novel cellular mechanism that represses genomic replication in response to genotoxic stress by inhibition of an essential DNA replication factor.

Genomic stability requires that cell cycle progression is tightly regulated and can be blocked at key transitions in response to genotoxic stress (38). In response to such stresses, eukaryotic cells activate pathways that both prevent entry into S phase and inhibit DNA synthesis in cells currently undergoing replication. Whereas certain mechanisms have been identified that, for example, block kinases necessary for S-phase progression (e.g., references 10, 11, and 19), other inhibitory pathways likely exist. Study of replication protein A (RPA), the primary single-stranded DNA binding protein in eukaryotes (31, 57), has shown that this factor is a target for inactivation in response both to genotoxic stress and heat shock (8, 13, 36, 37, 52, 54, 55). However, the mechanisms of inactivation remain poorly understood.

RPA is composed of three distinct subunits of ~70 (RPA1), 30 (RPA2), and 14 (RPA3) kDa and is an essential factor in many DNA processing reactions. Genetic and biochemical studies demonstrate that RPA has required roles both in the initiation and in the elongation stages of DNA replication (31, 57). Similarly, RPA is necessary for homologous recombination and for DNA repair events that use the recombination machinery (for example, see reference 53 and references therein). It is also indispensable for nucleotide excision repair (1). Along with stabilizing DNA in its single-stranded form, RPA supports the activity of other factors through obligate interactions. For example, simian virus 40 (SV40) DNA replication can be reconstituted with RPA of a metazoan origin but not with *Saccharomyces cerevisiae* RPA (6, 39). RPA is inti-

mately involved in the cellular checkpoint response as RPA recruits the ATR-ATRIP complex to sites of DNA damage and supports activation of the ATR kinase (59). RPA also recruits the replication factor C-like Rad17 complex to various DNA structures and assists the binding of the Rad9-Rad1-Hus1 complex (60).

As would be expected of a protein with multiple roles in DNA metabolism and in the response to DNA damage, RPA activity is regulated at various levels. The RPA2 subunit of RPA becomes phosphorylated in response to genotoxic stress by phosphatidylinositol 3-kinase-related kinases, including ATM and DNA-PK (see citations within references 5 and 52). Mutational analysis of the RPA2 phosphorylation sites indicates that RPA phosphorylation prevents recruitment of RPA to replication centers while having no effect on localization to sites of DNA damage (52). Downregulation of RPA activity also occurs by apparent phosphorylation-independent mechanisms. The most clearly identified pathway involves the inhibition of RPA activity by association with the nucleolar factor nucleolin (13, 54).

Nucleolin is an abundant protein that is required for the first step of pre-rRNA processing (22). Mutation of the genes encoding nucleolin homologues in budding and fission yeast disrupts balanced production of the small and large ribosomal subunits (24, 34, 35). Nucleolin has many other diverse activities, including regulation of transcription (20, 23, 26, 45, 58), modulation of mRNA stability (9, 48), and acting as a low-affinity receptor for human immunodeficiency virus on the cell surface (7, 41). In response to DNA damage conditions or heat shock, a significant fraction of the nucleolin pool relocates from the nucleolus to the nucleoplasm in a process stimulated by physical association with p53 (13, 14, 54). After heat shock, nucleolin-RPA complex formation is greatly stimulated, and

* Corresponding author. Mailing address: Department of Biochemistry, New York University School of Medicine, 550 First Ave., MSB-383, New York, NY 10016. Phone: (212) 263-8453. Fax: (212) 263-8166. E-mail: james.borowiec@med.nyu.edu.

formation of this complex is inhibitory to DNA replication in vitro (13, 54). In vivo, the mobilized nucleolin sequesters RPA at sites distinct from replication centers (13). The mobilization of nucleolin in response to heat shock thus represents a novel pathway for regulating DNA replication.

We examined the interaction of nucleolin and RPA in response to DNA damage. We found that, like heat shock, genotoxic stress strongly induces nucleolin-RPA complex formation. The RPA-interacting domain was localized to the 63-amino-acid (aa) glycine-arginine-rich (GAR) domain at the extreme C terminus of nucleolin. Expression of GAR or a nucleolin mutant with constitutive association with RPA causes a block in the cellular transit from G₁ into S phase. The nucleolin-mediated inhibition of chromosomal DNA replication could be prevented by overexpression of RPA2 to increase the cellular level of RPA. These data demonstrate a novel intra-S-phase checkpoint response in response to genotoxic stress through target of RPA by mobilized nucleolin.

MATERIALS AND METHODS

Construction of nucleolin and RPA2 expression vectors. For in vitro studies, human nucleolin and mutant nucleolin derivatives were expressed in *Saccharomyces cerevisiae* with N-terminal glutathione S-transferase (GST) tags and were purified as described below. The pKG-derived yeast plasmids that express full-length nucleolin (FL; aa 1 to 707), the N-terminal half of nucleolin (NT; aa 1 to 323), and the C-terminal half of nucleolin (CT; aa 323 to 707) were kindly provided by E. Rubin (University of Medicine and Dentistry of New Jersey [UMDNJ]). Other nucleolin variants, including the combined N terminus and first RNA-binding domain (RBD) (NT/RBD1; aa 1 to 390), the combined N terminus and the complete RBD region (NT/RBD1-4; aa 1 to 648), and the C-terminal GAR domain (GAR; aa 645 to 707), were inserted into the pKG vector by using standard PCR-mediated cloning procedures.

For in vivo studies, nucleolin or nucleolin derivatives were expressed with N-terminal green fluorescent protein (GFP), cyan fluorescent protein (CFP), or Myc epitope tags. GFP and CFP fusion proteins were constructed by using PCR cloning into the pEGFP-C1 or pECFP-C1 vectors (Clontech). Similarly, Myc-tagged nucleolin (FL or mutants) was expressed from the pEF6/Myc-HisA plasmid (Invitrogen), as modified by Vassin et al. (52) to prevent expression of the His tag or, for proliferation studies, from a modified pEGFP-C1 vector in which the GFP tag was replaced by the Myc tag. Human RPA2 containing an N-terminal yellow fluorescent protein (YFP) tag was generated by excising the RPA2 coding sequence from pENeGFP RPA34 (kindly provided by M. C. Cardoso) (50) into pEYFP-C1 vector (Clontech). The construction of the Myc-RPA2 expression vector was described previously (52). The pECFP-C1-H-Ras61L and pEYFP-N1-RasBD expression vectors were kindly provided by Trevor Bivona of Mark Philips laboratory (New York University [NYU] School of Medicine). All fusion constructs were sequenced and shown to be faithful copies of the corresponding genes.

Purification of proteins. GST-tagged nucleolin proteins were purified by the protocol of Haluska et al. (25). After transformation of *S. cerevisiae* JEL1 strain with the appropriate plasmid, cells were grown in synthetic defined (SD) medium under selection in 2% raffinose, and protein expression was induced by 2% galactose. Extracts from these cultures were made by disruption of the yeast cells by using 25- to 50- μ m glass beads in uracil RIPA buffer (50 mM Tris-HCl [pH 7.2], 150 mM NaCl, 0.1% sodium dodecyl sulfate [SDS], 1% Triton X-100, 1% sodium deoxycholate) with protease inhibitors (1 mM phenylmethylsulfonyl fluoride, 0.5 μ g of leupeptin/ml, 1 μ g of pepstatin/ml), 1 mM EDTA, and 1 mM dithiothreitol (DTT). Glutathione-Sepharose beads (Pharmacia) were then added to the clarified yeast extract, followed by incubation to bind the GST-nucleolin proteins. After three washes with a 10 \times bead volume of RIPA buffer, the GST-tagged proteins were eluted with 10 mM reduced glutathione and 50 mM Tris-HCl (pH 7.5). After overnight dialysis at 4°C against phosphate-buffered saline (PBS) and 20% glycerol, eluates were assayed for purity by SDS-polyacrylamide gel electrophoresis (PAGE) and Coomassie blue staining.

The human RPA heterotrimer was produced in *Escherichia coli* BL21 transformed with the p11dRPA vector and purified as described previously (29, 30).

Far-Western analysis. Far-Western blotting was carried out basically as described by Jayaraman et al. (32). Purified GST-tagged nucleolin (FL and mu-

nants) proteins were subjected to SDS-PAGE and then transferred to a nitrocellulose membrane. After two incubations in denaturation buffer (6 M guanidine-HCl in PBS) for 5 min at 4°C, the membrane was incubated six times in serial dilutions (1:1 [vol/vol]) of denaturation buffer, each dilution being with PBS containing 1 mM DTT. The membrane was blocked with PBS containing 0.1% Tween 20 (PBS-T) and 5% nonfat dry milk (NFD) for 45 min at room temperature and washed twice with PBS-T and 0.25% NFD. The membrane was then incubated with purified human RPA (0.2 μ g/ml) in PBS-T, 0.25% NFD, 1 mM DTT, and 2.5 mM phenylmethylsulfonyl fluoride for 2 h at room temperature and subsequently washed four times in PBS-T and 0.25% NFD. The presence of bound RPA was probed by using a mouse anti-RPA2 monoclonal antibody (SSB34A; NeoMarkers) and horseradish peroxidase-conjugated sheep anti-mouse antibody as the primary and secondary antibodies, respectively, and detected by using enhanced chemiluminescence (Amersham Biosciences).

In vitro DNA replication assay. The SV40-based in vitro DNA replication assay was described previously (52) and utilized a pBluescript SK+ phagemid (Stratagene) containing a 90-bp SV40 origin region segment (positions 5186 to 32) subcloned into the BamHI and XhoI sites (pBS-ori). Reaction mixtures (25 μ l) contained the following: 40 mM HEPES (pH 7.5); 40 mM creatine phosphate; 7 mM MgCl₂; 0.5 mM DTT; 4 mM ATP; 200 μ M concentrations each of CTP, GTP, and UTP; 100 μ M concentrations each of dATP, dGTP, and dTTP; 40 μ M [α -³²P]dCTP (3,000 cpm/pmol; Perkin-Elmer Life Sciences); 1.25 μ g of creatine phosphokinase; 150 ng of pBS-ori; 100 μ g of AS65 protein fraction prepared from HeLa cells; 200 ng of RPA; 200 to 400 ng of the GST fusion proteins; and 500 ng of SV40 large T antigen. The reaction mixtures were first preincubated on ice for 30 min without the addition of plasmid DNA, deoxynucleoside triphosphates, ATP, and creatine phosphokinase. After the addition of the remaining factors, the complete reaction mixture was further incubated at 37°C for 2 h. The replication activity was determined by precipitating the high-molecular-weight DNA with trichloroacetic acid and quantitating the amount of incorporated radioactivity in the precipitate by liquid scintillation counting.

Immunoprecipitation and immunoblotting. Plated U2-OS cells were transfected with 1 μ g of specified expression plasmids by using Effectene transfection reagent (Qiagen). The transfection efficiencies of each construct were similar when visualized at 24 h posttransfection. When required, cells were either treated with 1 μ M CPT or 2.5 mM hydroxyurea or exposed to 10 Gy of ionizing radiation or 30 J of UV light m⁻². The immunoprecipitation reaction was carried out by using the IMMUNOCatcher kit (Cytosignal) according to the manufacturer's instructions. Immunoprecipitated proteins were separated by using SDS-10% PAGE and transferred to a nitrocellulose membrane (Schleicher & Schuell). After incubation with the appropriate primary antibody, the membrane incubated with an horseradish peroxidase-conjugated goat anti-mouse or anti-rabbit secondary antibody, and the presence of bound proteins was detected with ECLplus (Amersham Pharmacia Biotech). The following antibodies were used for both detection and immunoprecipitation: RPA2, mouse monoclonal antibody SSB34A (NeoMarkers); RPA1, mouse monoclonal antibody Ab-1; nucleolin, either the MS3 mouse monoclonal or the H-250 rabbit polyclonal antibody (Santa Cruz Biotechnology); GFP, rabbit polyclonal antibody (Molecular Probes); Myc, rabbit polyclonal antibody (Upstate Biotechnology); p53, DO-1 mouse monoclonal antibody (Santa Cruz Biotechnology); (pSer15)p53, rabbit polyclonal antibody (Cell Signaling Technology); and p21, mouse monoclonal antibody (BD Biosciences/Pharmingen).

Immunofluorescence microscopy. To prepare for imaging, U2-OS cells grown on fibronectin-coated coverslips (BD Biosciences) were treated as described previously (15). Cells were fixed for 20 min at room temperature with 4% (wt/vol) formaldehyde in PBS, permeabilized with 0.5% Triton X-100, rinsed with PBS, and then incubated with PBS containing 0.5% Nonidet P-40. Coverslips were incubated with 1:100 dilution of the appropriate primary antibody for 1 h at room temperature. After three rinses with PBS containing 0.5% Tween 20, coverslips were incubated for 1 h at room temperature with 1:100 dilution of Texas Red- or fluorescein isothiocyanate-conjugated secondary antibody (Jackson ImmunoResearch Laboratories). Coverslips were then rinsed three times with PBS containing 0.5% Tween 20 and mounted onto glass slides. Fluorescent signals were detected by using either epifluorescence or confocal microscopy.

FRET. U2-OS cells were grown and cotransfected with the appropriate YFP- and CFP-tagged expression constructs in 35-mm uncoated glass bottom cell culture dishes (MatTek). Live cell images were obtained with a Zeiss LSM510 Meta laser scanning confocal microscope with a Plan-Apochromat \times 63 objective lens and a 30-mW Argon laser set at 50% of total output. CFP as the donor channel was excited with a 458-nm laserline, and CFP fluorescence was collected with a band-pass filter of 475 to 525 nm. YFP, the acceptor channel, was excited at 514 nm, and YFP emission was collected with a long-pass filter of 530 nm. The

fluorescence resonance energy transfer (FRET) channel consisted of CFP excited at 458 nm and YFP fluorescence collected with a long-pass filter of 530 nm. Photobleaching was performed with the 514-nm laser line set at 100% power with an average bleach time of 5 s. Specific regions of interest (ROIs) were chosen, and positive FRET was determined graphically based on the decrease of YFP signal, and the subsequent increase in the CFP fluorescence postbleaching. Although transfection of any combination of YFP-RPA2 and CFP-nucleolin (or nucleolin derivative) did not have notable deleterious effects on cell viability, only cells with a normal appearance and relatively low expression levels were tested.

BrdU incorporation assay and FACS. U2-OS cells were plated at 30% confluency in 60-mm dishes. Plates were mock transfected, transfected with 1 μ g of the Myc tag (empty) vector, or 1 μ g of the appropriate N-terminal Myc-tagged nucleolin expression construct. At 24 h posttransfection, the cells were incubated for 20 min with 10 μ M bromodeoxyuridine (BrdU). Cells were then washed twice with ice-cold PBS and collected by centrifugation at $180 \times g$ for 5 min at 4°C. Pelleted cells were carefully resuspended into 300 μ l of 4% (wt/vol) formaldehyde in PBS, fixed for 15 min at room temperature, and washed with PBS twice. Cells were then permeabilized for 15 min on ice with PBS containing 0.2% (vol/vol) Triton X-100 and 1% (wt/vol) bovine serum albumin (BSA), washed once with PBS, and then treated with PBS containing 0.25 mg of DNase/ml for 1 h at 37°C. Cells were incubated with 100 μ l of PBS containing rat anti-BrdU (Harlan Sera-Lab) and rabbit anti-Myc (Upstate Biotechnology) polyclonal antibodies and 2% (wt/vol) BSA for 40 min at 37°C. Cells were washed twice with PBS and incubated for 40 min at room temperature with 100 μ l of PBS containing anti-rabbit phycoerythrin-conjugated and anti-rat fluorescein isothiocyanate-conjugated antibodies (Jackson Laboratories) and 2% BSA. After preincubation of cells with 4 mM sodium citrate, 30 U of RNase A/ml, and 0.1% (vol/vol) Triton X-100 for 10 min at 37°C, the DNA was stained with 7-aminoactinomycin D (Sigma), and the cells were subjected to fluorescence-activated cell sorting (FACS) analysis.

[³H]thymidine uptake assay. U2-OS cells were plated into 24-well tissue culture plates in complete McCoy's media containing 10% fetal bovine serum (FBS). The cells were transfected with plasmids (100 ng) expressing one of the following proteins: Myc-tag, Myc-nucleolin TM, or Myc-nucleolin GAR. As indicated, cells were also cotransfected with various amounts of a Myc-RPA2 expression vector. After 6 to 8 h, the medium was changed to a low serum (0.1% FBS) condition and further incubated for 18 h. After recovery in complete medium for 8 to 10 h, the cells were incubated with [³H]thymidine (1 μ Ci/well) for 10 h. Cells were then washed with ice-cold PBS extensively and treated with 5% trichloroacetic acid for 30 min on ice. After further washes with ice-cold PBS, cells were solubilized in 0.5 N NaOH–0.5% (wt/vol) SDS and harvested, and the amount of incorporated radiolabel was determined with a scintillation counter.

RESULTS

Genotoxic stress induces RPA-nucleolin complex formation.

We previously showed that heat shock led to a significant increase in complex formation between endogenous nucleolin and RPA (13). We therefore determined whether this increase was specific for heat shock or a more general effect in response to stress. Human U2-OS osteosarcoma cells were treated with the radiomimetic agent camptothecin (CPT) to cause genotoxic stress (Fig. 1A). Although RPA-nucleolin complex formation was not found in control cells, these complexes were readily detected after CPT treatment with a transient increase in the level of complex formation noted. We estimate that ~5 to 10% of the RPA pool is coimmunoprecipitated with nucleolin at the peak level of complex formation, although this value would be an underestimate if the complex were transient or unstable under immunoprecipitation conditions. A similar induction of nucleolin-RPA complex formation was observed after treatment with hydroxyurea (to cause replicative stress; Fig. 1B) or exposure to ionizing radiation (10 Gy; Fig. 1C). Nucleolin was not seen to form a complex with RPA after exposure to UV radiation (Fig. 1D) similar to previous observations finding a lack of induced nucleolin-p53 complex and nucleolin relocalization after UV irradiation (14). Induction of

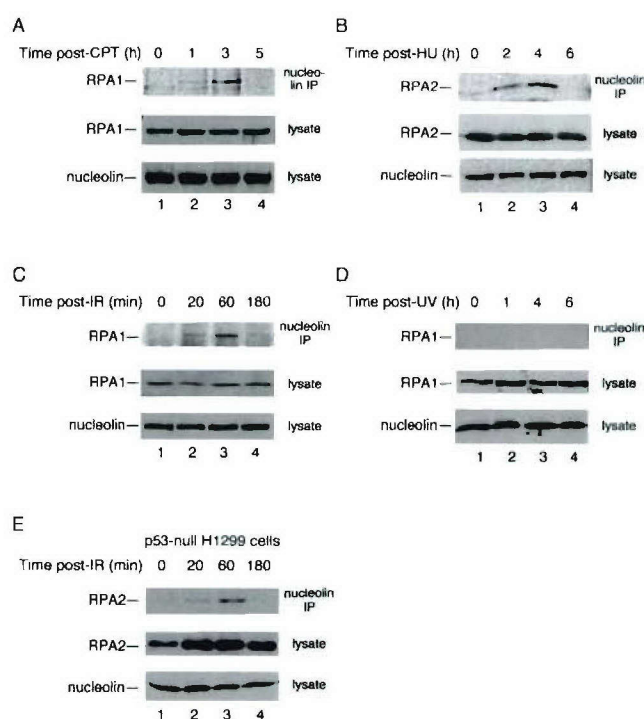


FIG. 1. Nucleolin-RPA complex formation is induced after genotoxic stress. Cell lysates were prepared from p53-positive U2-OS cells (A to D) and p53-null H1299 cells (E) at various times after exposure to various stress treatments as follows: 1 μ M CPT for 1 h (A), 2.5 mM hydroxyurea (HU) for 1 h (B), 10 Gy of ionizing radiation (IR) (C and E), and UV irradiation with a single dose of 30 J m⁻² (D). After each time point, nucleolin was immunoprecipitated from the lysate with a mouse monoclonal antibody to nucleolin. The precipitate was subjected to SDS-PAGE and immunoblotted for RPA with either an anti-RPA1 or anti-RPA2 antibody (as indicated). As loading controls, aliquots of the lysates were subjected to immunoblotting with anti-nucleolin, anti-RPA1, or anti-RPA2 antibodies.

nucleolin-RPA complex formation was observed in p53-null H1299 cells after CPT treatment (Fig. 1E). Therefore, although nucleolin relocalization from the nucleolus to the nucleoplasm is p53 dependent (14), this dependence does not extend to nucleolin-RPA complex formation. Note that previous studies from our laboratory indicated that complex formation is not mediated by the presence of DNA and can also be detected by precipitation of RPA rather than nucleolin (13). In general, enhanced nucleolin-RPA complex formation is not restricted to heat shock but is also detected after genotoxic stress.

RPA interacts with the nucleolin GAR domain in vitro. To better characterize the nucleolin-RPA complex, the region on human nucleolin that interacts with RPA was identified by far-Western analysis. Full-length nucleolin or nucleolin truncation mutants were expressed as GST-tagged fusion proteins in yeast and purified. The proteins tested were full-length nucleolin (termed nucleolin FL; aa 1 to 707), the nucleolin N terminus (NT; aa 1 to 323), the C terminus (CT; aa 323 to 707), the N terminus and the first RBD (NT/RBD1; aa 1 to 390), the N terminus and the RBD region (NT/RBD1-4; aa 1 to 648), and the extreme C-terminal GAR domain (GAR; aa 645 to 707) (Fig. 2A). Note that the NT/RBD1-4 construct lacks only

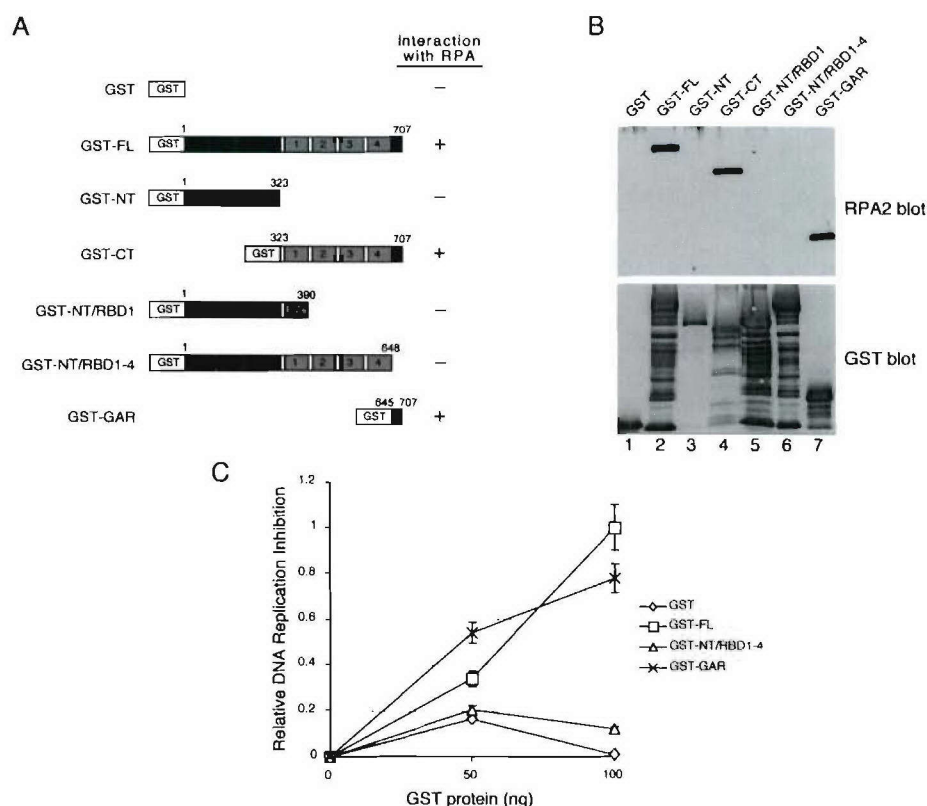


FIG. 2. The nucleolin RPA-binding domain inhibits SV40 DNA replication in vitro. (A) Schematic showing GST-tagged nucleolin and nucleolin mutant proteins as follows: full length (FL), amino terminus (NT), carboxy terminus (CT), amino terminus including the first RBD (NT/RBD1), the GAR deletion mutant (NT/RBD1-4), and only the C-terminal GAR domain (GAR). For each construct, the N-terminal acidic domain is indicated in dark gray; each of the four RBDs have light gray shading and are numbered, and the GAR domain is shown in black. (B) Far-Western analysis of the nucleolin-RPA interaction. Equivalent amounts (500 ng) of nucleolin FL (lane 2), NT (lane 3), CT (lane 4), NT/RBD1 (lane 5), NT/RBD1-4 (lane 6), and GAR (lane 7), with each containing an N-terminal GST tag, were separated by SDS-PAGE. GST alone was also electrophoresed as a control (lane 1). After transfer to a nitrocellulose membrane, the membrane was probed with purified RPA (0.2 μ g/ml) (upper panel, lanes 1 to 7). The binding of RPA was visualized by using an RPA2 antibody. To visualize GST-tagged proteins, the membrane was stripped and subjected to immunoblot analysis with a rabbit anti-GST antibody (lower panel, lanes 1 to 7). (C) An SV40 *ori*-containing plasmid (180 ng) was incubated with AS65 extract (100 μ g), T antigen (750 ng), RPA (200 ng), and purified GST-tagged nucleolin proteins (as indicated) for 2 h at 37°C (52). Both FL (□) and GAR (×) GST-tagged nucleolin proteins are proficient in inhibiting SV40 DNA replication in vitro, whereas the NT/RBD1-4 (△) GST-tagged nucleolin protein and GST alone (◇) are not. Replication activity was determined by precipitating the reaction mixtures with trichloroacetic acid and determining the amount of 32 P in the precipitate by scintillation counting. The data was plotted as the relative DNA replication inhibition compared to that determined by using 100 ng of GST-FL. The maximum degree of inhibition was to 68% that of control levels.

the GAR region. After SDS-PAGE and transfer to a nitrocellulose membrane, the immobilized proteins were renatured and incubated with purified RPA to allow for complex formation. The interaction between the fusion proteins and RPA was resolved by Western blotting with an RPA2 antibody (Fig. 2B, upper panel).

Nucleolin FL formed a complex with RPA (Fig. 2B, upper panel, lane 2), whereas GST alone did not (lane 1). Although no interaction with nucleolin NT was detected (lane 3), RPA bound to the C-terminal half of the protein (lane 4). Longer constructs of nucleolin NT that also contained the first RBD (NT/RBD1; lane 5) or the complete RBD domain (NT/RBD1-4; lane 6) were unable to rescue nucleolin-RPA complex formation. In contrast, RPA effectively bound the 63-aa GAR peptide lacking all other nucleolin domains. Stripping the blot and reprobing the membrane with anti-GST antibodies indicated that similar amounts of each GST fusion protein were loaded on the membrane (Fig. 2B, lower panel). These

data demonstrate that the nucleolin GAR domain is necessary and sufficient for RPA binding in vitro. A fraction of each GST construct was invariably present in a degraded form but only the largest FL, CT, or GAR species was observed to bind RPA. The GST constructs are degraded from the C-terminal end because N-terminal deletions would prevent reactivity to the anti-GST antibody (i.e., the GST is located on the N terminus of each construct). We therefore suggest that the extreme C terminus of the GAR domain is required for significant RPA binding.

Effect of the GAR domain on SV40 DNA replication in vitro.

We previously showed that SV40 DNA replication in vitro was inhibited by the addition of nucleolin, purified from human cells, which interfered with RPA action (13). Because our data indicate that the nucleolin GAR domain interacts with RPA, we similarly tested the effect of this peptide on SV40 DNA replication. GST-tagged nucleolin or nucleolin derivatives were purified, and titrated into a T-antigen-dependent SV40

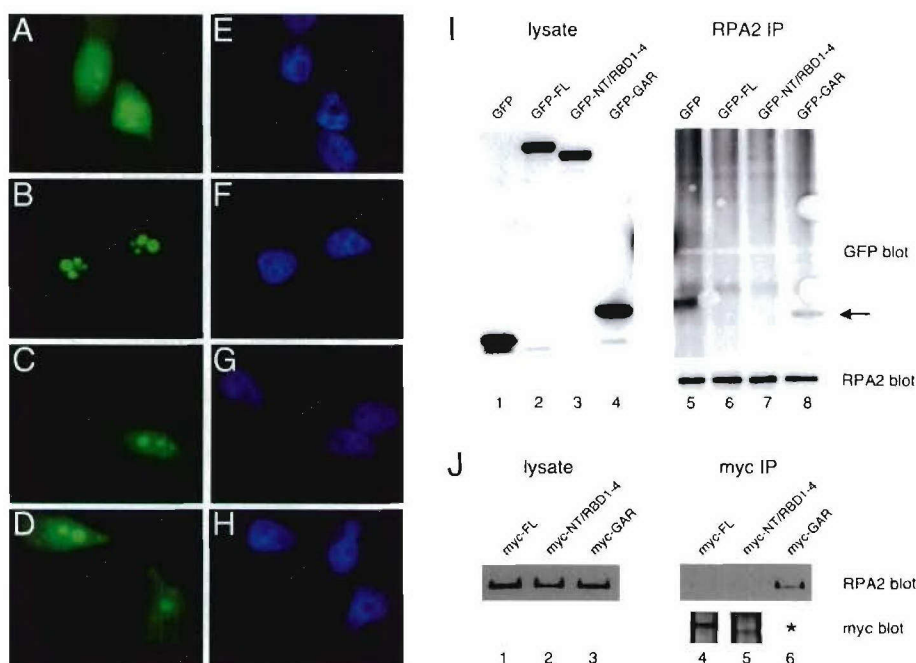


FIG. 3. Complex formation between the nucleolin GAR domain and RPA in vivo. (A to H) U2-OS cells were transfected with GFP alone (A and E) or the GFP-tagged nucleolin derivatives FL (B and F), NT/RBD1-4 (C and G), or GAR (D and H). At 24 h posttransfection, cells were fixed by treatment with 4% (wt/vol) formaldehyde for 30 min at room temperature and then imaged by epifluorescence microscopy. The staining patterns of the various GFP constructs are shown (A to D), as are images of the same cells stained with DAPI (4',6'-diamidino-2-phenylindole) (E to H). (I) Immunoprecipitation of endogenous RPA protein in U2-OS cells expressing GFP-tagged nucleolin FL (lane 6), NT/RBD1-4 (lane 7), or GAR (lane 8) or GFP alone (lane 5). The coprecipitation of the expressed GFP-tagged proteins with RPA is shown in the GFP blot. The arrow points to the coprecipitation of GFP-tagged GAR (lane 8). Corresponding lysates were assayed for similar levels of protein expression by blotting for GFP (lanes 1 to 4), whereas equivalent immunoprecipitation of RPA was verified by blotting for RPA2 (right side, lower panel). (J) Reverse immunoprecipitation experiment showing the coprecipitation of endogenous RPA in U2-OS cells expressing Myc-tagged nucleolin FL (lane 4), NT/RBD1-4 (lane 5), and GAR (lane 6). Myc-tagged nucleolin proteins were immunoprecipitated, and coprecipitation of RPA was determined by blotting for RPA2 (upper panel). The immunoprecipitated Myc-tagged proteins are also shown (lower panel). The asterisk indicates that the Myc-tagged GAR could not be detected because of its small size (5 kDa), preventing binding to nitrocellulose membrane during the transfer step. However, similar levels of myc staining were observed for the three constructs when transfected cells were examined by immunofluorescence microscopy (data not shown). The lysates were also blotted for RPA2 as a control (lanes 1 to 3).

DNA replication reaction (Fig. 2C). In reactions containing nucleolin FL or GAR, DNA synthesis was significantly inhibited as a function of the amount of nucleolin protein added. In contrast, no obvious inhibition was seen by addition of nucleolin NT/RBD1-4 or GST. Thus, nucleolin molecules that are capable of binding RPA also inhibit DNA replication in vitro.

Stress-dependent formation of the nucleolin FL-RPA complex. We examined the interaction of nucleolin and the nucleolin mutants with RPA in vivo. Because the cellular localization of nucleolin may be a determinant affecting its interaction with RPA (13), we first examined the localization of the different nucleolin derivatives. GFP-tagged nucleolin FL, NT/RBD1-4, and GAR were expressed in U2-OS cells, and the localization of the fusion proteins captured by indirect immunofluorescence microscopy. Nucleolin FL localized exclusively to nucleolar regions (Fig. 3B), as determined by colocalization with endogenous nucleolin and upstream binding factor (necessary for RNA polymerase I-mediated transcription of rRNA [27]) (data not shown). The NT/RBD1-4 and GAR proteins had primary localization in the nucleolus (Fig. 3C and D, respectively), although the level of nucleolar staining was higher for the NT/RBD1-4 mutant. A significant fraction of each mutant protein pool was located in the nucleoplasm, and both mutants

showed a weak but clear cytoplasmic signal. As expected, GFP alone was localized throughout the cell (Fig. 3A). These data are consistent with previous findings that the nucleolin RBD and GAR domains each contribute to nucleolar localization (12, 28, 40, 47).

The ability of various GFP-tagged nucleolin proteins to associate with endogenous RPA in vivo was tested by coimmunoprecipitation assays. RPA coprecipitated with the GAR domain but did not associate with the NT/RBD1-4 mutant (Fig. 3I, lanes 8 and 7, respectively). Nucleolin FL did not significantly complex with RPA under these nonstress conditions (lane 6) although, because of the higher background in the upper regions of the blot, we cannot rule out a low level of complex formation. To rule out the possibility that the large GFP moiety may sterically block nucleolin complex formation with RPA, reverse immunoprecipitation experiments were repeated with nucleolin tagged with a smaller Myc tag (Fig. 3J). Test of the Myc-tagged nucleolin proteins showed that only nucleolin GAR formed detectable complexes with endogenous RPA (lane 6), whereas nucleolin FL (lane 4) and NT/RBD1-4 (lane 5) did not. Note that detection of Myc-GAR in cell lysates by Western blotting was problematic because of poor association of this 5-kDa species with the nitrocellulose mem-

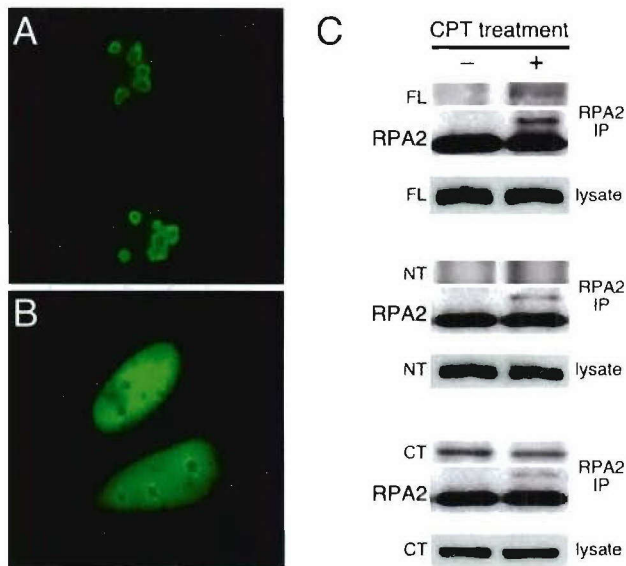


FIG. 4. Complex formation between nucleolin FL and endogenous RPA stimulated by genotoxic stress. (A and B) The cellular localization of GFP-tagged nucleolin FL expressed in U2-OS cells is shown in the absence of CPT treatment (A) and after treatment with 1 μ M CPT for 1 h and a 1-h recovery period (B). (C) Immunoprecipitation of endogenous RPA protein with RPA2 antibody in U2-OS cells expressing GFP-tagged nucleolin FL (top set), nucleolin NT (second set), or nucleolin CT (third set). Coprecipitation of the nucleolin proteins was examined in the absence of CPT treatment (–) and 2 h after treatment with 1 μ M CPT for 1 h (+) (upper panels). The same blot was reprobed with RPA2 antibody as a control for RPA immunoprecipitation (middle panels). Lysates were assayed for equivalent expression of GFP fusion proteins by probing with an anti-GFP antibody (lower panels).

brane. However, the levels of Myc-tagged nucleolin FL, NT/RBD1-4, and GAR were comparable when examined in parallel experiments by immunofluorescence microscopy, and their cellular localizations were similar to those observed for the analogous GFP fusion proteins (data not shown). In sum, these data indicate that the nucleolin GAR domain is sufficient to support complex formation with RPA *in vivo*. Concerning the lack of association between nucleolin FL and RPA *in vivo*, although in apparent contradiction with the results of the far Western analysis *in vitro* (above), these results are consistent with those showing a lack of complex formation between endogenous nucleolin and RPA in nonstressed cells (see Fig. 1, zero time points).

We next examined the effect of CPT treatment on GFP-tagged nucleolin FL localization and on the interaction of RPA with nucleolin FL and the nucleolin derivatives. Although nucleolin FL localized to the nucleolus in the absence of stress (Fig. 4A [see also Fig. 3B above]), incubation with CPT caused a significant fraction of the nucleolin FL pool to move to the nucleoplasm (Fig. 4B), similar to the behavior of endogenous nucleolin (13). In testing the interactions, RPA was observed to associate with nucleolin FL but only after CPT treatment (Fig. 4C, upper panel). In contrast, the NT construct lacking the GAR domain did not form a detectable complex with RPA irrespective of stress (Fig. 4C, middle panel). The CT construct that contains the GAR domain coprecipitated with RPA both

in the presence of CPT and in its absence, thus revealing a constitutive interaction (Fig. 4C, lower panel). The localizations of these truncated proteins were not affected by prior CPT treatment (data not shown). These data indicate that although the presence of the GAR is necessary to support detectable complex formation with RPA *in vivo*, detectable interaction of RPA with the full-length nucleolin also requires stress conditions such as caused by CPT treatment.

Nucleolin TM is able to mimic endogenous nucleolin under conditions of stress. To examine the question of whether nucleolin localization regulates nucleolin-RPA complex formation *in vivo*, we generated a nucleolin mutant with altered cellular localization. Preliminary studies by our laboratory indicate that the nucleolin phosphorylation pattern at CK2 sites changes in response to stress (K. Kim, M. Daras, and J. A. Borowiec, unpublished data). The three putative CK2 sites at positions S33, S187, and S209 were therefore converted to nonphosphorylatable alanines to generate nucleolin TM (for triple mutant). The localization of GFP-tagged nucleolin TM was examined in untreated U2-OS cells or in cells treated with CPT. Interestingly, nucleolin TM was found to have significant localization in the nucleoplasm in the absence of DNA damage (Fig. 5C) and resembled the localization of nucleolin FL in cells treated with CPT (Fig. 5B). After exposure of the cells to CPT, nucleolin TM was seen to have an even greater fraction of signal arising from the nucleoplasm (Fig. 5D). In testing interactions, the coprecipitation of nucleolin TM with RPA was found to be constitutive and independent of prior CPT treatment (Fig. 5E, lanes 3 and 4), in contrast to nucleolin FL (lanes 1 and 2). Therefore, a nucleolin mutant with a significant degree of nucleoplasmic localization in nonstressed cells also has a constitutive interaction with RPA.

Nucleolin-RPA complex formation examined by FRET. To examine whether a nucleoplasmic localization of nucleolin assists complex formation with RPA, we used FRET to determine the cellular site(s) of interaction. The middle subunit of heterotrimeric RPA (RPA2) was expressed as a YFP fusion, whereas nucleolin and the nucleolin derivatives were coupled to CFP. Previous studies testing GFP-RPA2 indicate that it behaves similarly to the endogenous RPA2 subunit, including the association with replication centers (50, 52). In cells transfected with both YFP-RPA2 and CFP-nucleolin FL, CPT treatment caused nucleolin relocalization (Fig. 6D) as seen above while having little notable effect on YFP-RPA2 (compare Fig. 6B and E). Although no significant FRET signal was detected in the absence of CPT treatment (Fig. 6C), a robust FRET signal was seen when these same doubly transfected cells were analyzed after CPT treatment (Fig. 6F). Because FRET is subject to artifactual detection due to CFP signal bleedthrough into the YFP channel, we performed acceptor photobleaching in which bleach of the YFP fluorescence stimulates the emission from CFP (Fig. 6G) (33). Cells that were either mock treated or treated with CPT were analyzed by using ROIs located in either the nucleolus or the nucleoplasm, and the average CFP signals from these experiments is shown. Consistent with the FRET images, no significant photobleach-dependent stimulation of the CFP signal was observed either in the nucleolus or the nucleoplasm without CPT. When cells were treated with CPT, a robust increase in the CFP signal was detected in the nucleoplasm and the nucleolus after photo-

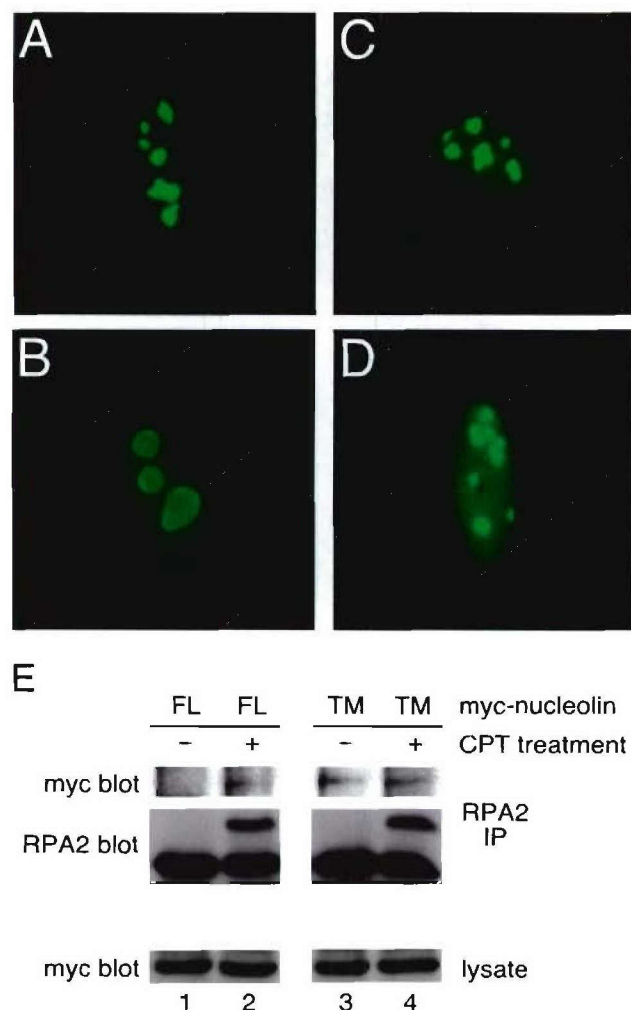


FIG. 5. The nucleolin TM mutant constitutively interacts with endogenous RPA. The subcellular localization of nucleolin FL (A and B) and nucleolin TM (C and D) in U2-OS cells was determined. At 24 h posttransfection, cells were either mock treated (A and C) or examined 2 h after treatment with 1 μ M CPT for 1 h (B and D). Cells were prepared for epifluorescence microscopy as described in Materials and Methods. (E) The coprecipitation of Myc-tagged nucleolin FL and TM with endogenous RPA in U2-OS cells was examined 24 h posttransfection either with or without prior CPT treatment (as described above). Endogenous RPA was precipitated with anti-RPA2 antibody, and the coprecipitation of Myc-tagged nucleolin FL or TM was visualized by Western blotting with an anti-Myc antibody (9E10).

bleaching. These FRET signals were quantitated and normalized against that found by nucleolin FL and RPA in the nucleoplasm after CPT treatment (Table 1).

We next performed similar FRET analyses with the nucleolin GAR and NT/RBD1-4 domains. Both nonstressed cells and cells treated with CPT were examined. The average normalized change in the CFP signal after YFP photobleaching is provided (Table 1). From these data, we found that the GAR domain of nucleolin interacts with RPA irrespective of the presence of CPT and equally well in the nucleolus and the nucleoplasm. Similarly, the nucleolin TM mutant showed a very strong FRET signal in both the nucleolus and the nucleoplasm in a CPT-independent fashion. In contrast, the NT-

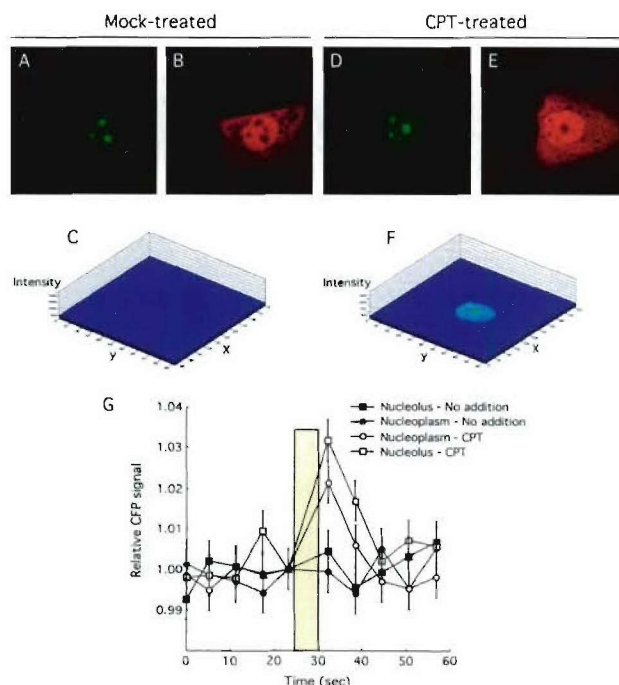


FIG. 6. Nucleolin FL-RPA complex formation occurs both in the nucleolus and in the nucleoplasm after stress. (A to F) U2-OS cells were transfected with CFP-nucleolin and YFP-RPA2 and either mock treated or treated with 1 μ M CPT for 1.5 h prior to imaging. Cells were then imaged to capture the CFP-nucleolin signal (A and D), the YFP-RPA2 signal (B and E), or the FRET signal obtained by transfer of the CFP emission energy to YFP (C and F). The FRET images are shown with a pseudo three-dimensional display with the intensity of staining given on the z axis. (G) Acceptor photobleaching analysis of nucleolin-RPA complex formation. The CFP signal from various (ca. 10 to 15) ROIs was determined at 6-s intervals. After the fifth scan, the YFP fluor was photobleached at 514 nm with an average bleach time of 5 s. An increase in the CFP after photobleaching of the YFP signal is indicative of bona fide FRET (33).

RBD construct was not found to interact with RPA in either the nucleolus or the nucleoplasm and without apparent effect from the CPT. We note that these latter data are subject to the standard concerns of false-negative FRET results due to potential improper orientation of the two fluorescent tags. As a positive control, we show a significant FRET signal from the H-Ras 61L with the Ras-binding domain of Raf1 in the cytoplasm (4). As expected, no FRET signal arises from cells expressing the H-Ras 61L and RPA2 or in cells expressing CFP-nucleolin alone. We also show that heat shock induces a stronger FRET signal compared to CPT treatment, which parallels our previous immunoprecipitation findings that heat shock also greatly stimulated the nucleolin-RPA complex formation (13). It is interesting that heat shock also has a much greater effect on chromosomal DNA replication (an approximately 70 to 85% reduction [see, for example, references 13 and 55] compared to genotoxic stress (an approximately 50% reduction [see, for example, reference 42]). In sum, along with confirming that the nucleolin FL-RPA interaction is stress dependent, these data also indicate that nucleolin-RPA complex formation is stimulated in both the nucleolus and the nucleoplasm after genotoxic stress.

TABLE 1. Effect of stress and cellular localization on FRET intensity

Constructs transfected ^a	Location	Stress status	Relative increase in CFP signal after addition of YFP bleach (%)
Nucleolin FL/RPA2	Nucleoplasm	None	<15
Nucleolin FL/RPA2	Nucleolus	None	<15
Nucleolin FL/RPA2	Nucleoplasm	CPT	100
Nucleolin FL/RPA2	Nucleolus	CPT	68
Nucleolin FL/RPA2	Nucleoplasm	HS	164
Nucleolin FL/RPA2	Nucleolus	HS	<15
Nucleolin GAR/RPA2	Nucleoplasm	None	128
Nucleolin GAR/RPA2	Nucleolus	None	101
Nucleolin GAR/RPA2	Nucleoplasm	CPT	91
Nucleolin GAR/RPA2	Nucleolus	CPT	89
Nucleolin TM/RPA2	Nucleoplasm	None	134
Nucleolin TM/RPA2	Nucleolus	None	170
Nucleolin TM/RPA2	Nucleoplasm	CPT	163
Nucleolin TM/RPA2	Nucleolus	CPT	150
Nucleolin RBD/RPA2	Nucleoplasm or nucleolus	None	<15
Nucleolin RBD/RPA2	Nucleoplasm or nucleolus	CPT	<15
Nucleolin FL only	Nucleoplasm or nucleolus	CPT	<15
H-Ras61L/RPA2	Nucleoplasm or nucleolus	None	<15
H-Ras61L/Ras-binding domain	Cytoplasm	None	42

^a Acceptor photobleaching analyses were carried out on U2-OS cells transfected with various expression constructs. As indicated, cells were either mock treated, stressed with 1 μ M CPT for 1.5 h, or subjected to a 44°C heat shock (HS) for 15 min prior to analysis. The YFP in each examined ROI was subjected to photobleaching, and the change in intensity of the CFP signal was quantitated. After the averaging of data from >10 ROI for each condition, these data were normalized against the increase in CFP signal detected for CFP-nucleolin FL and YFP-RPA2 in the nucleoplasm after CPT treatment. All nucleolin derivatives and H-Ras61L were expressed with N-terminal CFP tags; RPA2 contained an N-terminal YFP tag, whereas the Ras-binding domain was tagged with YFP on C terminus.

Cell cycle arrest upon overexpression with either nucleolin GAR or TM. We found previously that heat shock mobilizes nucleolin to move to the nucleoplasm, whereupon it binds RPA at sites distinct from the DNA replication centers (13). These data predict that expression of nucleolin derivatives that bind RPA in nonstressed cells will cause a G₁/S arrest. The effect of nucleolin TM and GAR expression on cell cycle progression were therefore investigated by FACS. Both the non-transfected control and the vector control showed a similar distribution, indicating that transfection alone did not inhibit cell cycle transit (Fig. 7A). Expression of nucleolin FL led to only a slight increase in G₁-phase cells. However, much more significant effects were observed in cells transfected with nucleolin TM or GAR. The expression of nucleolin GAR resulted in an increase in the G₁ population to 52% of cells compared to 36% of vector-transfected cells. We also detected a decrease in S-phase cells from 39% in vector-transfected cells to 23% in GAR-transfected cells. Expression of nucleolin TM had a similar influence on cell cycle progression with G₁- and S-phase cells contributing 53 and 25%, respectively, of the total cell pool. In each case, the fraction of G₂ cells remained constant. Thus, the expression of nucleolin GAR or TM was sufficient to elicit an arrest in the cell cycle, leading to the accumulation of cells in G₁ and a decrease in cells in S phase. We note that the overall degree of replication inhibition in the GAR- or TM-transfected cells (a >40% decrease) is similar to that observed after ionizing irradiation (42).

DNA replication inhibition overcome by overexpression of RPA2. If the inhibition of DNA replication by nucleolin GAR or TM were truly mediated through RPA, then overexpression of heterotrimeric RPA might overcome this inhibition of DNA synthesis. A method of increasing RPA levels arose from our finding that changes in RPA2 levels have coordinate effects on

the level of the RPA1 subunit. That is, a decrease in RPA2 levels due to the use of RNAi leads to a corresponding decrease in RPA1 levels (D. Curanovic and J. A. Borowiec, unpublished results), a finding also recently reported by others (16). Similarly, overexpression of Myc-RPA2 caused a parallel increase in the level of RPA1 protein, when examined either by Western blotting (Fig. 7B) or immunofluorescence microscopy (data not shown). Since stable association of the RPA1 and RPA2 subunits requires the smallest RPA3 subunit (which available antibodies only poorly detect), these data indicate that changes in the level of RPA2 regulate the level of RPA in cells. Overexpression of RPA2 thereby provides a method to more directly examine the nucleolin-RPA interplay in inhibiting chromosomal DNA replication.

To test this method, U2-OS cells were transfected with either nucleolin GAR or TM, and the level of DNA replication was measured by determining thymidine incorporation (Fig. 7C). Corroborating the results of the FACS analysis, expression of either nucleolin construct inhibited DNA synthesis by ca. 50%. In parallel reactions, these cells were cotransfected with increasing levels of RPA2. We observed that the degree of replication inhibition caused either by nucleolin GAR or TM expression was progressively reduced by transfection of the Myc-RPA2 expression vector. The stimulatory effect of RPA2 overexpression was somewhat more pronounced in nucleolin TM-transfected cells compared to GAR-transfected cells, for unknown reasons. Transfecting higher levels of RPA2 vector (i.e., 100 ng) caused some toxic effects on cell viability (data not shown). These data strongly indicate that nucleolin can inhibit DNA synthesis by direct interaction with RPA.

Nucleolin GAR expression does not activate p53. It is possible that the expression of the GAR domain causes a cellular stress response and therefore only inhibits cell cycle progres-

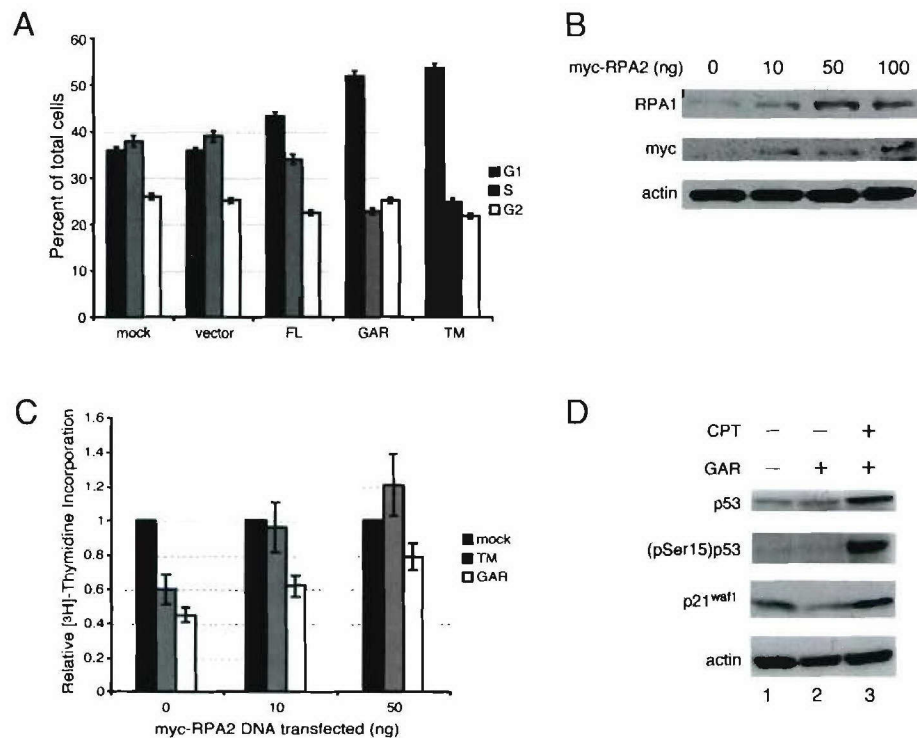


FIG. 7. RPA overexpression rescues the inhibition of DNA replication caused by nucleolin GAR or TM. (A) Cell cycle distribution of U2-OS cells transfected with nucleolin and nucleolin mutants. FACS analysis was performed 24 h after transfection with N-terminal Myc-tagged nucleolin constructs. The DNA content was quantitated by using the DNA intercalating agent 7-aminoactinomycin D, and cells in S phase were identified by determining BrdU incorporation. (B) Overexpression of myc-tagged RPA2 leads to a corresponding increase in the level of RPA1. Lysates from U2-OS cells transfected with various amounts of myc-tagged RPA2 (10, 50, and 100 ng) were analyzed by Western blotting for the level of RPA1 (first panel). Myc-tagged RPA2 expression (second panel) and β -actin (third panel) are shown as transfection and loading controls, respectively. (C) [3 H]thymidine incorporation assay shows that expression of Myc-tagged RPA2 (leading to higher levels of RPA) can rescue the reduction in DNA synthesis caused by expression of nucleolin TM or nucleolin GAR. Each set of U2-OS cells (mock transfected, nucleolin TM transfected, and nucleolin GAR transfected) were cotransfected with 0, 10, or 50 ng of Myc-tagged RPA2. The data are plotted showing the relative amounts of [3 H]thymidine incorporation compared to the mock-treated cells at each level of Myc-RPA2 transfected. Expression of Myc-RPA2 alone slightly inhibited cellular DNA synthesis with transfection of 10 ng of the expression construct causing a 16% reduction in [3 H]thymidine incorporation. This resulted from inhibitory effects of pEF6/Myc vector transfection rather than expression of Myc-RPA2 per se (data not shown). (D) The nucleolin-mediated checkpoint response does not involve p53 activation. Lysates from U2-OS cells expressing GFP-tagged nucleolin GAR (lanes 2 and 3) or GFP alone (lane 1) were examined after mock treatment (lanes 1 and 2) or 2 h posttreatment with 1 μ M CPT for 1 h (lane 3). Lysates were analyzed by Western blotting for total p53 levels (top panel), p53 phosphorylation at serine 15 (second panel), p21^{waf1}, and the loading control, β -actin.

sion indirectly. As a test of this possibility, we examined the effect of GAR expression on p53 activation in U2-OS cells (which express wild-type p53). Expression of nucleolin GAR did not increase p53 levels (Fig. 7D, upper panel) or the level of p53 phosphorylated on Ser15, a site modified by the ATM and ATR kinases in response to genotoxic stress (49, 51). The lack of Ser15 phosphorylation demonstrates that p53 and, indirectly, ATM and ATR do not become activated in response to GAR expression (Fig. 7D, second panel). Aliquots of these lysates were probed for the presence of p21^{waf1}, a key stress-induced inhibitor of cyclin-dependent kinases whose expression results in a G₁/S arrest. No changes in the level of p21^{waf1} were detected in response to GAR expression (Fig. 7D, third panel). In contrast, treatment of cells with CPT was found to simultaneously stimulate the levels of p53, (pSer15)p53, and p21^{waf1}. The block in cell cycle progression caused by expression of nucleolin GAR is therefore unrelated to p53 activation, induction of p21, or, likely, activation of ATM or ATR. In-

stead, our data indicate that nucleolin can itself inhibit DNA replication by binding to RPA and inhibiting RPA activity.

DISCUSSION

In response to genotoxic insult and other stress conditions, eukaryotic cells in S phase use multiple mechanisms to reduce the level of ongoing DNA replication and thereby minimize the detrimental repercussions to the genome. Certain stress response pathways inhibit S-phase kinase complexes Cdk2/cyclin E (10, 19) and Cdc7/Dbf4 (11) whose activities are necessary to allow an origin of replication to fire. Another route apparently mediating the S-phase checkpoint targets the Mre11 recombinational DNA repair complex (43). In contrast, the pathway that we identify involves the inhibition of an essential DNA replication factor, RPA, by stress-dependent complex formation with nucleolin. In this pathway, our data indicate that nucleolin becomes activated in response to stress,

leading to heightened complex formation in both the nucleolus and the nucleoplasm. This induced nucleolin-RPA complex can block cellular transit through the G₁/S boundary and inhibit DNA replication during S phase. Furthermore, the nucleolin-mediated inhibition can be diminished by heightened expression of RPA.

What is the mechanism by which nucleolin inhibits cell cycle progression? We find that GST-tagged nucleolin FL and the GAR domain each can inhibit SV40 DNA replication *in vitro*, recapitulating similar inhibitory effects that were observed when endogenous nucleolin purified from human cells was tested (13). Although our studies did not find an inhibitory effect of nucleolin on RPA binding to single-stranded DNA, we do find that nucleolin can inhibit the binding of RPA to duplex molecules containing a central nonpaired region (data not shown). Such data suggest that the nucleolin-RPA complex is selectively inhibitory to the initiation stages of replication. However, we have recently presented data indicating that RPA does not randomly bind to single-stranded DNA at a chromosomal DNA replication fork but is instead actively loaded by a component of the replication machinery (52). Thus, complex formation with nucleolin has the potential to prevent RPA from productive loading onto single-stranded DNA at a replication fork *in vivo*. Both of these processes could inhibit DNA replication *in vivo* and cause a reduction in DNA synthesis. Overall, our data indicate that a direct interaction between the GAR domain of nucleolin and RPA is sufficient for replication inhibition *in vivo*.

Our data lead to the model that genotoxic stress activates nucleolin, such that the GAR domain becomes exposed for complex formation with RPA. In support of this model, consider the following data. First, although the GAR domain is required to bind RPA, nucleolin FL also requires stress conditions to bind RPA. Second, the nucleolin TM molecule that constitutively binds RPA was mutated at three N-terminal positions, whereas the RPA-interacting GAR domain is located on the extreme C terminus of nucleolin. Third, nucleolin relocalization to the nucleoplasm, although an outcome of genotoxic stress and heat shock, is not required for RPA complex formation because our FRET data show interaction in the nucleolus, as well as in the nucleoplasm. Fourth, a requirement for changes in RPA modification does not appear to be required as the GAR domain binds RPA in a stress-independent fashion. Along these same lines, preliminary evidence obtained from test of a hyperphosphorylation mimic of RPA (RPA₂₁) (52) showed no significant effects on nucleolin complex formation compared to RPA_{2wt} (data not shown). We postulate that changes in nucleolin modification promote conformational changes which remove steric constraints preventing RPA complex formation. Although expression of nucleolin TM or GAR do not *cause* apparent ATM or ATR activation, it is quite possible that activation of these kinases by genotoxic stress facilitates nucleolin-RPA complex formation, a possibility under investigation.

Our FRET data indicate that nucleolin-RPA complex formation occurs both in the nucleoplasm and in the nucleolus and hence nucleolin relocalization is not required for these two proteins to interact. Even so, nucleolin relocalization probably facilitates interaction with RPA. The nucleolus comprises ca. 10 to 15% of the nuclear volume in human cells (e.g., see

reference 18) and a nucleoplasmic localization would provide a larger volume in which complex formation can occur. Although p53 is not required for nucleolin-RPA complex formation, nucleolin relocalization is strongly dependent on p53 (14) (see also below), suggesting that p53 might stimulate the nucleolin-RPA interaction. Testing the ability of p53-positive (U2-OS) and negative (H1299) cells to induce nucleolin-RPA complex formation after stress did not reveal any obvious differences. That said, these cells have genetic differences other than p53 that preclude our drawing firm conclusions on the potential role of p53 in facilitating complex formation at this time.

The mechanism of nucleolin relocalization remains somewhat unclear. Previous study has found that movement of a portion of the nucleolin pool to the nucleoplasm is greatly facilitated by p53 (14). Because genotoxic stress transiently induces nucleolin and p53 complex formation (14), increased nucleoplasmic levels of appropriately modified p53 and nucleolin may lead to more complex formation and hence a net nucleoplasmic flow of nucleolin. The lack of requirement for p53 in supporting nucleolin-RPA complex formation would indicate that an event(s), such as changes to the nucleolin modification state, occurs prior to nucleolin-RPA and nucleolin-p53 complex formation. This event would lead to the apparently independent increase in the association of nucleolin with either p53 or RPA. Along with a p53 requirement in supporting nucleolin mobilization from the nucleolus in response to stress, it has also been recently proposed that p53 activation by stress itself involves nucleolar disruption (ND) (46). In this model, ND interrupts a requisite nucleolar export pathway for p53 destined for degradation. If this model is correct, ND initiates p53 activation, which itself leads to increased ND.

We identified the nucleolin GAR domain as being necessary for interaction with RPA *in vitro* and *in vivo*. The GAR domain is contained within ~63 residues and includes more than 10 RGG or FGG repeats. Similar RGG/FGG repeat sequences are found in other RNA-binding proteins, including hnRNP A1, hnRNP U, and fibrillarin (3). The RGG region forms a β -spiral structure and binds nonspecifically to single- and double-stranded RNA and DNA (21). The GAR domain of nucleolin interacts with various ribosomal subunits, including L3 (22), and, along with its ability to bind RNA, presumably explains the role of the nucleolin GAR domain in supporting efficient nucleolar localization (12, 28, 40, 47). The nucleolin GAR domain also contains a 12-residue unique lysine-rich element at the extreme C terminus. Our far-Western analysis indicates that nucleolin molecules with small C-terminal deletions do not support RPA binding, suggesting that RPA may bind this unique C-terminal end. Additional studies will be needed to determine the relative contributions of the RGG region and the unique element in supporting complex formation with RPA.

It is becoming clear that the nucleolus is a critical cellular body whose components regulate cell cycle progression. For example, p19^{ARF} (p14^{ARF} in humans) localizes to the nucleolus, where it can bind and sequester the p53 antagonist MDM2 and thereby cause p53 stabilization (56). Similarly, the binding of the human MDM2 RING domain to ATP stimulates nucleolar localization in the absence of p14^{ARF} (44). The yeast Yph1p protein is a BRCT domain-containing nucleolar factor

whose depletion causes both G₁ and G₂ arrest (17). With regard to mitotic progression, it has been found that exit from mitosis is controlled by the Cdc14 protein phosphatase that is sequestered in the nucleolus until anaphase (2). These and other observations, combined with our findings that nucleolus also serves a dual role in ribosome biogenesis and inhibiting S-phase progression in response to genotoxic stress, highlights the importance of the nucleolus in serving to integrate cell growth and cell stress pathways.

ACKNOWLEDGMENTS

We thank John Hirsch for assistance with FACS analysis, Eric Rubin (UMDNJ) for providing the GST-nucleolin expression vectors, Cristina Cardoso for the pENeGFP RPA34 plasmid, and Trevor Bivona and Mark Philips (NYU School of Medicine) for kindly providing the H-Ras and Ras-binding-domain constructs and other reagents and for their invaluable advice on FRET. We also thank Angus Wilson for insightful comments on our studies and Vitaly Vassin for helpful discussions.

This study was supported by NIH grant AI29963, DOD Breast Cancer Research Program DAMD17-03-1-0299, Philip Morris grant 15-B0001-42171, the NYU Cancer Institute, and the Rita J. and Stanley Kaplan Comprehensive Cancer Center (NCI P30CA16087). Purchase of the confocal microscope was funded by the Shared Instrumentation Grant Program of the NIH (S10 RR017970).

REFERENCES

- Araujo, S. J., and R. D. Wood. 1999. Protein complexes in nucleotide excision repair. *Mutat. Res.* 435:23–33.
- Bembek, J., and H. Yu. 2003. Regulation of CDC14: pathways and checkpoints of mitotic exit. *Front. Biosci.* 8:d1275–d1287.
- Biamonti, G., and S. Riva. 1994. New insights into the auxiliary domains of eukaryotic RNA binding proteins. *FEBS Lett.* 340:1–8.
- Bivona, T. G., I. Perez De Castro, I. M. Ahearn, T. M. Grana, V. K. Chiu, P. J. Lockyer, P. J. Cullen, A. Pellicer, A. D. Cox, and M. R. Philips. 2003. Phospholipase C γ activates Ras on the Golgi apparatus by means of Ras-GRP1. *Nature* 424:694–698.
- Block, W. D., Y. Yu, and S. P. Lees-Miller. 2004. Phosphatidyl inositol 3-kinase-like serine/threonine protein kinases (PIKKs) are required for DNA damage-induced phosphorylation of the 32-kDa subunit of replication protein A at threonine 21. *Nucleic Acids Res.* 32:997–1005.
- Brill, S. J., and B. Stillman. 1989. Yeast replication factor-A functions in the unwinding of the SV40 origin of replication. *Nature* 342:92–95.
- Callebaut, C., J. Blanco, N. Benkirane, B. Krust, E. Jacotot, G. Guichard, N. Seddiki, J. Svab, E. Dam, S. Muller, J. P. Briand, and A. G. Hovanessian. 1998. Identification of V3 loop-binding proteins as potential receptors implicated in the binding of HIV particles to CD4⁺ cells. *J. Biol. Chem.* 273:21988–21997.
- Carty, M. P., M. Zernik-Kobak, S. McGrath, and K. Dixon. 1994. UV light-induced DNA synthesis arrest in HeLa cells is associated with changes in phosphorylation of human single-stranded DNA-binding protein. *EMBO J.* 13:2114–2123.
- Chen, C. Y., R. Gherzi, J. S. Andersen, G. Gaietta, K. Jurchott, H. D. Royer, M. Mann, and M. Karin. 2000. Nucleolin and YB-1 are required for JNK-mediated interleukin-2 mRNA stabilization during T-cell activation. *Genes Dev.* 14:1236–1248.
- Costanzo, V., K. Robertson, C. Y. Ying, E. Kim, E. Avvedimento, M. Gottesman, D. Grieco, and J. Gautier. 2000. Reconstitution of an ATM-dependent checkpoint that inhibits chromosomal DNA replication following DNA damage. *Mol. Cell* 6:649–659.
- Costanzo, V., D. Shechter, P. J. Lupardus, K. A. Cimprich, M. Gottesman, and J. Gautier. 2003. An ATR- and Cdc7-dependent DNA damage checkpoint that inhibits initiation of DNA replication. *Mol. Cell* 11:203–213.
- Creancier, L., H. Prats, C. Zanibellato, F. Amalric, and B. Bugler. 1993. Determination of the functional domains involved in nucleolar targeting of nucleolin. *Mol. Biol. Cell* 4:1239–1250.
- Daniely, Y., and J. A. Borowiec. 2000. Formation of a complex between nucleolin and replication protein A after cell stress prevents initiation of DNA replication. *J. Cell Biol.* 149:799–810.
- Daniely, Y., D. D. Dimitrova, and J. A. Borowiec. 2002. Stress-dependent nucleolin mobilization mediated by p53-nucleolin complex formation. *Mol. Cell. Biol.* 22:6014–6022.
- Dimitrova, D. S., and D. M. Gilbert. 2000. Stability and nuclear distribution of mammalian replication protein A heterotrimeric complex. *Exp. Cell Res.* 254:321–327.
- Dodson, G. E., Y. Shi, and R. S. Tibbetts. 2004. DNA replication defects, spontaneous DNA damage, and ATM-dependent checkpoint activation in replication protein A-deficient cells. *J. Biol. Chem.* 279:34010–34014.
- Du, Y. C., and B. Stillman. 2002. Yph1p, an ORC-interacting protein: potential links between cell proliferation control, DNA replication, and ribosome biogenesis. *Cell* 109:835–848.
- Elias, E., N. Lalun, M. Lorenzato, L. Blache, P. Chelidze, M. F. O'Donohue, D. Ploton, and H. Bobichon. 2003. Cell-cycle-dependent three-dimensional redistribution of nuclear proteins. P120, pKi-67, and SC35 splicing factor, in the presence of the topoisomerase I inhibitor camptothecin. *Exp. Cell Res.* 291:176–188.
- Falck, J., N. Mailand, R. G. Syljuasen, J. Bartek, and J. Lukas. 2001. The ATM-Chk2-Cdc25A checkpoint pathway guards against radioresistant DNA synthesis. *Nature* 410:842–847.
- Gabellini, D., M. R. Green, and R. Tupler. 2002. Inappropriate gene activation in FSHD: a repressor complex binds a chromosomal repeat deleted in dystrophic muscle. *Cell* 110:339–348.
- Ghisolfi, L., G. Joseph, F. Amalric, and M. Erard. 1992. The glycine-rich domain of nucleolin has an unusual supersecondary structure responsible for its RNA-helix-destabilizing properties. *J. Biol. Chem.* 267:2955–2959.
- Ginisty, H., H. Sicard, B. Roger, and P. Bouvet. 1999. Structure and functions of nucleolin. *J. Cell Sci.* 112:761–772.
- Griinstein, E., P. Wernet, P. J. Snijders, F. Rosl, I. Weinert, W. Jia, R. Kraft, C. Schewe, M. Schwabe, S. Hauptmann, M. Dietel, C. J. Meijer, and H. D. Royer. 2002. Nucleolin as activator of human papillomavirus type 18 onco-gene transcription in cervical cancer. *J. Exp. Med.* 196:1067–1078.
- Gulli, M. P., J. P. Girard, D. Zabetakis, B. Lapeyre, T. Melese, and M. Caizergues-Ferrer. 1995. gar2 is a nucleolar protein from *Schizosaccharomyces pombe* required for 18S rRNA and 40S ribosomal subunit accumulation. *Nucleic Acids Res.* 23:1912–1918.
- Haluska, P., Jr., A. Saleem, T. K. Edwards, and E. H. Rubin. 1998. Interaction between the N terminus of human topoisomerase I and SV40 large T antigen. *Nucleic Acids Res.* 26:1841–1847.
- Hanakah, L. A., L. A. Dempsey, M. J. Li, and N. Maizels. 1997. Nucleolin is one component of the B cell-specific transcription factor and switch region binding protein, LR1. *Proc. Natl. Acad. Sci. USA* 94:3605–3610.
- Hannan, K. M., R. D. Hannan, and L. I. Rothblum. 1998. Transcription by RNA polymerase I. *Front. Biosci.* 3:d376–d398.
- Heine, M., M. L. Rankin, and P. J. DiMario. 1993. The Gly/Arg-rich (GAR) domain of *Xenopus* nucleolin facilitates in vitro nucleic acid binding and in vivo nucleolar localization. *Mol. Biol. Cell* 4:1189–1204.
- Henricksen, L. A., C. B. Umbricht, and M. S. Wold. 1994. Recombinant replication protein A: expression, complex formation, and functional characterization. *J. Biol. Chem.* 269:11121–11132.
- Ifode, C., and J. A. Borowiec. 1998. Unwinding of origin-specific structures by human replication protein A occurs in a two-step process. *Nucleic Acids Res.* 26:5636–5643.
- Ifode, C., Y. Daniely, and J. A. Borowiec. 1999. Replication protein A (RPA): the eukaryotic SSB. *Crit. Rev. Biochem. Mol. Biol.* 34:141–180.
- Jayaraman, L., N. C. Moorthy, K. G. Murthy, J. L. Manley, M. Bustin, and C. Prives. 1998. High mobility group protein-1 (HMG-1) is a unique activator of p53. *Genes Dev.* 12:462–472.
- Karpova, T. S., C. T. Baumann, L. He, X. Wu, A. Grammer, P. Lipsky, G. L. Hager, and J. G. McNally. 2003. Fluorescence resonance energy transfer from cyan to yellow fluorescent protein detected by acceptor photobleaching using confocal microscopy and a single laser. *J. Microsc.* 209:56–70.
- Kondo, K., and M. Inouye. 1992. Yeast NSR1 protein that has structural similarity to mammalian nucleolin is involved in pre-rRNA processing. *J. Biol. Chem.* 267:16252–16258.
- Lee, W. C., D. Zabetakis, and T. Melese. 1992. NSR1 is required for pre-rRNA processing and for the proper maintenance of steady-state levels of ribosomal subunits. *Mol. Cell. Biol.* 12:3865–3871.
- Liu, J. S., S. R. Kuo, M. M. McHugh, T. A. Beerman, and T. Melendy. 2000. Adozelesin triggers DNA damage response pathways and arrests SV40 DNA replication through replication protein A inactivation. *J. Biol. Chem.* 275:1391–1397.
- Liu, J. S., S. R. Kuo, X. Yin, T. A. Beerman, and T. Melendy. 2001. DNA damage by the enediyne C-1027 results in the inhibition of DNA replication by loss of replication protein A function and activation of DNA-dependent protein kinase. *Biochemistry* 40:14661–14668.
- Luch, A. 2002. Cell cycle control and cell division: implications for chemically induced carcinogenesis. *Chembiochem* 3:506–516.
- Matsumoto, T., T. Eki, and J. Hurwitz. 1990. Studies on the initiation and elongation reactions in the simian virus 40 DNA replication system. *Proc. Natl. Acad. Sci. USA* 87:9712–9716.
- Messmer, B., and C. Dreyer. 1993. Requirements for nuclear translocation and nucleolar accumulation of nucleolin of *Xenopus laevis*. *Eur. J. Cell Biol.* 61:369–382.
- Nisole, S., B. Krust, C. Callebaut, G. Guichard, S. Muller, J. P. Briand, and A. G. Hovanessian. 1999. The anti-HIV pseudopeptide HB-19 forms a complex with the cell-surface-expressed nucleolin independent of heparan sulfate proteoglycans. *J. Biol. Chem.* 274:27875–27884.

42. Painter, R. B., and B. R. Young. 1980. Radiosensitivity in ataxia-telangiectasia: a new explanation. *Proc. Natl. Acad. Sci. USA* **77**:7315–7317.
43. Petrini, J. H. 2000. The Mre11 complex and ATM: collaborating to navigate S phase. *Curr. Opin. Cell Biol.* **12**:293–296.
44. Poyurovsky, M. V., X. Jacq, C. Ma, O. Karni-Schmidt, P. J. Parker, M. Chalfie, J. L. Manley, and C. Prives. 2003. Nucleotide binding by the Mdm2 RING domain facilitates Arf-independent Mdm2 nucleolar localization. *Mol. Cell* **12**:875–887.
45. Roger, B., A. Moisand, F. Amalric, and P. Bouvet. 2002. Repression of RNA polymerase I transcription by nucleolin is independent of the RNA sequence that is transcribed. *J. Biol. Chem.* **277**:10209–10219.
46. Rubbi, C. P., and J. Milner. 2003. Disruption of the nucleolus mediates stabilization of p53 in response to DNA damage and other stresses. *EMBO J.* **22**:6068–6077.
47. Schmidt-Zachmann, M. S., and E. A. Nigg. 1993. Protein localization to the nucleolus: a search for targeting domains in nucleolin. *J. Cell Sci.* **105**:799–806.
48. Sengupta, T. K., S. Bandyopadhyay, D. J. Fernandes, and E. K. Spicer. 2003. Identification of nucleolin as an AU-rich element binding protein involved in *bc1-2* mRNA stabilization. *J. Biol. Chem.* **279**:10855–10863.
49. Siliciano, J. D., C. E. Canman, Y. Taya, K. Sakaguchi, E. Appella, and M. B. Kastan. 1997. DNA damage induces phosphorylation of the amino terminus of p53. *Genes Dev.* **11**:3471–3481.
50. Sporbert, A., A. Gahl, R. Ankerhold, H. Leonhardt, and M. C. Cardoso. 2002. DNA polymerase clamp shows little turnover at established replication sites but sequential de novo assembly at adjacent origin clusters. *Mol. Cell* **10**:1355–1365.
51. Tibbetts, R. S., K. M. Brumbaugh, J. M. Williams, J. N. Sarkaria, W. A. Cliby, S. Y. Shieh, Y. Taya, C. Prives, and R. T. Abraham. 1999. A role for ATR in the DNA damage-induced phosphorylation of p53. *Genes Dev.* **13**:152–157.
52. Vassin, V. M., M. S. Wold, and J. A. Borowiec. 2004. Replication protein A (RPA) phosphorylation prevents RPA association with replication centers. *Mol. Cell. Biol.* **24**:1930–1943.
53. Wang, X., and J. E. Haber. 2004. Role of *Saccharomyces* single-stranded DNA-binding protein RPA in the strand invasion step of double-strand break repair. *PLoS Biol.* **2**:104–112.
54. Wang, Y., J. Guan, H. Wang, D. Leeper, and G. Iliakis. 2001. Regulation of DNA replication after heat shock by replication protein A-nucleolin interactions. *J. Biol. Chem.* **276**:20579–20588.
55. Wang, Y., A. R. Perrault, and G. Iliakis. 1998. Replication protein A as a potential regulator of DNA replication in cells exposed to hyperthermia. *Radiat. Res.* **149**:284–293.
56. Weber, J. D., L. J. Taylor, M. F. Roussel, C. J. Sherr, and D. Bar-Sagi. 1999. Nucleolar Arf sequesters Mdm2 and activates p53. *Nat. Cell Biol.* **1**:20–26.
57. Wold, M. S. 1997. Replication protein A: a heterotrimeric, single-stranded DNA-binding protein required for eukaryotic DNA metabolism. *Annu. Rev. Biochem.* **66**:61–92.
58. Ying, G. G., P. Proost, J. van Damme, M. Bruschi, M. Introna, and J. Golay. 2000. Nucleolin, a novel partner for the Myb transcription factor family that regulates their activity. *J. Biol. Chem.* **275**:4152–4158.
59. Zou, L., and S. J. Elledge. 2003. Sensing DNA damage through ATRIP recognition of RPA-ssDNA complexes. *Science* **300**:1542–1548.
60. Zou, L., D. Liu, and S. J. Elledge. 2003. Replication protein A-mediated recruitment and activation of Rad17 complexes. *Proc. Natl. Acad. Sci. USA* **100**:13827–13832.

Replication Protein A (RPA) Phosphorylation Prevents RPA Association with Replication Centers

Vitaly M. Vassin,¹ Marc S. Wold,² and James A. Borowiec^{1*}

Department of Biochemistry and New York University Cancer Institute, New York University School of Medicine, New York, New York 10016,¹ and Department of Biochemistry, University of Iowa College of Medicine, Iowa City, Iowa 52242²

Received 11 August 2003/Returned for modification 15 September 2003/Accepted 24 November 2003

Mammalian replication protein A (RPA) undergoes DNA damage-dependent phosphorylation at numerous sites on the N terminus of the RPA2 subunit. To understand the functional significance of RPA phosphorylation, we expressed RPA2 variants in which the phosphorylation sites were converted to aspartate (RPA2_D) or alanine (RPA2_A). Although RPA2_D was incorporated into RPA heterotrimers and supported simian virus 40 DNA replication in vitro, the RPA2_D mutant was selectively unable to associate with replication centers in vivo. In cells containing greatly reduced levels of endogenous RPA2, RPA2_D again did not localize to replication sites, indicating that the defect in supporting chromosomal DNA replication is not due to competition with the wild-type protein. Use of phosphospecific antibodies demonstrated that endogenous hyperphosphorylated RPA behaves similarly to RPA2_D. In contrast, under DNA damage or replication stress conditions, RPA2_D, like RPA2_A and wild-type RPA2, was competent to associate with DNA damage foci as determined by colocalization with γ -H2AX. We conclude that RPA2 phosphorylation prevents RPA association with replication centers in vivo and potentially serves as a marker for sites of DNA damage.

DNA-damaging stress leads to the inception of a variety of cellular responses that serve to minimize mutation and prevent genomic instability. In particular, the cell cycle checkpoint apparatus is activated to block S phase entry and, in those cells in the replicative phase, to both inhibit firing of late origins of DNA replication and avert the collapse of replication forks blocked by damage (3). The DNA repair machinery is mobilized in concert to repair lesions and to allow eventual restart of stalled replication forks. One factor that plays essential roles both during DNA replication and in the repair- and recombination-mediated recovery from damage is replication protein A (RPA), the eukaryotic single-stranded (ss) DNA-binding protein (27, 52).

RPA is a heterotrimeric protein consisting, in mammalian cells, of ~70- (RPA1), 30- (RPA2), and 14 (RPA3)-kDa subunits. During DNA replication, RPA acts at the fork, stabilizing ssDNA and facilitating nascent strand synthesis by the replicative DNA polymerases. Under DNA-damaging conditions, RPA-ssDNA complexes act to recruit and activate a key checkpoint mediator consisting of the ATR and ATRIP (ATR-interacting protein) protein-kinase complex (54). At DNA damage-dependent nuclear foci, RPA interacts with repair and recombination components to process double-strand DNA breaks and other lesions (19). RPA activity is regulated by various stress conditions. In particular, heat shock (12, 47, 48), exposure to UV radiation (9), and treatment with DNA-alkylating agents (30) each cause the generation of an RPA species that is unable to support DNA replication in vitro. In the case of heat shock, the inhibition of RPA activity is mediated

by a stress-dependent association with the nucleolar protein nucleolin (12, 47).

In an area with potential regulatory significance, RPA undergoes both stress-dependent and -independent phosphorylation on the extreme N terminus of the RPA2 subunit. A basal level of RPA modification by cyclin-cdk complexes occurs at two sites (16, 35). Following stress, such as exposure to ionizing (31) or UV (9) radiation, or treatment with radiomimetic agents, such as camptothecin (CPT) (42), human RPA2 can be phosphorylated at five or more additional sites out of a possible seven by the phosphatidylinositol 3-kinase-related kinases (PIKKs) DNA-PK, ATM, and perhaps ATR (7, 10, 17, 18, 31, 33, 35, 46, 53). ATM and ATR are activated in response to DNA damage and replication stress, and they modify various effectors that facilitate the damage and cell cycle checkpoint responses (1). DNA-PK is required directly in the repair of double-strand DNA breaks and in V(D)J recombination (15). These data could suggest that the function of stress-dependent modification of RPA is to repress DNA replication or to promote recovery from DNA damage, but there are as yet no compelling data for either role. While the results of certain studies suggest that RPA modification by PIKKs may lead to the inhibition of DNA replication in vitro and in vivo (9, 37), direct testing of this possibility has not shown any appreciable effects of RPA phosphorylation on binding to ssDNA or on replication in vitro using a simian virus 40 (SV40)-based assay (7, 23).

Because previous work has primarily studied the effects of mammalian RPA phosphorylation using in vitro systems, it is possible that the modulation of RPA activity by phosphorylation might be observed only in the cellular milieu. Testing this hypothesis, we found that RPA2 phosphorylation mutants that mimic the hyperphosphorylated form were unable to localize to replication centers in normal cells. Interestingly, binding of

* Corresponding author. Mailing address: Dept. of Biochemistry and New York University Cancer Institute, New York University School of Medicine, New York, NY 10016. Phone: (212) 263-8453. Fax: (212) 263-8166. E-mail: james.borowiec@med.nyu.edu.

the hyperphosphorylation mimic to DNA damage foci was unaffected, as determined by colocalization with the DNA damage marker γ -H2AX. Similar behavior was observed with endogenous hyperphosphorylated RPA. We conclude that RPA phosphorylation following damage both prevents RPA from catalyzing DNA replication and potentially serves as a marker to recruit repair factors to sites of DNA damage.

MATERIALS AND METHODS

Cell lines and stress treatments. U2-OS and HeLa cells were maintained in McCoy's 5 M and Dulbecco's modified Eagle's media, respectively, supplemented with 10% fetal bovine serum and 50 μ g of gentamicin/ml. When the effect of stress was examined, the cells were treated with either 1 μ M CPT (Sigma) for 1 or 3 h, 2.5 mM hydroxyurea (HU; Sigma) for either 1 or 3 h, or 7 μ M aphidicolin (Sigma) for 3 h. To inhibit the cellular checkpoint response, cells were treated with 5 mM caffeine for 30 min prior to stress. Transfection experiments were performed using Effectene (Qiagen).

Generation of RPA2 mutant constructs. To generate the myc-RPA2_{wt} and myc-RPA2_D mammalian expression vectors, the human RPA2 genes from plasmids p11dtRPA and p11dtRPA-32Asp8 (4, 24) were inserted into the *Xba*I and *Bsr*BI sites of the pEF6/Myc-HisA vector (Invitrogen), resulting in pERPA2_{wt} and pERPA2_D. Expression of the His₆ tag from pEF6/Myc-HisA was prevented by mutating the ATG codon at position 1863 to a TGA codon. Vectors expressing the intermediate RPA2 phosphorylation mutants and RPA2_A were constructed by a combination of site-directed mutagenesis of either pERPA2_{wt} or pERPA2_D (as appropriate) at positions 23, 29, and 33 and replacement of larger segments of the RPA2 N terminus with synthetic oligonucleotides encoding mutant phosphorylation regions. Detailed cloning procedures are available upon request.

Protein purification and in vitro replication assay. The RPA_{RPA2wt} and RPA_{RPA2D} heterotrimers were expressed in *Escherichia coli* BL21 transformed with p11dtRPA and p11dtRPA-32Asp8, respectively, and purified as described previously (24, 26). The SV40 large tumor (T) antigen used for SV40 DNA replication reactions was prepared from extracts of Si9 cells infected with the recombinant baculovirus Ac941SVT (5) and purified using immunoaffinity chromatography (6). The AS65 fraction lacking RPA was prepared from HeLa cell extracts by ammonium sulfate fractionation according to the method of Wobbe et al. (51). SV40 DNA replication reaction mixtures (50 μ l) containing 40 mM creatine phosphate (diTris salt; pH 7.8); 7 mM MgCl₂; 4 mM ATP; 25 μ g of creatine kinase/ml; 0.4 mM dithiothreitol; 200 μ M (each) CTP, GTP, and UTP; 100 μ M (each) dATP, dGTP, and dCTP; 25 μ M [³H]dTTP (~500 cpm/pmol); 0.2 μ g of the *ori*-containing plasmid pSV01ΔEP (50); 200 μ g of the AS65 fraction; 0 to 700 ng of RPA_{RPA2wt} or RPA_{RPA2D}; and 750 ng of SV40 T antigen were incubated at 37°C for 2 h. Replication activity was determined by precipitating the high-molecular-weight DNA with trichloroacetic acid and quantitating the amount of ³H in the precipitate by scintillation counting. To examine the *Dpn*I resistance of the replication products, replication reaction mixtures containing 600 ng of either RPA_{RPA2wt} or RPA_{RPA2D} and 100 μ M [α -³²P]dCTP (1,000 cpm/pmol) to label the replication products were incubated at 37°C for 2.5 h. Following removal of protein by phenol extraction, the DNA products were first linearized by digestion with *Pst*I and then either mock treated or incubated with 2.5 U of *Dpn*I to cleave nonreplicated DNA. The digestion products were separated by electrophoresis through a 1.1% agarose gel and visualized both by ethidium bromide staining and by autoradiography.

Immunoprecipitation and immunoblotting. Transfected U2-OS cells were lysed in lysis buffer (50 mM Tris-HCl, pH 7.4, 150 mM NaCl, 1% [vol/vol] NP-40, 1 mM phenylmethylsulfonyl fluoride, 0.1 mM Na₃VO₄, 1 mM NaF, and 1 μ g each of aprotinin, leupeptin, and pepstatin per ml). The cell extracts were then incubated at 4°C for 2 h with 70A anti-RPA1 monoclonal antibody (28) conjugated to CNBr-activated Sepharose beads (Amersham Biosciences). The immunoprecipitate was washed five times with lysis buffer and resolved by sodium dodecyl sulfate-polyacrylamide gel electrophoresis (SDS-PAGE) (13% [wt/vol] polyacrylamide). To test RPA2 phosphorylation and myc-RPA2 expression, cells were directly lysed in SDS-PAGE sample buffer and proteins were separated by SDS-PAGE. For phosphatase treatment, cells were lysed in λ protein phosphatase buffer (New England Biolabs) containing 1% Triton X-100 and 1 μ g each of aprotinin, leupeptin, and pepstatin per ml. Cell lysates (~20 μ g of protein) were then incubated with 400 U of λ protein phosphatase for 30 min at 30°C or mock treated in the presence of protein phosphatase inhibitors (0.1 mM Na₃VO₄, 1 mM NaF). The Western blots were developed with an anti-RPA2 34A mouse

monoclonal antibody (28) or a rabbit polyclonal anti-pSer4/pSer8-RPA2 antibody obtained from Bethyl Laboratories, Inc. (Montgomery, Tex.). Proteins were detected using enhanced chemiluminescence (Amersham Biosciences).

Cell cycle assay. Forty-eight hours posttransfection, cells were incubated with 10 μ M bromodeoxyuridine (BrdU). After a 30-min incubation, the cells were fixed and processed according to the BrdU Flow Kit manual (BD Pharmingen). Following incubation with rat anti-BrdU (Harlan Sera-Lab) and rabbit anti-myc (Upstate Biotechnology) antibodies, the cells were stained with anti-rat fluorescein isothiocyanate-conjugated and anti-rabbit phycoerythrin-conjugated secondary antibodies (Jackson ImmunoResearch Laboratories). The DNA was stained with 7-aminoactinomycin D, and the cells were subjected to fluorescence-activated cell sorting (FACS) analysis.

Immunofluorescence microscopy. Transfected cells were processed by two methods. To test protein expression and transfection efficiency, the cells were first washed with phosphate-buffered saline (PBS), fixed with 4% (wt/vol) formaldehyde in PBS for 15 min at room temperature, and then extracted with PBS containing 0.5% (vol/vol) Triton X-100 for 5 min. To study chromatin-bound proteins, the cells were extracted with 0.5% (vol/vol) Triton X-100 for 5 min prior to fixation as described previously (13). When required, cells were incubated in media containing 10 μ M BrdU for 10 min prior to harvest. For detection of incorporated BrdU, DNA was denatured with HCl using standard procedures. RPA2 silencing was achieved using a short interfering RNA (siRNA) duplex targeted to the 5'-CCUAGUUUACAAUCUGUU sequence found in the 3' noncoding region of RPA2 mRNA. Prepared cells were incubated, as required, with rabbit anti-myc (Upstate Biotechnology), mouse anti-RPA1 70A and anti-RPA2 34A (28), rabbit anti-pSer4/pSer8-RPA2 (Bethyl Laboratories), rat anti-BrdU (Harlan Sera-Lab), and mouse anti- γ H2AX (Upstate Biotechnology) antibodies. Following staining with the appropriate secondary antibodies (Jackson ImmunoResearch Laboratories), the cells were examined by epifluorescence microscopy using a Zeiss Axiophot microscope. To calculate the relative frequency of myc-RPA2-positive cells (see Fig. 6H and 8M), the fraction of cells transfected with myc-RPA2_{wt} or the myc-tagged RPA mutants was first determined by processing cells without prior Triton X-100 extraction (e.g., $F_{\text{transfection:wt}}$ and $F_{\text{transfection:D4}}$). Separately, the fraction of cells showing significant chromatin staining was also determined (e.g., $F_{\text{chromatin:wt}}$ and $F_{\text{chromatin:D4}}$). The relative frequency of cells that were positive, for example, for myc-RPA2_{D4} chromatin staining was calculated using the following formula: relative frequency = $(F_{\text{chromatin:D4}}/F_{\text{transfection:D4}})/(F_{\text{chromatin:wt}}/F_{\text{transfection:wt}}) \cdot 100\%$. Each value determined was the result of three independent experiments.

RESULTS

The RPA2_D phosphorylation mimic localizes to the nucleus but is not chromatin bound. To understand the functional significance of RPA phosphorylation, we generated various human RPA2 constructs in which subsets of the nine potential N-terminal phosphorylation sites were mutated. Previous studies have shown that two of the RPA2 sites (S23 and S29) are phosphorylated in a cell cycle-dependent manner by cyclin-cdk2 complexes (16, 35). At least five of the other seven (S4, S8, S11, S12, S13, T21, and S33) can be phosphorylated in response to UV irradiation (53). Ionizing irradiation and treatment with the radiomimetic agent CPT cause similar RPA hyperphosphorylation and likely modification of most if not all of these same sites (31, 42). Various data strongly suggest that the PIKK members DNA-PK and ATM, and likely ATR, can independently modify the RPA stress-dependent sites (7, 10, 17, 18, 31, 33, 35, 46), although only two (T21 and S33) have canonical SQ/TQ sequences that are PIKK targets (1). Both of the cyclin-cdk2 sites and six of the stress-dependent sites (S8, S11, S12, S13, T21, and S33) were replaced by aspartate to mimic phosphate (generating the RPA2_D mutant; see Fig. 6G for a schematic showing the construction of this and other mutants). Although an aspartate residue is not the same as phosphoserine or phosphothreonine, the use of aspartate residues to imitate phosphate has been shown in many cases to have identical effects on protein structure and activity (25, 49).

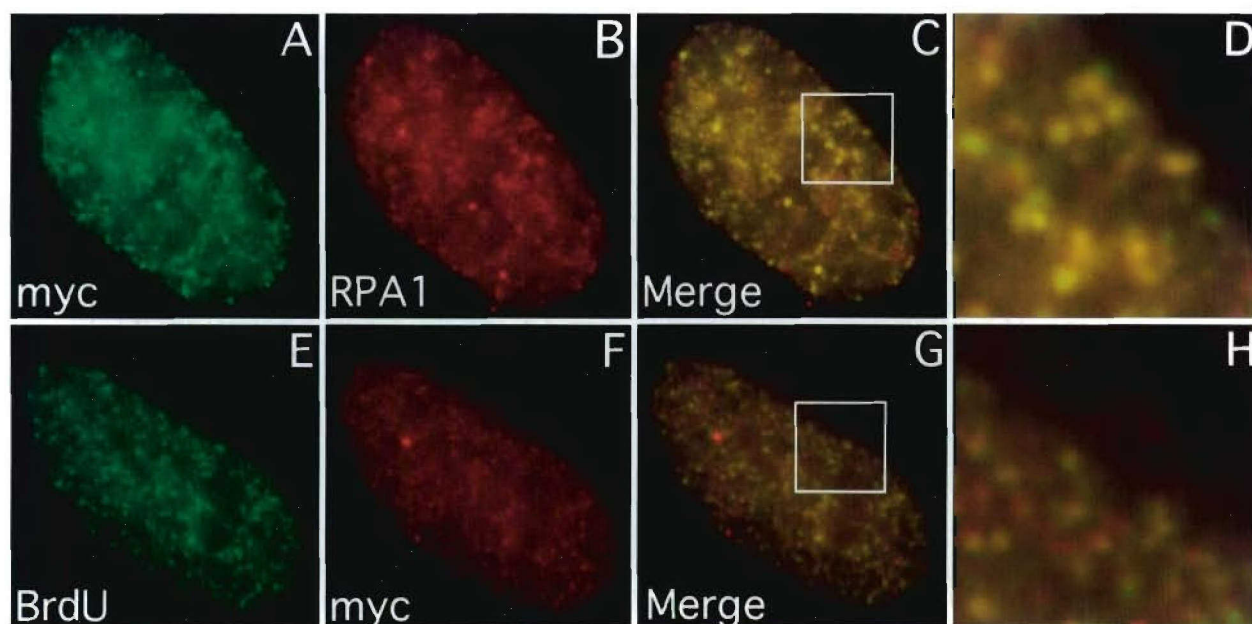


FIG. 1. The myc-RPA2_{wt} subunit colocalizes with endogenous RPA1 and DNA replication centers. U2-OS cells were transfected with a vector expressing myc-RPA2_{wt}. To allow visualization of chromatin-bound myc-RPA, the cells were first extracted with 0.5% Triton X-100 for 5 min and then fixed with formaldehyde. (E to H) To detect sites of DNA replication, BrdU was added to the medium 10 min before the cells were prepared for epifluorescence microscopy. As indicated, the cells were then stained with anti-myc (A and F), anti-RPA1 (B), or anti-BrdU (E) antibody. The extent of myc-RPA2_{wt} and endogenous RPA1 colocalization is shown (C), with enlargement of a particular nuclear region (boxed) (D). BrdU and myc-RPA2_{wt} colocalization are similarly shown (G and H).

In the RPA2_A mutant, these same eight sites were converted to alanines to prevent phosphorylation (see also Fig. 6G). All of the mutants and the wild-type RPA2 control (RPA2_{wt}) contained a C-terminal myc tag.

The RPA2_{wt} subunit was expressed in human U2-OS cells. To detect the chromatin-bound fraction of RPA2, transfected cells were extracted with nonionic detergent prior to formaldehyde fixation (13). Under such conditions, RPA bound to chromatin in nuclear replication foci can be selectively visualized. The transfected RPA2_{wt} subunit nearly completely colocalized with the endogenous RPA1 and exhibited a punctate distribution throughout the nucleus, consistent with its recruitment to DNA replication centers (Fig. 1A to D). To confirm this observation, transfected cells were pulse-labeled with BrdU prior to fixation, and the sites of RPA2_{wt} localization and BrdU incorporation were examined. As expected, the RPA2_{wt} subunit showed nearly complete colocalization with replicating chromatin (Fig. 1E to H). Taken together, these results indicate that the recombinant RPA2_{wt} subunit can functionally replace endogenous RPA2 in supporting chromosomal DNA replication.

We next examined the localization of the RPA2_A and RPA2_D mutants. Transfected cells were examined both without and with prior detergent extraction to reveal transfection efficiency and to show the fraction bound to chromatin, respectively. The distribution of RPA2_A on chromatin (Fig. 2L) was virtually identical to the replication pattern seen with endogenous RPA2 (data not shown) and the RPA2_{wt} variant (Fig. 2D) and showed nearly complete colocalization with endogenous RPA1 (Fig. 2K and data not shown). RPA2 phosphorylation is therefore not required for association with replication centers.

In dramatic contrast, we did not observe chromatin staining for RPA2_D (Fig. 2H), even though the RPA2_D mutant was expressed to an equivalent similar to that of the RPA2_{wt} construct (Fig. 2F and B, respectively). Similar experiments were performed with RPA2_D and RPA2_{wt} expressed as fusion proteins with green fluorescent protein. While a modest RPA2_{wt} signal was detected, we did not observe an appreciable level of chromatin binding for RPA2_D (data not shown). We therefore find that mutation of RPA2 to a hyperphosphorylation mimic greatly reduces its localization to DNA replication centers.

In addition to the possibility that phosphorylation of RPA inhibits its normal participation at the DNA replication fork *in vivo*, other explanations exist. One is that the myc-RPA2_D subunit is unable to complex with the other RPA subunits. To examine this, lysates prepared from cells transfected with the RPA2_{wt} and RPA2_D expression vectors were subjected to immunoprecipitation with an anti-RPA1 antibody and immunoblotted for the presence of RPA2. The two myc-RPA2 variants, as well as the endogenous RPA2, efficiently coprecipitated with the RPA1 subunit (Fig. 3A, lanes 1 to 3). The RPA2_D protein was also found in the lysate at levels comparable to those of RPA2_{wt}, suggesting that the two proteins have similar stabilities (lanes 5 and 6). Because RPA1 and RPA2 complex formation requires the RPA3 subunit (24, 44), these data indicate that the two mutants form RPA heterotrimers with equivalent efficiencies.

To establish if heterotrimeric RPA containing the RPA2_D subunit (RPA_{RPA2D}) was inherently unable to function in DNA replication, we tested the abilities of RPA_{RPA2D} and RPA_{RPA2wt} to support SV40 DNA replication *in vitro*. With the exception of the viral large T antigen, SV40 replication is

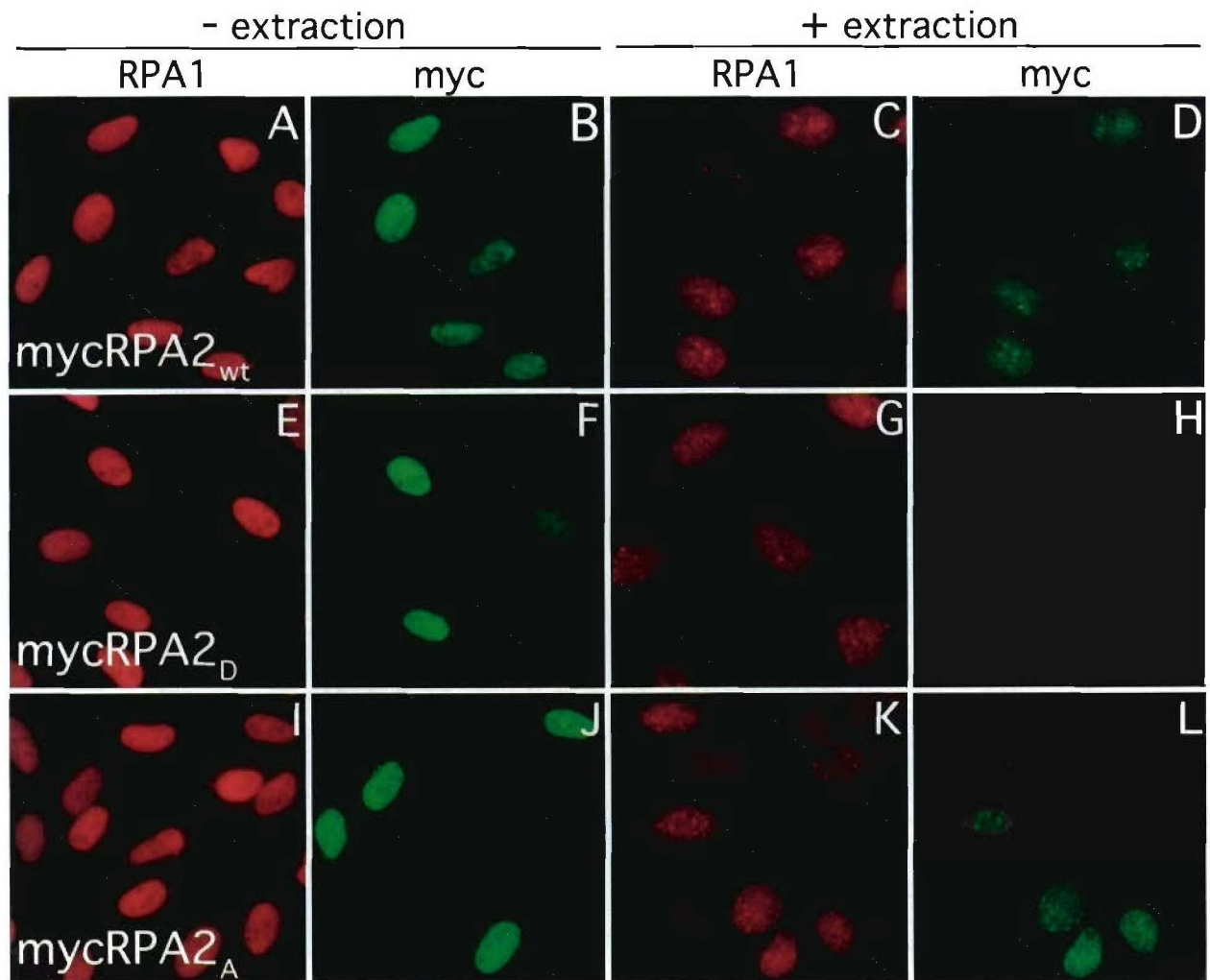


FIG. 2. Lack of association of the RPA2_D mutant with chromatin in unstressed cells. U2-OS cells were transfected with a vector expressing myc-RPA2_{wt} (A to D), myc-RPA2_D (E to H), or myc-RPA2_A (I to L). (C, D, G, H, K, and L) To allow visualization of chromatin-bound myc-RPA, cells were first extracted with 0.5% Triton X-100 for 5 min and then fixed with formaldehyde (+ extraction). (A, B, E, F, I, and J) To assay for transfection efficiency, cells were also fixed without prior extraction (– extraction). The cells were then stained with anti-myc (B, D, F, H, J, and L) or anti-RPA1 (A, C, E, G, I, and K) antibody.

catalyzed by host cell components (8, 22). The SV40 system can thus provide a relatively comprehensive test of the ability of RPA to interact functionally with ssDNA and the DNA replication machinery. Previous work by J. Hurwitz and colleagues has shown that separation of human cell extracts by ammonium sulfate precipitation yields two required fractions (AS30 and AS65), with RPA found to be the only essential factor within the AS30 fraction (51). Because the AS65 fraction lacks RPA, the activities of different RPA variants can be assayed by their abilities to complement the AS65 fraction in supporting SV40 DNA replication. The RPA_{RPA2D} and RPA_{RPA2wt} variants were produced in *E. coli* and purified to homogeneity (Fig. 3B). Use of the AS65 fraction alone showed no significant DNA replication activity (Fig. 3C). The addition of either heterotrimeric RPA complex supported T-antigen-dependent viral DNA replication to similar extents, and the activities of the two RPA variants were similar over a range of levels (Fig. 3C). The reaction products synthesized in

the presence of RPA_{RPA2D} or RPA_{RPA2wt} were equally resistant to *DpnI*, demonstrating that they were bona fide DNA replication products and not due to repair synthesis (Fig. 3D). RPA_{RPA2D} is therefore functionally active in supporting DNA replication in vitro. RPA_{RPA2D} was also found to bind normally to short ssDNA oligonucleotides (4). These results are not completely unexpected, as it was shown previously that the RPA phosphorylation state does not appreciably affect the ability of RPA to function in viral DNA replication or in DNA repair (2, 7, 36). In sum, mutation of the seven serines and one threonine in the N terminus of RPA2 to negatively charged aspartate residues does not have any apparent effect on the inherent activity of the heterotrimeric protein.

We next examined the possibility that expression of the RPA2_D mutant generates a signal that shuts down cellular DNA synthesis and thus indirectly prevents RPA2_D from associating with chromatin. To address this issue, cells were transfected with the RPA2_{wt} or RPA2_D expression construct

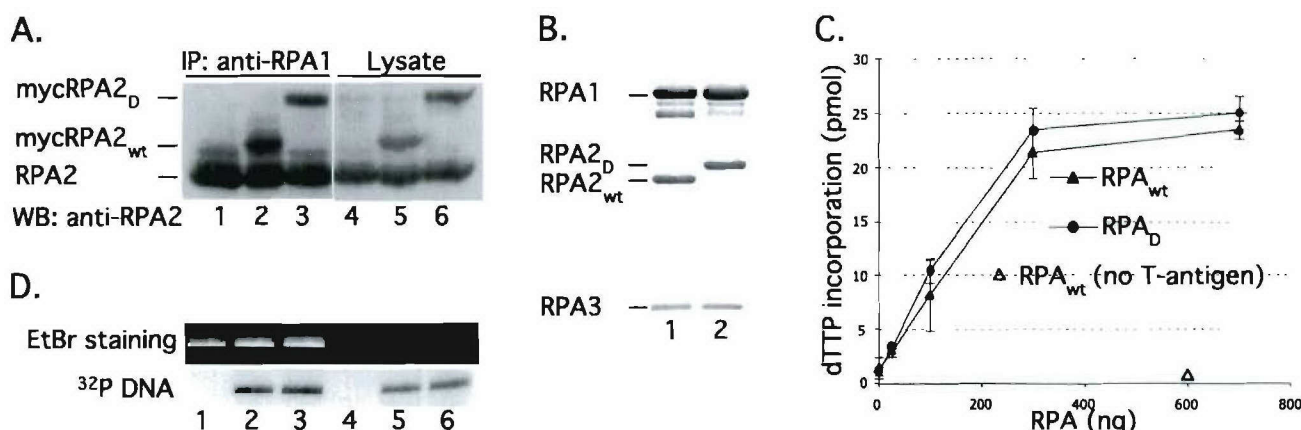


FIG. 3. RPA2_D-containing RPA heterotrimers are replication competent. (A) U2-OS cells were transfected with empty vector (lanes 1 and 4), myc-RPA2_{wt} (lanes 2 and 5), or myc-RPA2_D (lanes 3 and 6). Lysates were prepared from each batch of transfected cells, and the lysates were subjected to immunoprecipitation using anti-RPA1 antibodies. Immunoprecipitates (IP) (lanes 1 to 3) and aliquots of the lysates (lanes 4 to 6) were then analyzed for the presence of RPA2 by Western blotting analysis using RPA2 antibodies (which recognize both transfected and endogenous RPA2). (B and C) RPA heterotrimers that contained either RPA2_{wt} (lane 1) or RPA2_D (lane 2) were expressed in *E. coli*, purified, and analyzed by SDS-PAGE and Coomassie blue staining (B). The purified RPA was then assayed for the ability to support SV40 DNA replication in combination with an AS65 fraction purified from HeLa cells (51) (C). The open triangle shows that only background levels of DNA synthesis occur in reactions containing RPA2_D but lacking T antigen. Similar results were observed using RPA2_D. (D) SV40 DNA replication reactions were performed in the presence of [α -³²P]dCTP to label the replication products as described in Materials and Methods. The reaction mixtures contained 600 ng of either RPA_{RPA2wt} (lanes 1, 2, 4, and 5) or RPA_{RPA2D} (lanes 3 and 6) and either lacked T antigen (lanes 1 and 4) or contained 750 ng of T antigen (lanes 2, 3, 5, and 6). After isolation, the DNA replication products were first linearized by restriction digestion and then either mock treated (lanes 1 to 3) or incubated with DpnI to cleave nonreplicated DNA (lanes 4 to 6). The digestion products were then subjected to agarose gel electrophoresis, and the images of the ethidium bromide (EtBr)-stained gel (to show the total level of DNA) and the autoradiograph of the gel (to visualize ³²P-labeled reaction products) are provided. The observed bands correspond to the linearized SV40 origin-containing plasmid.

and pulse-labeled with BrdU. The cells were then subjected to FACS based on three signals: the level of myc-RPA2, DNA content, and BrdU incorporation. In addition to confirming that the two RPA2 variants were expressed at comparable levels (Fig. 4A and C), it was found that the percentages of cells in S phase were similar regardless of whether the cells were transfected with RPA2_{wt} (Fig. 4B), RPA2_D (Fig. 4D), or empty vector (not shown). Although the percentage of cells in S phase was somewhat high compared to other experiments, perhaps because of transfection conditions, the fractions of cells in S phase were routinely found to be similar for RPA2_{wt} and RPA2_D. We conclude that expression of RPA2_D does not significantly affect cell cycle progression.

RPA2_D is unable to complement the loss of endogenous RPA2. The data presented above suggested that the RPA2_{wt} subunit, but not RPA2_D, would be able to complement the loss of endogenous RPA2 and support chromosomal DNA replication. To test this possibility, cells were depleted of cellular RPA2 by using an siRNA molecule directed against the 3' noncoding sequence of RPA2. The RPA2 expression cassettes do not contain the siRNA-targeted sequences, and hence the myc-RPA2 RNA produced from these vehicles is resistant to siRNA-mediated degradation. Visualization of RPA2 in these siRNA-treated cells by epifluorescence microscopy showed an apparent reduction of the RPA2 signal to nearly background level in >90% of the cells (compare Fig. 5D with A). Western blotting analysis indicated that RPA2 levels were reduced by >95% (data not shown). Upon cotransfection with myc-RPA2_{wt}, a significant fraction of the cells demonstrated a robust myc signal bound to chromatin, with the pattern of bind-

ing similar to that seen in replicating cells (Fig. 5C). In contrast, little or no myc-RPA2_D was found associated with chromatin (Fig. 5F), even though comparable levels of RPA2_{wt} and RPA2_D expression were detected in nonextracted cells (Fig. 5B and E, respectively). We therefore conclude that RPA2_D, unlike RPA2_{wt}, is unable to complement the loss of endogenous RPA2 and support DNA replication. These data also indicate that RPA_{RPA2D} is not prevented from binding ssDNA because of competition with the endogenous RPA but rather is inherently unable to productively interact with the DNA replication machinery.

RPA association with replication centers is dependent on the RPA2 N terminus negative charge. We next examined whether mutation of particular serine or threonine residues to aspartate was responsible for the lack of RPA2_D association with replication centers or whether it was a consequence of the heightened negative charge at the RPA2 N terminus. We first constructed serine-to-aspartate substitutions at the cyclin-cdk2 sites S23 and S29 (RPA2_{D2}) (Fig. 6G). S29 is invariably modified in each form of phosphorylated RPA (53), and thus, the RPA2_{D2} mutant resembles the form found in the initial steps of the RPA phosphorylation pathway. Further intermediate RPA2 mutants were designed to roughly follow the phosphorylation pathway, as suggested by the data of Zernik-Kobak and colleagues (53). However, it must be mentioned that the exact pathway of RPA2 modification from the hypophosphorylated to the hyperphosphorylated form is not known, and it is unlikely that a strict order of modification occurs in vivo. Additional serine-to-aspartate changes were generated in the background of the RPA2_{D2} mutant, with a total of three (RPA2_{D3},

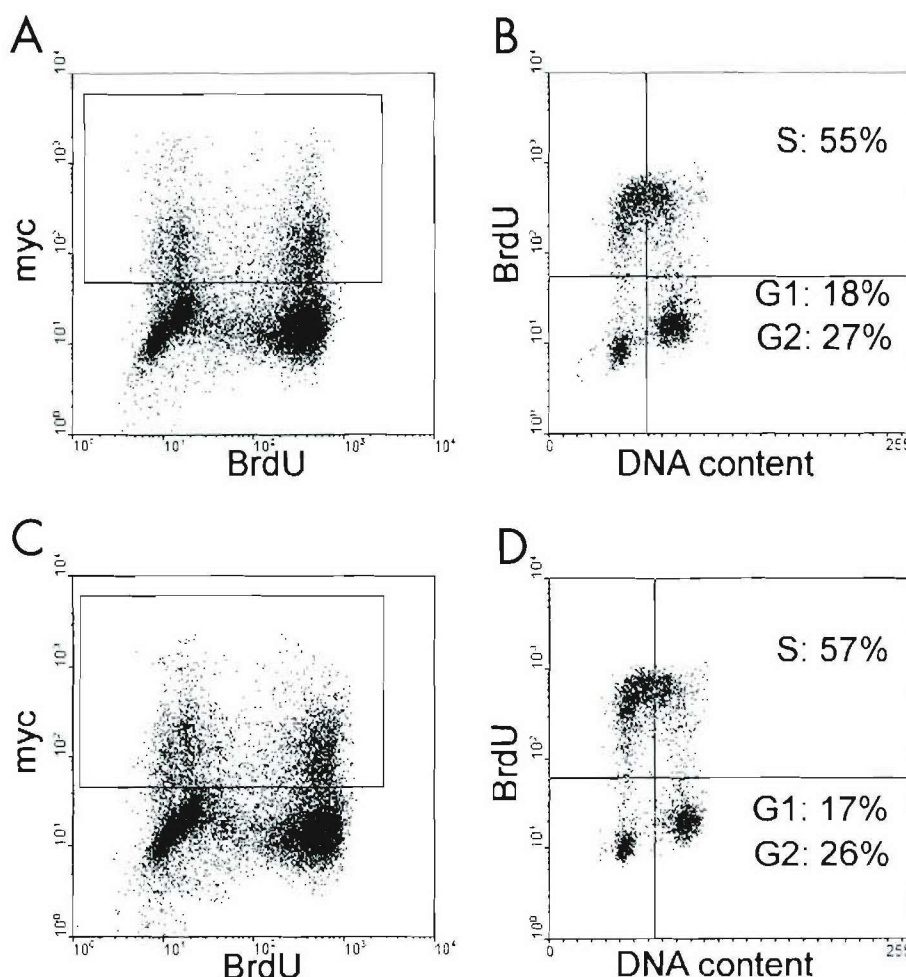


FIG. 4. Expression of RPA2_D does not affect cell cycle progression. Cells transfected with myc-RPA2_{wt} (A and B) or myc-RPA2_D (C and D) were incubated with 10 μ M BrdU for 30 min prior to harvest. The cells were then subjected to FACS analysis using a pairwise analysis of the levels of myc and BrdU signals. Transfected cells (with significant myc signals [boxed regions in panels A and C]) were further analyzed for the BrdU signal and the amount of DNA. (B and D) Fractions of cells in G₁, S, and G₂ phases. For each plot, the x and y axes indicate fluorescence intensities of the different signals.

and RPA2_{D31}), four (RPA2_{D4} and RPA2_{D41}), or five (RPA2_{D5}) positions mutated. The sites mutated in these RPA2 variants are also found to be modified in RPA with an intermediate phosphorylation state in vivo.

Transfection of U2-OS cells indicated that all of the intermediate RPA2 mutants were expressed at similar levels (Fig. 6A and B and data not shown). Relative to RPA2_{wt}, the RPA2 mutants with two or three Ser→Asp changes had two notable effects: (i) a modestly reduced fraction of transfected cells showing mutant RPA2 bound to chromatin (Fig. 6H) and (ii) a reduction in the intensity of RPA2 bound to chromatin (see below). More dramatic effects were observed when four or five serines were converted. For RPA2_{D41}, the fraction of cells with significant chromatin binding was threefold less than for RPA2_{wt}, and this fraction was reduced to 8% for the RPA2_{D5} mutant (Fig. 6H). The intensities of chromatin staining for the intermediate RPA2 mutants were also greatly reduced in individual cells, as demonstrated by comparing the average staining patterns of cells transfected with RPA2_{wt} and RPA2_{D41} (Fig. 6C and D, respectively [taken with identical exposure times]).

The decrease in association of RPA2 with replication centers was most strongly correlated with the number of aspartate residues rather than with changes at any particular positions. The notion that the mutation of serines to aspartates per se (i.e., irrespective of the changes in the RPA2 negative charge) causes decreased RPA binding to replication centers is argued against because the N terminus of RPA2 is not critical for DNA replication in vitro for mammalian RPA (23) or in vivo for yeast RPA (38). These data therefore suggest that the increase in net negative charge afforded by the increased number of aspartate residues is the primary factor regulating RPA binding to chromatin. Although the location of the aspartate residues did not appear to have major effects on RPA2 activity, we did note that mutation of the S33 site, known as a consensus sequence for PIKKs, appeared to have a somewhat more deleterious effect.

RPA2_D is recruited to DNA damage foci following genotoxic stress. Under DNA damage conditions, a significant change occurs in the nuclear distribution of RPA, with the more diffuse punctate pattern seen during DNA replication transform-

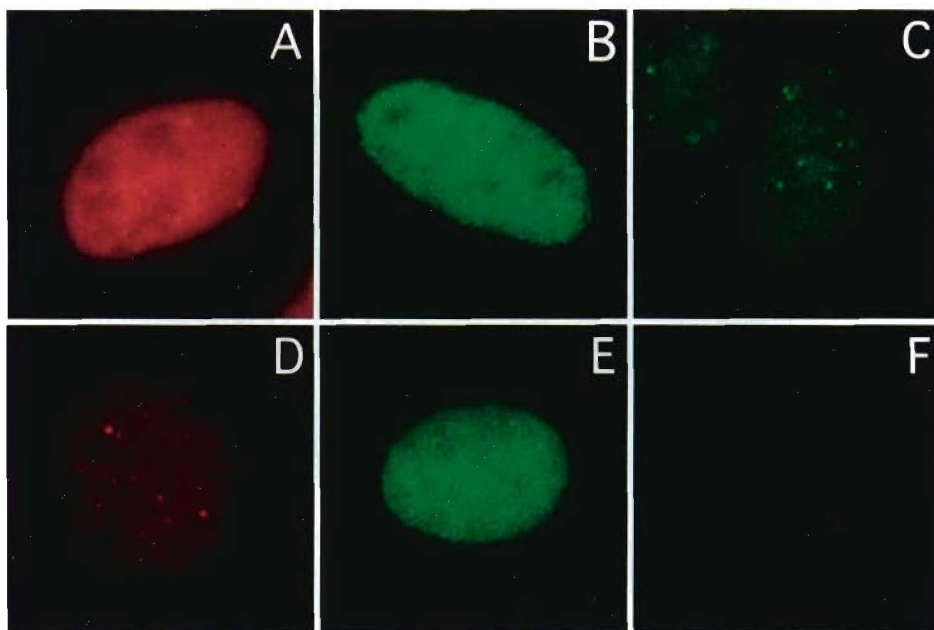


FIG. 5. Lack of RPA2_D chromatin association in cells lacking endogenous RPA2. U2-OS cells were incubated with a control (i.e., scrambled) siRNA (A) or an siRNA specific for the 3' noncoding region of the RPA2 mRNA (B to F). The cells were simultaneously cotransfected with an empty control vector (D), myc-RPA2_{wt} (B and C), or myc-RPA2_D (E and F). Forty-eight hours posttransfection, the cells were extracted with 0.5% (vol/vol) Triton X-100 for 5 min prior to formaldehyde fixation to reveal RPA associated with chromatin (C and F) or were fixed to show total endogenous or transfected RPA2 (A, B, D, and E). The cells were then stained with anti-RPA2 (A and D) or anti-myc (panels B, C, E, and F) antibody and then visualized by epifluorescence microscopy. Cells with representative signals were chosen.

ing to bright, well-distinguished foci. In this state, RPA colocalizes with a number of repair and checkpoint proteins (e.g., ATR and Rad51) and is thought to demarcate the sites of DNA repair and/or unrepairable lesions (19, 20, 39, 54). Such stress conditions cause a subset of the endogenous RPA pool to become hyperphosphorylated (see below). We therefore reexamined the behavior of RPA2_D and RPA2_A in cells undergoing genotoxic stress.

Cells were transfected with the RPA2_{wt}, RPA2_A, or RPA2_D expression construct and then treated with CPT. CPT inhibits topoisomerase I, indirectly causing DNA double-strand breaks, and leads to rapid and massive RPA phosphorylation (42). Similar to RPA2_{wt} (Fig. 7A to C), the RPA2_A variant colocalized with RPA1 in bright foci following CPT treatment (Fig. 7G to I). Very similar foci were observed for endogenous RPA2 (not shown). Thus, the phosphorylation-defective RPA2_A variant is apparently competent to bind chromatin both in normal (above [Fig. 2L]) and in stressed cells.

In sharp contrast to the inability of RPA2_D to stably associate with replication centers, CPT treatment caused the RPA2_D variant to colocalize with RPA1 in DNA damage foci (Fig. 7D to F). The number and distribution of these foci, as well as the intensity of staining, were indistinguishable from those observed with the RPA2_{wt} (and RPA2_A) construct. Thus, although the RPA2_D mutant is unable to localize to replication centers, this defect does not extend to the involvement of RPA2_D in the DNA damage response.

We determined if the CPT-dependent recruitment of RPA2_D to DNA damage foci was applicable to other stresses. We tested HU and aphidicolin, agents that do not directly cause DNA damage but rather result in stalling of the DNA

replication fork. As cells were incubated with HU from 1 to 3 h (Fig. 8E and F), a progressive increase in RPA2_D association with chromatin was observed, with most cells demonstrating a dispersed staining pattern. A fraction of cells exhibited distinctive foci, and these showed significant colocalization with γ -H2AX, the phosphorylated form of histone variant H2AX that is a marker for sites of DNA damage (Fig. 8I to L) (40). Similar effects of HU were noted on cells transfected with RPA2_{wt} (Fig. 8A and B). In contrast, treatment with aphidicolin for 3 h did not stimulate RPA2_D association with chromatin (Fig. 8M; data not shown), demonstrating reduced toxicity of aphidicolin relative to HU under these conditions. Exposure to ionizing radiation (10 Gy) gave rise to staining patterns of RPA2_{wt} and RPA2_D similar to that found with CPT (data not shown).

In the functional absence of the budding yeast homologs of ATR and its downstream effector Chk1 (Mec1p and Rad53, respectively), replication forks have a greater propensity to collapse when encountering DNA damage, yielding unregulated production of long ssDNA regions (32, 43, 45). We therefore hypothesized that addition of caffeine, an inhibitor of the ATR-ATM-dependent checkpoint response (21, 41), to HU-treated cells would similarly lead to replication fork degradation. This in turn would cause faster induction of DNA damage foci and of RPA2_D localization. To test this hypothesis, RPA2_{wt} or RPA2_D-transfected cells were treated with HU for 1 or 3 h in the presence of caffeine. Particularly for RPA2_D, addition of caffeine dramatically increased the number and intensity of RPA2 foci at both the 1- and 3-h time points (Fig. 8G and H). Quantification of the effects on myc-RPA2 localization demonstrated that caffeine greatly increased the frac-

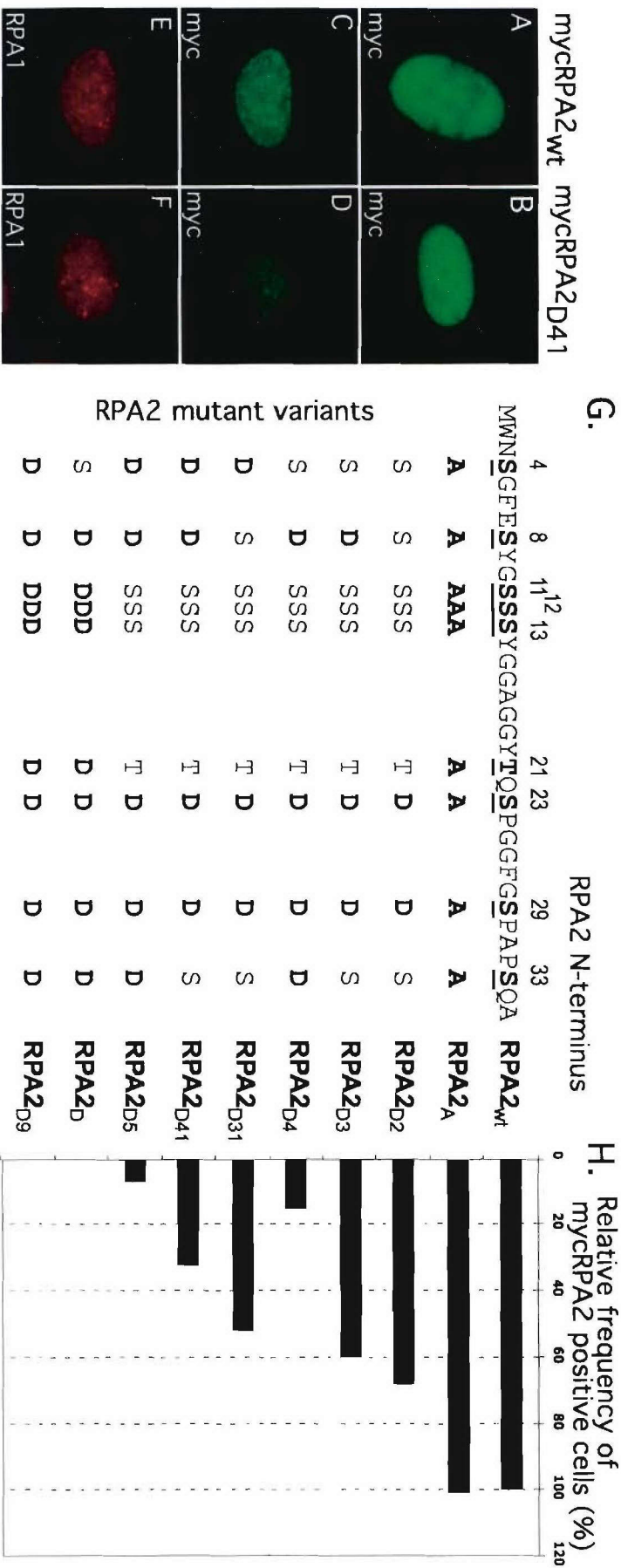


FIG. 6. Increase in negative charge at the RPA2 N terminus decreases frequency of myc-positive cells. (A to F) Cells were transfected with myc-RPA2^{wt} or myc-RPA2^{D41} as indicated. Representative epifluorescence images showing total myc-RPA2 staining (no extraction (A and B)), chromatin-bound myc-RPA2 (C and D), and chromatin-bound RPA1 (E and F) are shown. (G and H) Serines and threonine (boldface and underlined) at the potential phosphorylation sites in the N terminus of the RPA2 subunit were replaced with alanines (A) or aspartates (D) as indicated. Cells expressing these myc-tagged RPA2 mutants were then analyzed by immunofluorescence microscopy for the presence of myc-RPA2 bound to chromatin and, in parallel reactions, for transfection efficiency. The relative frequencies of myc-RPA2 positive cells were calculated as described in Materials and Methods.

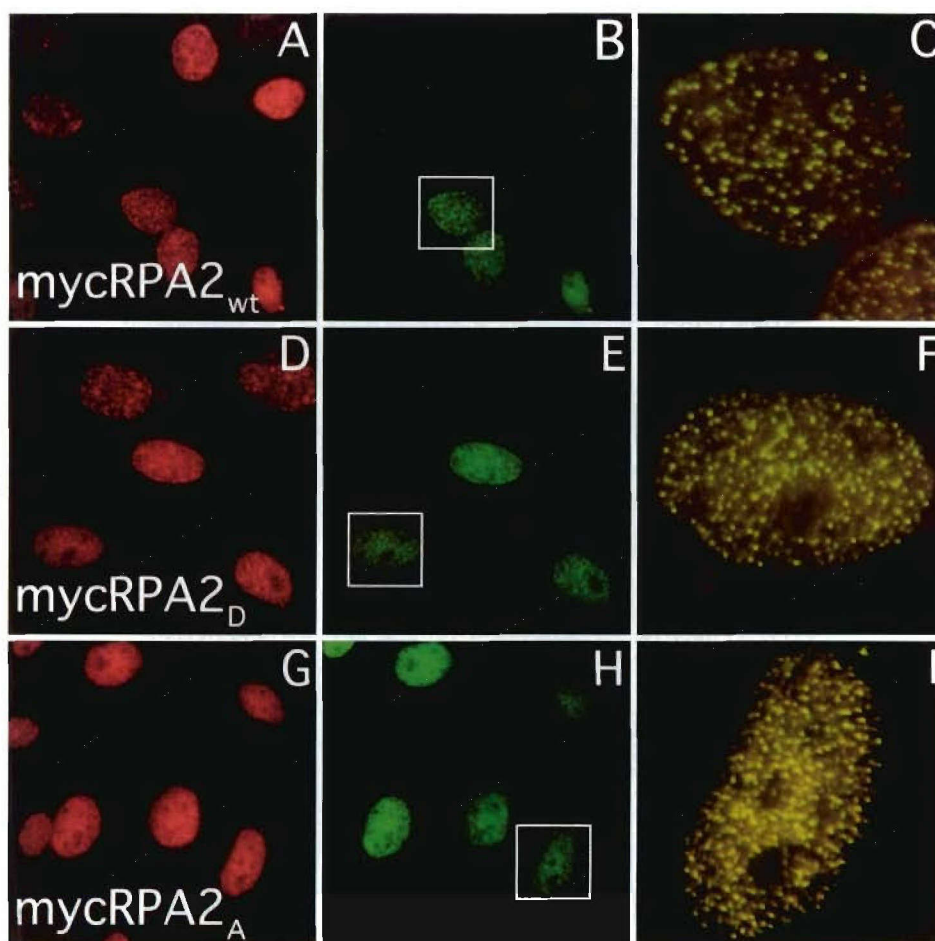


FIG. 7. RPA2_D binds chromatin and colocalizes with RPA1 after CPT treatment. U2-OS cells were transfected with myc-RPA2_{wt} (A to C), myc-RPA2_D (D to F), or myc-RPA2_A (G to I) vector. Forty-eight hours posttransfection, the cells were incubated with 1 μ M CPT for 3 h, extracted with 0.5% (vol/vol) Triton X-100 for 5 min, fixed, and stained with anti-RPA1 (A, D, and G) and anti-myc (B, E, and H) antibodies. (C, F, and I) Colocalization of the two stains, enlarged from the boxed regions.

tion of HU-treated cells with significant RPA2_D and RPA2_{wt} signals (Fig. 8M).

The effects of these various stress conditions on endogenous RPA phosphorylation were also examined (Fig. 8N). Those stress conditions that resulted in significant RPA2_D chromatin binding also caused increased phosphorylation of endogenous RPA2, although CPT caused modification of a greater fraction of the RPA pool, as well as phosphorylation of more RPA2 sites, than HU. Enhanced phosphorylation of RPA following a 1-h treatment with HU and caffeine was occasionally seen. Consistent with our results showing the inability of aphidicolin to stimulate the chromatin binding of RPA2_D, aphidicolin also did not induce RPA2 phosphorylation. Because caffeine has been demonstrated to be an inhibitor of ATM and ATR kinase activities (21, 41), the observed hyperphosphorylation of RPA probably results from the caffeine-insensitive activity of DNA-PK that is stimulated by collapsed replication forks. However, we note that a recent study found that caffeine can inhibit the checkpoint response without inhibiting ATR-ATM kinase activity *in vivo* (11), leaving open the possibility that these kinases may still be responsible. In any case, these data indicate that the rate and extent of RPA2_D (and RPA2_{wt})

localization to sites of DNA damage correlate with the degree of DNA damage sustained during stress.

Localization of endogenous hyperphosphorylated RPA. The properties of endogenous hyperphosphorylated RPA were examined using an antibody generated against an RPA2 peptide doubly phosphorylated on serine residues 4 and 8. Lysates prepared from untreated or CPT-treated U2-OS cells were probed with either a general RPA2 antibody or the pSer4/pSer8-RPA antibody (Fig. 9J). The phosphospecific antibody selectively recognized a species from CPT-treated cells that comigrated with hyperphosphorylated RPA2 by Western blotting analysis. Prior incubation of the CPT-treated lysates with phosphatase resulted in the loss of both the hyperphosphorylated RPA2 form and reactivity by the phosphospecific antibody. We conclude that the phosphospecific antibody recognizes a hyperphosphorylated RPA2 species that is modified on Ser4 and Ser8.

The phosphospecific antibodies were used to examine the localization of the pSer4/pSer8 form of RPA in untreated U2-OS cells and in cells treated with HU alone or with HU and caffeine. In control cells or in cells treated only with HU (Fig. 9D and E), little if any pSer4/pSer8-RPA staining was detected. Following

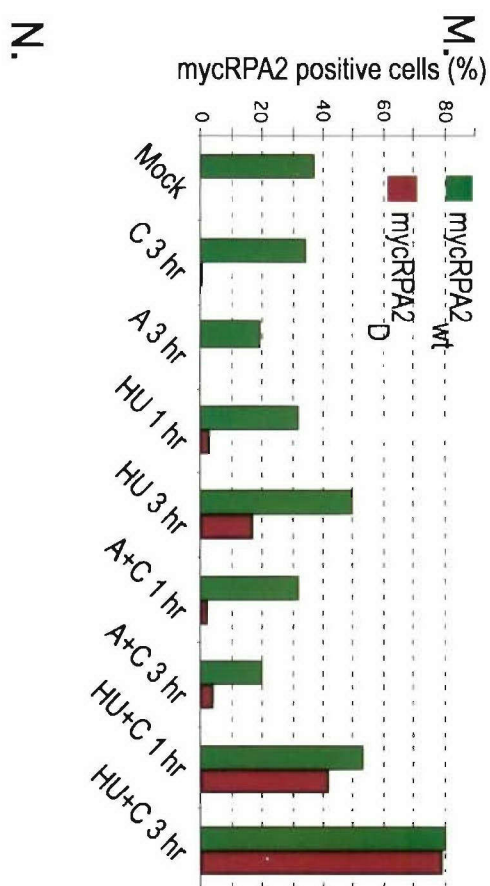
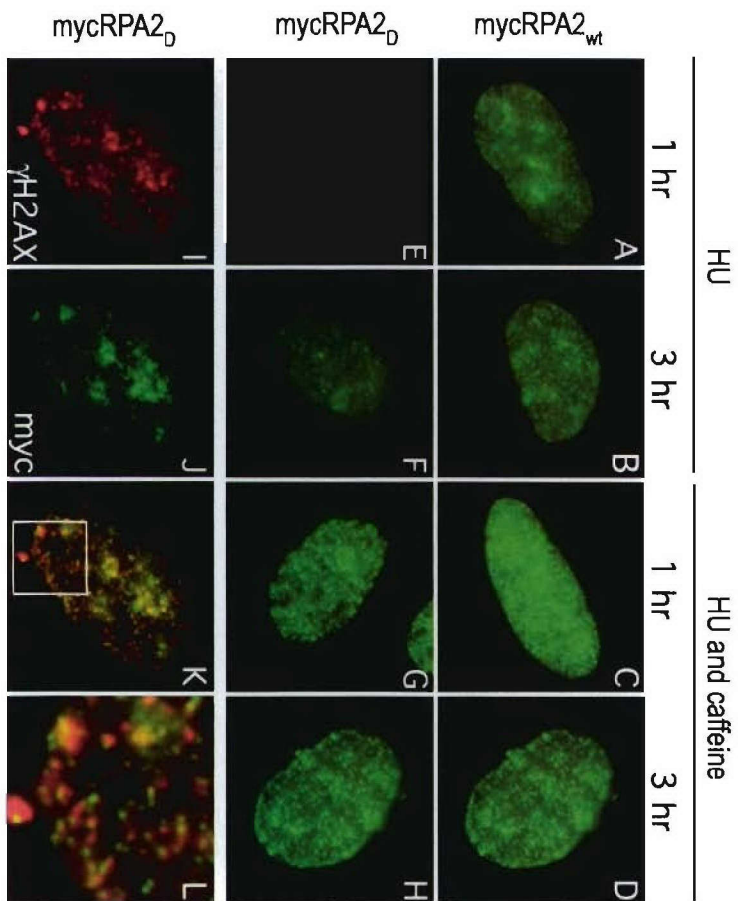


FIG. 8. Collapse of DNA replication forks stimulates RPA loading to damaged DNA. (A to H) U2-OS cells were transfected with plasmids expressing either myc-RPA2_{wt} or myc-RPA2_D as indicated for 48 h. The cells were then treated with 2.5 mM HU for either 1 (A and E) or 3 (B and F) h in the absence of caffeine or treated with HU for 1 (C and G) or 3 (D and H) h in the presence of 5 mM caffeine. The cells were then treated with Triton X-100 extracted and then stained for myc-RPA. (I to L) Colocalization of myc-RPA2_{wt} with sites of DNA damage. U2-OS cells were transfected with a myc-RPA2_D-expressing plasmid. Forty-eight hours posttransfection, the cells were treated with 2.5 mM HU for 3 h and then extracted with 0.5% Triton X-100 and fixed. The cells were stained with γ-H2AX (I) and myc-RPA (J). The staining pattern of a representative cell and the image of the merged staining patterns (K) are provided. (L) One section (boxed) of the composite image is shown enlarged to reveal the degree of signal overlap. (M) Graph showing the fractions of myc-RPA2-transfected cells with a significant chromatin-bound myc-RPA2_{wt} (green bars) or myc-RPA2_D (brown bars) signal. The fractions of cells showing chromatin-bound RPA were quantified by visual inspection of 100 to 200 cells. The bar graph values were calculated as described in Materials and Methods. Note that although RPA2_{wt} staining is consistently detected in a greater fraction of cells than RPA2_D staining, this result is expected because RPA2_{wt} can be observed both at replication centers and at DNA damage foci while RPA2_D localizes only to damage foci. (N) Effects of stress and caffeine treatment on endogenous RPA2 phosphorylation. U2-OS cells were mock treated (mock) or treated with either 1 μM CPT for 1 or 3 h, 2.5 mM HU for 1 or 3 h, 5 mM caffeine (c) for 3 h, 2.5 mM HU for 1 or 3 h in the presence of 5 mM caffeine or with 7 μM aphidicolin (A) for 3 h and 7 μM aphidicolin for 1 or 3 h in the presence of 5 mM caffeine. The band labeled RPA2' represents nonphosphorylated RPA, while P-RPA2 indicates the position of phosphorylated RPA.

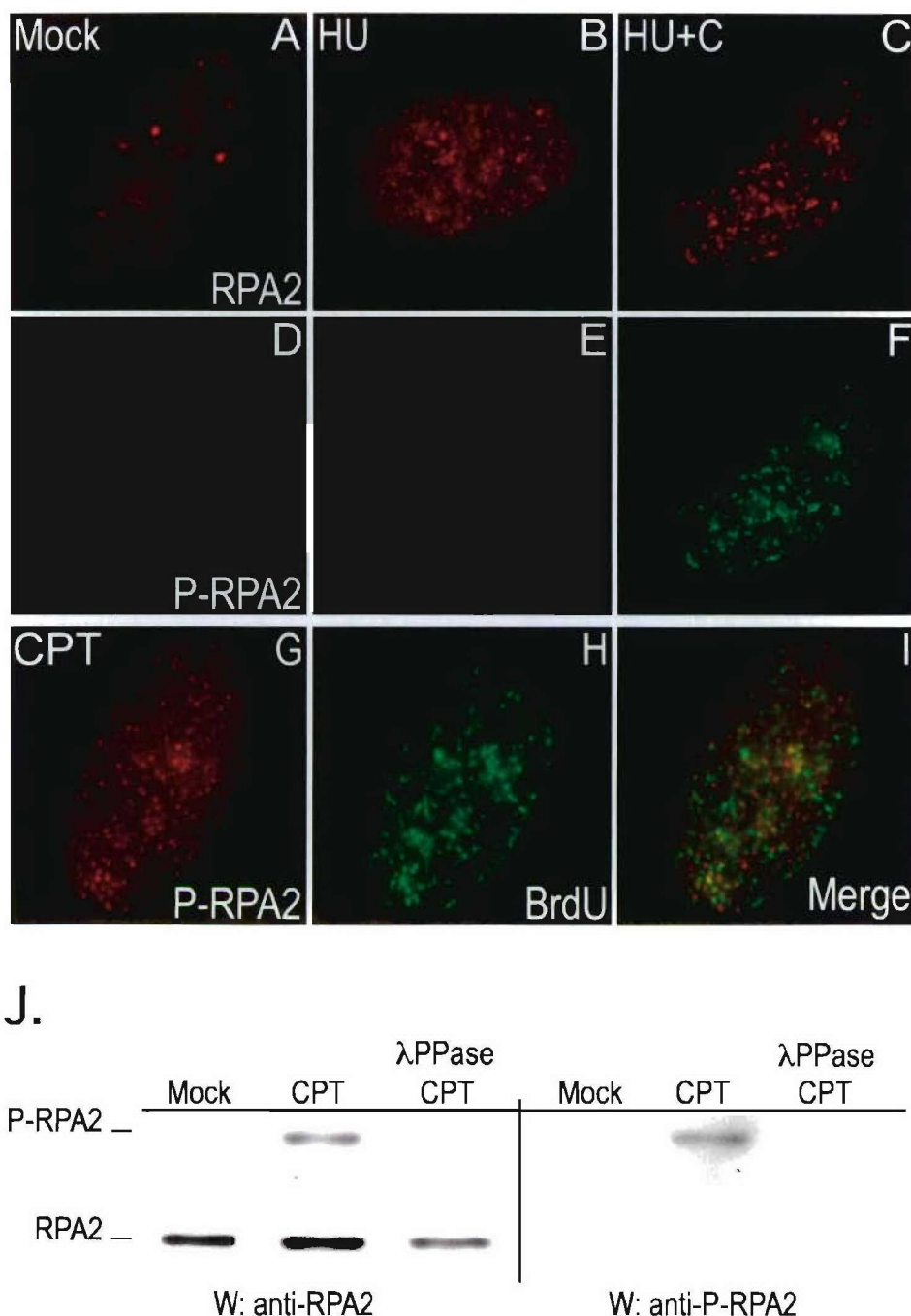


FIG. 9. Endogenous phosphorylated RPA (P-RPA2) does not localize to sites of DNA synthesis. (A to F) U2-OS cells were either mock treated (A and D) or treated with 2.5 mM HU for 3 h (B and E) or with 2.5 mM HU and 5 mM caffeine for 3 h (C and F). The cells were extracted to visualize the chromatin-bound form of RPA, fixed, and then stained either with anti-RPA2 (A to C) or anti-pSer4/pSer8-RPA2 (D to F) antibody. (G to I) U2-OS cells were either mock treated or treated with 1 μ M CPT for 30 min, followed by an additional 2.5-h incubation in medium lacking CPT. The cells were incubated with 10 μ M BrdU for 15 min prior to being processed. The cells were then extracted to visualize the chromatin-bound form of RPA, fixed, and stained either with anti-pSer4/pSer8-RPA2 (G) or anti-BrdU (H) antibody. (I) Merged staining pattern. (J) Extracts prepared from mock-treated or CPT-treated (1 μ M for 3 h) cells were subjected to Western blotting (W) analyses using either anti-RPA2 (34A) monoclonal antibody (anti-RPA2) or a rabbit anti-pSer4/pSer8-RPA2 antibody (anti-P-RPA2). CPT-treated extracts were also incubated with λ protein phosphatase (λ PPase), as indicated.

treatment with both HU and caffeine, the cells showed a dramatic increase in pSer4/pSer8-RPA staining (Fig. 9F). The staining pattern was nearly identical to that of total RPA2 (compare Fig. 9C and F), and also showed good overlap with γ -H2AX staining

(data not shown). The colocalization of pSer4/pSer8-RPA with sites of DNA synthesis was also examined. Cells were treated with CPT and then incubated with BrdU. The areas of pSer4/pSer8-RPA staining did not colocalize with sites of remaining DNA

synthesis to any significant degree (Fig. 9L). A majority of the RPA pool is hyperphosphorylated under these conditions (Fig. 8N), rendering similar experiments using general RPA2 antibodies uninformative. We conclude that the hyperphosphorylated form of RPA localizes only to chromatin following DNA damage and is not significantly associated with sites of chromosomal DNA synthesis.

DISCUSSION

We find that the RPA2_D mutant that mimics the hyperphosphorylated state is prevented from stable association with replication centers in vivo. The lack of association with sites of DNA synthesis is also observed for endogenous hyperphosphorylated RPA and is not a result of competition with the non-phosphorylated protein. Importantly, the RPA_{RPA2D} protein has activity equivalent to the wild-type protein both in ssDNA binding (4) and in SV40 DNA replication in vitro. The inherent activity of hyperphosphorylated RPA or RPA_{RPA2D} in vivo also appears normal because genotoxic stress causes these RPA species to localize to DNA damage foci similarly to endogenous RPA2 and RPA2_w. Our data therefore indicate that the chromosomal DNA replication machine has the ability to discriminate between RPA species with different phosphorylation states. In addition to providing a means to regulate RPA loading and hence DNA replication, RPA phosphorylation also has the potential to mark sites of DNA damage or replication stress for recruitment of repair factors.

Our data suggest a novel feature of eukaryotic DNA replication, namely, that RPA is actively loaded onto the ssDNA by the chromosomal replication machinery. This model arises from the fact that RPA_{RPA2D}, and by inference hyperphosphorylated RPA, is inherently active in binding the ssDNA at a DNA replication fork but is unable to do so in vivo. The most logical explanation is that, as the duplex DNA is unwound by the advancing DNA helicase, the hypophosphorylated RPA is loaded onto the ssDNA by protein components of the replication fork machinery. One could easily envision, for example, that the minichromosome maintenance (MCM) complex, suggested to be the eukaryotic replicative helicase (29) and known to interact with RPA (55), would load RPA molecules in a step-by-step fashion as the ssDNA is generated. Selective binding of nonphosphorylated RPA (i.e., endogenous RPA, RPA_{RPA2W}, or RPA_{RPA2A}) to MCM would therefore allow this RPA species to bind only to unwound DNA. (The MCM complex is not involved in SV40 DNA replication.) However, RPA interacts with various proteins, including the DNA polymerase α -DNA primase complex (14), and RPA phosphorylation has been found to inhibit the association with DNA polymerase α (34). Thus, discrimination of the RPA phosphorylation state can be achieved by these or other replication factors. One alternative model that does not require concerted RPA loading would involve a discrimination filter that prevents access of the phosphorylated RPA to the replication fork. The nature of such a filter would be difficult to envisage.

DNA-damaging stress relieves the inhibition of RPA_{RPA2D} chromatin binding and causes RPA_{RPA2D} association with DNA damage foci, as evident by colocalization with γ -H2AX. That HU causes RPA_{RPA2D} foci to form and increases the

level of RPA2 phosphorylation while aphidicolin does neither indicates that replication fork blockage is not sufficient for RPA_{RPA2D} chromatin binding but that the presence of DNA damage or aberrant replication fork structures is also required. This conclusion is strengthened by our observation that inhibition of ATR- or ATM-mediated checkpoint response by caffeine stimulates the rate of RPA association with DNA damage foci. Mutation of MEC1, the *Saccharomyces cerevisiae* ATR homolog, is known to cause the collapse of DNA replication forks that have been stalled by treatment with HU or methyl methanesulfonate (32, 45), and such treatment leads to the production of long ssDNA regions (43). Because of the high affinity of RPA for ssDNA (27, 52), we propose that the increased availability of ssDNA releases the constraints on RPA loading seen during normal S-phase progression. Thus, under damage conditions, the RPA phosphorylation state no longer regulates the association of RPA with chromatin.

Our data indicate that hyperphosphorylated RPA is preferentially associated with sites of DNA damage. The specific association of repair factors with this modified form of RPA would therefore provide a mechanism to recruit repair factors to sites of DNA damage. Interestingly, the ATRIP-ATR complex has been found to sense damaged DNA by recognition of RPA-ssDNA complexes. Clearly, RPA phosphorylation has the potential to regulate the binding of ATRIP-ATR and thereby modify the cellular checkpoint response. Although our examination of RPA2_D expression did not detect any notable effects on cell cycle progression, it will be interesting to examine whether RPA2_D and RPA2_A expression in cells lacking endogenous RPA alters cellular proliferative capacity or response to DNA damage.

Finally, our data indicate that hyperphosphorylation of RPA can limit its ability to support chromosomal DNA replication. It is unlikely that this mechanism alone could cause significant reductions in the level of DNA synthesis during genotoxic stress. Under severe stress conditions, such as 1-h exposure to 1 μ M CPT (Fig. 8N) or irradiation with 30 J of UV light/m² (53), the hyperphosphorylated form of RPA contributes ~50% of the total RPA pool prepared from asynchronous cells. Even though the fraction of hyperphosphorylated RPA may be higher in S-phase cells, these data suggest that enough hypophosphorylated RPA would be available to sustain DNA replication. That being said, we and others have found that stress conditions also lead to the inhibition of RPA activity by other processes (9, 30, 48), including sequestration of RPA by nucleolin (12, 47). Combined, these data suggest that inhibition of RPA activity by multiple mechanisms can serve to repress chromosomal DNA replication following stress.

ACKNOWLEDGMENTS

We thank Kyung Kim and Diana Dimitrova for helpful discussions during the course of these experiments, Kristine Carta for expert technical assistance, and John Hirsch for assistance with FACS analysis.

J.A.B. was supported by NIH grant AI29963, DOD Breast Cancer Research Program DAMD17-03-1-0299, Philip Morris grant 15-B0001-42171, and the NYU Cancer Institute and the Rita J. and Stanley Kaplan Comprehensive Cancer Center (NCI P30CA16087). M.S.W. was supported by NIH grant GM44721.

REFERENCES

1. Abraham, R. T. 2001. Cell cycle checkpoint signaling through the ATM and ATR kinases. *Genes Dev.* 15:2177-2196.

2. Ariza, R. R., S. M. Keyse, J. G. Moggs, and R. D. Wood. 1996. Reversible protein phosphorylation modulates nucleotide excision repair of damaged DNA by human cell extracts. *Nucleic Acids Res.* **24**:433–440.
3. Bartek, J., and J. Lukas. 2001. Mammalian G1- and S-phase checkpoints in response to DNA damage. *Curr. Opin. Cell Biol.* **13**:738–747.
4. Binz, S. K., Y. Lao, D. F. Lowry, and M. S. Wold. 2003. The phosphorylation domain of the 32-kDa subunit of replication protein A modulates RPA-DNA interactions: evidence for an intersubunit interaction. *J. Biol. Chem.* **278**:35584–35591.
5. Borowiec, J. 1992. Inhibition of structural changes in the simian virus 40 core origin of replication by mutation of essential origin sequences. *J. Virol.* **66**:5248–5255.
6. Borowiec, J. A., F. B. Dean, and J. Hurwitz. 1991. Differential induction of structural changes in the simian virus 40 origin of replication by T antigen. *J. Virol.* **65**:1228–1235.
7. Brush, G. S., C. W. Anderson, and T. J. Kelly. 1994. The DNA-activated protein kinase is required for the phosphorylation of replication protein A during simian virus 40 DNA replication. *Proc. Natl. Acad. Sci. USA* **91**:12520–12524.
8. Bullock, P. A. 1997. The initiation of simian virus 40 DNA replication *in vitro*. *Crit. Rev. Biochem. Mol. Biol.* **32**:503–568.
9. Carty, M. P., M. Zernik-Kobak, S. McGrath, and K. Dixon. 1994. UV light-induced DNA synthesis arrest in HeLa cells is associated with changes in phosphorylation of human single-stranded DNA-binding protein. *EMBO J.* **13**:2114–2123.
10. Chan, D. W., S. C. Son, W. Block, R. Ye, K. K. Khanna, M. S. Wold, P. Douglas, A. A. Goodarzi, J. Pelley, Y. Taya, M. F. Lavin, and S. P. Lees-Miller. 2000. Purification and characterization of ATM from human placenta: A manganese-dependent, wortmannin-sensitive serine/threonine protein kinase. *J. Biol. Chem.* **275**:7803–7810.
11. Cortez, D. 2003. Caffeine inhibits checkpoint responses without inhibiting the ataxia-telangiectasia-mutated (ATM) and ATM- and Rad3-related (ATR) protein kinases. *J. Biol. Chem.* **278**:37139–37145.
12. Daniely, Y., and J. A. Borowiec. 2000. Formation of a complex between nucleolin and replication protein A after cell stress prevents initiation of DNA replication. *J. Cell Biol.* **149**:799–810.
13. Dimitrova, D. S., and D. M. Gilbert. 2000. Stability and nuclear distribution of mammalian replication protein A heterotrimeric complex. *Exp. Cell Res.* **254**:321–327.
14. Dornreiter, I., L. F. Erdile, I. U. Gilbert, D. von Winkler, T. J. Kelly, and E. Fanning. 1992. Interaction of DNA polymerase α -primase with cellular replication protein A and SV40 T antigen. *EMBO J.* **11**:769–776.
15. Durocher, D., and S. P. Jackson. 2001. DNA-PK, ATM and ATR as sensors of DNA damage: variations on a theme? *Curr. Opin. Cell Biol.* **13**:225–231.
16. Dutta, A., and B. Stillman. 1992. cdc2 family kinases phosphorylate a human cell DNA replication factor, RPA, and activate DNA replication. *EMBO J.* **11**:2189–2199.
17. Fotedar, R., and J. M. Roberts. 1992. Cell cycle regulated phosphorylation of RPA-32 occurs within the replication initiation complex. *EMBO J.* **11**:2177–2187.
18. Gately, D. P., J. C. Hittle, G. K. T. Chan, and T. J. Yen. 1998. Characterization of ATM expression, localization, and associated DNA-dependent protein kinase activity. *Mol. Biol. Cell* **9**:2361–2374.
19. Golub, E. I., R. C. Gupta, T. Haaf, M. S. Wold, and C. M. Radding. 1998. Interaction of human Rad51 recombination protein with single-stranded DNA binding protein. RPA. *Nucleic Acids Res.* **26**:5388–5393.
20. Haaf, T., E. Raderschall, G. Reddy, D. C. Ward, C. M. Radding, and E. I. Golub. 1999. Sequestration of mammalian Rad51-recombination protein into micronuclei. *J. Cell Biol.* **144**:11–20.
21. Hall-Jackson, C. A., D. A. Cross, N. Morrice, and C. Smythe. 1999. ATR is a caffeine-sensitive, DNA-activated protein kinase with a substrate specificity distinct from DNA-PK. *Oncogene* **18**:6707–6713.
22. Hassell, J. A., and B. T. Brinton. 1996. SV40 and polyomavirus DNA replication, p. 639–677. *In* M. L. DePamphilis (ed.), *DNA replication in eukaryotic cells*. Cold Spring Harbor Laboratory Press, Cold Spring Harbor, N.Y.
23. Henricksen, L. A., T. Carter, A. Dutta, and M. S. Wold. 1996. Phosphorylation of human replication protein A by the DNA-dependent protein kinase is involved in the modulation of DNA replication. *Nucleic Acids Res.* **24**:3107–3112.
24. Henricksen, L. A., C. B. Umbrecht, and M. S. Wold. 1994. Recombinant replication protein A: expression, complex formation, and functional characterization. *J. Biol. Chem.* **269**:11121–11132.
25. Huang, W., and R. L. Erikson. 1994. Constitutive activation of Mek1 by mutation of serine phosphorylation sites. *Proc. Natl. Acad. Sci. USA* **91**:8960–8963.
26. Ifthode, C., and J. A. Borowiec. 1998. Unwinding of origin-specific structures by human replication protein A occurs in a two-step process. *Nucleic Acids Res.* **26**:5636–5643.
27. Ifthode, C., Y. Daniely, and J. A. Borowiec. 1999. Replication protein A (RPA): the eukaryotic SSB. *Crit. Rev. Biochem. Mol. Biol.* **34**:141–180.
28. Kenny, M. K., U. Schlegel, H. Furneaux, and J. Hurwitz. 1990. The role of human single-stranded DNA binding protein and its individual subunits in simian virus 40 DNA replication. *J. Biol. Chem.* **265**:7693–7700.
29. Lei, M., and B. K. Tye. 2001. Initiating DNA synthesis: from recruiting to activating the MCM complex. *J. Cell Sci.* **114**:1447–1454.
30. Liu, J. S., S. R. Kuo, M. M. McHugh, T. A. Beerman, and T. Melendy. 2000. Adofolesin triggers DNA damage response pathways and arrests SV40 DNA replication through replication protein A inactivation. *J. Biol. Chem.* **275**:1391–1397.
31. Liu, V. F., and D. T. Weaver. 1993. The ionizing radiation-induced replication protein A phosphorylation response differs between ataxia telangiectasia and normal human cells. *Mol. Cell Biol.* **13**:7222–7231.
32. Lopes, M., C. Cotta-Ramusino, A. Pellicoli, G. Liberati, P. Plevani, M. Muzi-Falconi, C. S. Newton, and M. Foiani. 2001. The DNA replication checkpoint response stabilizes stalled replication forks. *Nature* **412**:557–561.
33. Niu, H., H. Erdjument-Bromage, Z. Q. Pan, S. H. Lee, P. Tempst, and J. Hurwitz. 1997. Mapping of amino acid residues in the p34 subunit of human single-stranded DNA-binding protein phosphorylated by DNA-dependent protein kinase and Cdc2 kinase *in vitro*. *J. Biol. Chem.* **272**:12634–12641.
34. Oakley, G. G., S. M. Patrick, J. Yao, M. P. Carty, J. J. Turchi, and K. Dixon. 2003. RPA phosphorylation in mitosis alters DNA binding and protein-protein interactions. *Biochemistry* **42**:3255–3264.
35. Pan, Z.-Q., A. A. Amin, E. Gibbs, H. Niu, and J. Hurwitz. 1994. Phosphorylation of the p34 subunit of human single-stranded-DNA-binding protein in cyclin A-activated G₁ extracts is catalyzed by cdk-cyclin A complex and DNA-dependent protein kinase. *Proc. Natl. Acad. Sci. USA* **91**:8343–8347.
36. Pan, Z.-Q., C. H. Park, A. A. Amin, J. Hurwitz, and A. Sancar. 1995. Phosphorylated and unphosphorylated forms of human single-stranded DNA-binding protein are equally active in simian virus 40 DNA replication and in nucleotide excision repair. *Proc. Natl. Acad. Sci. USA* **92**:4636–4640.
37. Park, J. S., S. J. Park, X. Peng, M. Wang, M. A. Yu, and S. H. Lee. 1999. Involvement of DNA-dependent protein kinase in UV-induced replication arrest. *J. Biol. Chem.* **274**:32520–32527.
38. Philipova, D., J. R. Mullen, H. S. Maniar, J. Lu, C. Gu, and S. J. Brill. 1996. A hierarchy of SSB protomers in replication protein A. *Genes Dev.* **10**:2222–2233.
39. Raderschall, E., E. I. Golub, and T. Haaf. 1999. Nuclear foci of mammalian recombination proteins are located at single-stranded DNA regions formed after DNA damage. *Proc. Natl. Acad. Sci. USA* **96**:1921–1926.
40. Redon, C., D. Pilch, E. Rogakou, O. Sedelnikova, K. Newrock, and W. Bonner. 2002. Histone H2A variants H2AX and H2AZ. *Curr. Opin. Genet. Dev.* **12**:162–169.
41. Sarkaria, J. N., E. C. Busby, R. S. Tibbetts, P. Roos, Y. Taya, L. M. Karnitz, and R. T. Abraham. 1999. Inhibition of ATM and ATR kinase activities by the radiosensitizing agent, caffeine. *Cancer Res.* **59**:4375–4382.
42. Shao, R. G., C. X. Cao, H. Zhang, K. W. Kohn, M. S. Wold, and Y. Pommier. 1999. Replication-mediated DNA damage by camptothecin induces phosphorylation of RPA by DNA-dependent protein kinase and dissociates RPA: DNA-PK complexes. *EMBO J.* **18**:1397–1406.
43. Sogo, J. M., M. Lopes, and M. Foiani. 2002. Fork reversal and ssDNA accumulation at stalled replication forks owing to checkpoint defects. *Science* **297**:599–602.
44. Stigger, E., F. B. Dean, J. Hurwitz, and S.-H. Lee. 1994. Reconstitution of functional human single-stranded DNA-binding protein from individual subunits expressed by recombinant baculoviruses. *Proc. Natl. Acad. Sci. USA* **91**:579–583.
45. Tercero, J. A., and J. F. Diffley. 2001. Regulation of DNA replication fork progression through damaged DNA by the Mec1/Rad53 checkpoint. *Nature* **412**:553–557.
46. Wang, H., J. Guan, A. R. Perrault, Y. Wang, and G. Iliakis. 2001. Replication protein A2 phosphorylation after DNA damage by the coordinated action of ataxia telangiectasia-mutated and DNA-dependent protein kinase. *Cancer Res.* **61**:8554–8563.
47. Wang, Y., J. Guan, H. Wang, D. Leeper, and G. Iliakis. 2001. Regulation of DNA replication after heat shock by replication protein A-nucleolin interactions. *J. Biol. Chem.* **276**:20579–20588.
48. Wang, Y., A. R. Perrault, and G. Iliakis. 1998. Replication protein A as a potential regulator of DNA replication in cells exposed to hyperthermia. *Radiat. Res.* **149**:284–293.
49. Wittekind, M., J. Reizer, J. Deutscher, M. H. Saier, and R. E. Klevit. 1989. Common structural changes accompany the functional inactivation of HPr by seryl phosphorylation or by serine to aspartate substitution. *Biochemistry* **28**:9908–9912.
50. Wobbe, C. R., F. Dean, L. Weissbach, and J. Hurwitz. 1985. *In vitro* replication of duplex circular DNA containing the simian virus 40 DNA origin site. *Proc. Natl. Acad. Sci. USA* **82**:5710–5714.
51. Wobbe, C. R., L. Weissbach, J. A. Borowiec, F. B. Dean, Y. Murakami, P. Bullock, and J. Hurwitz. 1987. Replication of simian virus 40 origin-containing DNA *in vitro* with purified proteins. *Proc. Natl. Acad. Sci. USA* **84**:1834–1838.

52. **Wold, M. S.** 1997. Replication protein A: a heterotrimeric, single-stranded DNA-binding protein required for eukaryotic DNA metabolism. *Annu. Rev. Biochem.* **66**:61–92.
53. **Zernik-Kobak, M., K. Vasunia, M. Connelly, C. W. Anderson, and K. Dixon.** 1997. Sites of UV-induced phosphorylation of the p34 subunit of replication protein A from HeLa cells. *J. Biol. Chem.* **272**:23896–23904.
54. **Zou, L., and S. J. Elledge.** 2003. Sensing DNA damage through ATRIP recognition of RPA-ssDNA complexes. *Science* **300**:1542–1548.
55. **Zou, L., and B. Stillman.** 2000. Assembly of a complex containing Cdc45p, replication protein A, and Mcm2p at replication origins controlled by S-phase cyclin-dependent kinases and Cdc7p-Dbf4p kinase. *Mol. Cell. Biol.* **20**:3086–3096.

Views and Commentaries

The Toposome

A New Twist on Topoisomerase II α

James A. Borowiec

Correspondence to: James A. Borowiec, Department of Biochemistry, New York University Cancer Institute, New York University School of Medicine, 550 First Ave., New York, New York 10016 USA; Tel.: 212.263.8453; Fax: 212.263.8166; Email: james.borowiec@med.nyu.edu

Received 03/19/04; Accepted 03/22/04

Previously published online as a *Cell Cycle* Epublication:
<http://www.landesbioscience.com/journals/cc/abstract.php?id=871>

KEY WORDS

topoisomerase II α , condensin, heterochromatin, RNA processing

ACKNOWLEDGMENTS

Work in the author's laboratory is supported by NIH grant AI29963, DOD Breast Cancer Research Program DAMD17-03-1-0299, and Philip Morris grant 15-B0001-42171.

As a small boy, I frequently visited nearby woods where a favored pastime was to overturn rocks on the forest floor. More often than not, I would discover a new sub-rocca world teeming with life. Nowadays, having less time to gambol through the woods and my curiosity focusing on biological questions, a similar enjoyment can be obtained from learning of ties of known factors to unanticipated processes. An example is provided by various recent findings relating to Topoisomerase II α (Topo II), including the work of Lee and colleagues who found that this enzyme can be isolated in a complex containing factors involved in RNA processing and transcription.¹

Topo II has been known to play key roles at two primary stages during the cell cycle. In preparation for mitosis and cytokinesis, Topo II acts in concert with the condensin complex² to condense the chromosomes 10,000-fold into the mitotic structures. A second requirement for Topo II arises because the process of DNA replication invariably leads to entanglement of the chromosomes, links between DNA molecules that must be resolved or the genomic information becomes endangered. Decatenation activity is primarily provided by Topo II which functions as the sister chromatids are preparing to segregate to the opposite cellular poles. Both condensation and decatenation utilize the ATP-dependent strand passage activity of Topo II.

When biochemically screening for novel nuclear kinases that modify RNA processing factors containing serine/arginine (SR) dipeptide repeats, Lee et al isolated a large complex, termed the toposome, containing a known SR kinase, SRPK1.¹ Modification of SR proteins by members of the SRPK and functionally related Clk/Sty families promotes nuclear import and recruitment to nascent transcripts for RNA splicing.³ In addition to containing other factors with known roles in transcription (RNA helicase A and SSRP1), pre-mRNA splicing (PRP8 and hnRNP C), and RNA processing (Rhl/Gu), the toposome complex also contained Topo II. That the association is functionally meaningful is indicated by the finding that the toposome has higher decatenation activity on chromatin substrates compared to isolated Topo II, and forms in a cell cycle-regulated manner with highest levels detected during mitosis.

The findings have a touch of déjà vu to the functional association of Topo II with condensin, a pentameric complex comprised by SMC2, SMC4, CapG, CapD2, and CapH/Barren. The CapH/Barren subunit of condensin can both bind Topo II and stimulate its relaxation activity, and these two factors colocalize on mitotic figures.⁴ Conditional knockouts of the SMC2 subunit in chicken cells are defective in proper localization of Topo II on mitotic chromosomes, and reduce Topo II levels at centromeres.⁵ Future characterization of the toposome will require similar investigation of the possible colocalization of Topo II with the other toposome factors on mitotic chromosomes. Such studies will not only reveal whether the toposome is bound to chromatin during mitosis, but indicate if the toposome complex occurs at all Topo II bound sites or only a subset of these targets. It is known that the sequences with which Topo II associates in vitro are somewhat different than those it binds in vivo. Moreover, chromatin structure has a strong influence on the binding preference of Topo II to centromeric sites.⁶ Thus, it is conceivable that formation of the toposome alters the binding preferences of Topo II to particular chromatin structures. If apparent toposome complexes exist on mitotic chromosomes, the effect of disruption or inhibition of toposome components other than Topo II should provide unambiguous answers as to whether the major role of the toposome relates to the known roles of Topo II in chromosome condensation and separation.

As mentioned above, Lee et al observed that the toposome apparently assembles as cells are entering mitosis, as only low levels of the complex were seen in cells at the G₁/S boundary or in S phase. Topo II has heightened phosphorylation at the G₂/M transition and this is apparently catalyzed by protein kinase C (PKC) and p34cdc2.^{7,8} Therefore, it would not be unexpected that modification increases the affinity of Topo II for other toposome components.

Test of the effects of mutation of the PKC and p34cdc2 sites on Topo II would clarify the significance of phosphorylation on toposome formation, and separate these effects from direct changes in Topo II activity per se. Recent evidence also demonstrates that *S. cerevisiae* and *Xenopus* Topo II undergo conjugation to SUMO, with disruption of this modification resulting in defective sister chromatid dissociation and centromere cohesion.^{9,10} In *Xenopus*, SUMO conjugation occurs during mitosis,¹⁰ and this modification clearly has the potential to regulate Topo II-protein interactions. Other toposome components are also modified by phosphorylation, acetylation, etc., and reciprocal changes in the modification patterns of these other factors could also regulate toposome formation.

What is the significance of the association of the RNA splicing and processing components with the toposome? Recent data by other laboratories lead to the suggestion that the toposome may be involved in heterochromatin formation. Topo II has a dynamic association with nuclear speckles that are thought to represent depots of splicing factors, and this pool is in equilibrium with Topo II involved in RNA polymerase II transcription.¹¹ Topo II also localizes to heterochromatic regions in a DNA replication-dependent fashion.¹¹ These data can be coupled to the finding that two different histone deacetylases (HDAC1 and HDAC2) physically interact with Topo II with reciprocal regulation of their activities.¹² Because of the emerging role for short noncoding RNA molecules in assembling heterochromatin,¹³ a possibility to be entertained is that Topo II is coupled to the RNAi machinery via toposome components. The toposome would therefore facilitate the maintenance of heterochromatin structure following passage of the DNA replication fork.

Lastly, because Topo II is an abundant factor on chromatin during mitosis, association with Topo II in the toposome may allow for the proper distribution of splicing factors to daughter cells as passenger proteins. During mitosis, a large number of factors, many involved in RNA processing or ribosome biogenesis such as fibrillarin, nucleophosmin, and ribosomal protein S1, become associated with condensed chromosomes.¹⁴ Among other roles (e.g., protection of mitotic chromosomes), chromosome association has been postulated to allow relatively equal partitioning of such factors to daughter cells.

Clearly, many questions are raised by the intriguing association of Topo II with RNA processing and transcription factors in the toposome. The literature is now becoming rife with examples of proteins that have distinct activities in, at first glance, unrelated processes. The work of my own laboratory finds that nucleolin, a protein with established roles in ribosome biogenesis and pre-rRNA processing, can also inhibit DNA replication following heat shock and genotoxic stress.^{15,16} As our understanding of biological processes matures, an important but arduous goal will be to decipher how the disparate processes of the cell are integrated into a unified whole.

References

1. Lee C-G, Hague LK, Li H, Donnelly R. Identification of toposome, a novel multisubunit complex containing topoisomerase II α . *Cell Cycle* 2004; In press.
2. Hirano T, Kobayashi R, Hirano M. Condensins, chromosome condensation protein complexes containing XCAP-C, XCAP-E and a *Xenopus* homolog of the *Drosophila* Barren protein. *Cell* 1997; 89:511-21.
3. Sanford JR, Longman D, Caceres JE. Multiple roles of the SR protein family in splicing regulation. *Prog Mol Subcell Biol* 2003; 31:33-58.
4. Bhat MA, Philp AV, Glover DM, Bellen HJ. Chromatid segregation at anaphase requires the barren product, a novel chromosome-associated protein that interacts with Topoisomerase II. *Cell* 1996; 87:1103-14.
5. Hudson DF, Vagnarelli P, Gassmann R, Earnshaw WC. Condensin is required for nonhistone protein assembly and structural integrity of vertebrate mitotic chromosomes. *Dev Cell* 2003; 5:323-36.
6. Spence JM, Critcher R, Ebersole TA, Valdivia MM, Earnshaw WC, Fukagawa T, et al. Colocalization of centromere activity, proteins and topoisomerase II within a subdomain of the major human X α -satellite array. *EMBO J* 2002; 21:5269-80.
7. Wells NJ, Fry AM, Guano F, Norbury C, Hickson ID. Cell cycle phase-specific phosphorylation of human topoisomerase II α . Evidence of a role for protein kinase C. *J Biol Chem* 1995; 270:28357-63.
8. Wells NJ, Hickson ID. Human topoisomerase II α is phosphorylated in a cell-cycle phase-dependent manner by a proline-directed kinase. *Eur J Biochem* 1995; 231:491-7.
9. Bachant J, Alcasabas A, Blat Y, Kleckner N, Elledge SJ. The SUMO-1 isopeptidase Smt4 is linked to centromeric cohesion through SUMO-1 modification of DNA topoisomerase II. *Mol Cell* 2002; 9:1169-82.
10. Azuma Y, Arnaoutov A, Dasso M. SUMO-2/3 regulates topoisomerase II in mitosis. *J Cell Biol* 2003; 163:477-87.
11. Agostinho M, Rino J, Braga J, Ferreira F, Steffensen S, Ferreira J. Human topoisomerase II α : Targeting to subchromosomal sites of activity during interphase and mitosis. *Mol Biol Cell* 2004; In press.
12. Tsai SC, Valkov N, Yang WM, Gump J, Sullivan D, Seto E. Histone deacetylase interacts directly with DNA topoisomerase II. *Nat Genet* 2000; 26:349-53.
13. Grewal SI, Moazed D. Heterochromatin and epigenetic control of gene expression. *Science* 2003; 301:798-802.
14. Hernandez-Verdun D, Gautier T. The chromosome periphery during mitosis. *Bioessays* 1994; 16:179-85.
15. Daniely Y, Borowiec JA. Formation of a complex between nucleolin and replication protein A after cell stress prevents initiation of DNA replication. *J Cell Biol* 2000; 149:799-810.
16. Daniely Y, Dimitrova DD, Borowiec JA. Stress-dependent nucleolin mobilization mediated by p53-nucleolin complex formation. *Mol Cell Biol* 2002; 22:6014-22.